Analysis of a filter with adaptive zeros for direct non-stationary multi-frequency estimation and tracking

Julio Vargas

A thesis submitted for the degree of Doctor of Philosophy.
The University of Edinburgh.
August 2001

Abstract

Direct multi-frequency estimation and tracking using a filter with adaptive zeros is the centre of the study in this thesis. The applicability of this approach is tested with the analysis of temporally and spatially sampled signals and proves to be a simple but useful tool for analysis.

General ideas and analysis techniques related to the study of non-stationary sinusoids are explained in chapters 2 and 3. There, several approaches oriented to the extraction of information from these kind of signals are described, including a brief description of potential applications in the areas of communication and speech processing.

The proposed approach to estimate multiple frequency trajectories and amplitude envelopes of multiple non-stationary sinusoids is then presented in chapter 4. There, the ideas are focused on the design of an algorithm to adapt the zeros of a filter, structured in cascade form, to track multiple non-stationary frequencies. Although this approach has been used in the past to analyse non-stationary multicomponent exponentials signals, the novel technique introduces a new gradient-based algorithm focused on the direct estimation and tracking of the instantaneous frequency of each component of the signal.

A second algorithm is also proposed in chapter 4 to estimate the amplitude envelope of a non-stationary sinusoid relying on two consecutive samples. This algorithm is extended to the multicomponent case by first isolating each sinusoid, relying on a cascade of notch filters. The theoretical propositions are validated in computer simulations of the algorithm for the case of synthetic signals, a bat sonar signal and a voiced segment of speech.

In chapter five, a spatial filter in decomposed form is used to analyse computer simulations of signals from a linear array of uniformly spaced sensors over which impinge multiple non-stationary plane waves. The ideas exploited constitute an extension to the spatial domain of direct frequency estimation using gradient-descent techniques. The resulting decoupled adaptive filter allows the tracking of the instantaneous spatial frequency of each component of the directional signal, which is equivalent to tracking the angle at which the different plane waves impinge on the array.

Acknowledgements

I would like to thank Dr. Steve McLaughlin for his constant support and supervision and Professor Bernie Mulgrew for carefully reading this thesis.

I would also like to thank my wife Ligia and my son Francisco for their unlimited love.

Finally, I want to recognise the good atmosphere surrounding the Signal and Systems Group thanks to the contribution of all its members. Thanks you all!!.

Contents

List of figures

List of tables

Acronyms

NSME	Non-stationary multicomponent exponential signal
TDAR	Time dependent autoregressive model
STFT	Short-time Fourier transform
LAF	Local autocorrelation function
GLAF	Generalised local autocorrelation function
WV	Wigner-Ville distribution
CW	Choi-Williams distribution
LTI	Linear time invariant
FIR	Finite impulse response filters
SSE	Summed squared errors
MSE	Mean square error
LMS	Least mean squares algorithm
RLS	Recursive least squares algorithm
CRLS-SA	Cascade recursive least squares with subsection adaptation
SNR	Signal to noise ratio
ULA	Uniformly spaced linear array of sensors
ED	Eigenvalue decomposition

Nomenclature

$a(n)$	Amplitude of sinuoidal signal
$\phi(n)$	Phase of sinusoidal signal
$\omega(n)$	Frequency of sinusoidal signal
$\hat{a}(n)$	Estimate of the amplitude of sinusoidal signal
$\hat{\phi}(n)$	Estimate of the phase of sinusoidal signal
$\hat{\omega}(n)$	Estimate of the frequency of sinusoidal signal
$H(\cdot)$	Hilbert transform
$*$	Convolution operation
$\Psi(\cdot)$	Teager-Kaiser energy operator

Time-dependent autoregressive modeling

$\{c_k(n)\}$	Parameters of the model
$\beta_i(n)$	Expansion functions
$\mathbf{R}$	Expanded correlation matrix
$p(n)$	Instantaneous pole of the signal

Time-Frequency distributions

E	Energy of the signal
$P(t,\Omega)$	Time-frequency density
$R(t,\tau)$	Local auto-correlation function
$GR(t,\tau)$	Generalised local auto-correlation function
$\kappa(t,\tau)$	Kernel function (time-lag expression)
$\zeta(Omega,\tau)$	Kernel function (frequency-lag expression)

FIR filter

$d(n)$	Desired signal
$c(n)$	Filter unit sample response
$\mathbf{c}$	Vector of filter coefficients
$E[\cdot]$	Expectation operator
$e(n)$	Error signal
$\mathbf{R_s}$	Autocorrelation of $\mathbf{s}(n)$
$\mathbf{r_{ds}}$	Crosscorrelation of $d(n)$ and $s(n)$
$\mathbf{R_{ds}}$	Matrix of crosscorrelations and autocorrrelations of $d(n)$ and $s(n)$
ξ	Summed square error (SSE)
$\hat{P}_s[exp(j\omega)]$	Estimated spectrum of s(n)

FIR filter structured in lattice

$\nabla_{\mathbf{c}^*}\xi$	Gradient of ξ respect to $\mathbf{c}^*$
e_{i-1}^f	Forward error of the $i-th$ section
e_{i-1}^b	Backward error of the $i-th$ section
Γ_i	Reflection coefficient of the $i-th$ section
$\nabla_{\Gamma_i^*}\xi_i^f$	Gradient of ξ_i^f respect to Γ_i^*
ξ_i^f	Variance of the output forward error
μ	Step size
λ_{max}	Maximum eigenvalue
$POW(\cdot)$	Power of the enclosed variable

Recursive least squares algorithm

λ	Forgetting factor

Cascade recursive least squares with subsection adaptation

Φ_k	Gradient corresponding to the $k-th$ section

$\mathbf{R}_k$	Autocorrelation matrix corresponding to the $k-th$ section
$C_k(q,n)$	Filter corresponding to the $k-th$ section

Adaptive zero: temporal domain

$\xi(n)$	Instantaneous residual energy
$\psi(n)$	Instantaneous complex phase
$\varpi(n)$	Instantaneous complex frequency
$\frac{1}{\mu}$	Inertia of the adaptation process
m	Expanded time index
$sr_k(n)$	$k-th$ real valued component
$z_k(n)$	Instantaneous $k-th$ zero
$p_k(n)$	Instantaneous $k-th$ pole
sup(n)	Super pole
suz(n)	Super zero
$P_k(n,q^{-1})$	$k-th$ Predictor filter
$\tilde{sr}_k$ $k-th$	Real valued semiresidual component
$\mathbf{c}_k(n)$	Coefficients of the $k-th$ section
$\theta_k(m)$	Parameters of the $k-th$ zero
μ_θ	Inverse of inertia
$\bar{\tilde{sr}}_k$	$k-th$ Normalised real valued semiresidual component
$J^t_{\bar{a}_k/\theta_k}$	Jacobian of transformation ($k-th$ section).
$\vec{U}(\cdot)$	Unitary vector
zv	Zero estimation error
ωv	Frequency estimation error
ρv	Damping factor estimation error

Notch filter

$N_k(n,q^{-1})$	Notch filter
$NC(n,q^{-1})$	Cascade of notch filters

Array of sensors

$X(m,t)$	Output of the $m-th$ element of the array
$A(t)$	Amplitude of the signal
Ω_c	Carrier frequency
$\omega(t)$	Electrical angle (intersensor shift)
$\theta(t)$	Angle of arrival
λ	Wavelength
d	Intersensor distance
$x(m,n)$	Sampled complex baseband signal from the $m-th$ element of the array
$a(n)$	Sampled amplitude of the signal
$\eta(m,n)$	$m-th$ sensor noise
$\omega(n)$	Electrical angle (intersensor shift) in discrete time
$\theta(n)$	Angle of arrival in discrete time
σ^2	Noise power
$\mathbf{x}(n)$	Vector of samples
$\mathbf{a}(n)$	Vector of amplitudes
$\vec{\eta}(n)$	Noise vector
$\mathbf{B}(n)$	Direction matrix
$\mathbf{x}$	Vector of array output
$\mathbf{b}_l(n)$	$l-th$ direction vector
$\mathbf{R_x}$	Autocorrelation matrix of the array output
$\mathbf{R_s}$	Signal autocorrelation matrix
$\mathbf{V_s}$	Matrix of signal eigenvectors
$PD[exp(j\Omega)]$	Pseudo-spectral function
$C(q^{-1})$	Spatial filter
$c(k)$	$k-th$ Coefficients of the spatial filter
$\bar{c}(k)$	$k-th$ Normalised coefficients of the spatial filter
$\bar{\mathbf{c}}$	Normalised vector of coefficients of the spatial filter
$V_i(q^{-1})$	$i-th$ Spatial eigenfilter
$v(k)$	$k-th$ Paramters of the spatial eigenfilter
$\mathbf{v}$	Vector of coefficients of the spatial eigen-filter
z_l	$l-th$ Zero of the spatial filter

Adaptive zeros: spatial domain

ξ	Mean square error
$\mathbf{wtot}$	Total spatial filter
$\mathbf{w}_l$	$l-th$ section of the spatial filter
$\prod(*)$	Multiple convolutions operation
$\mathbf{Q}$	Correlation of two spatially shifted output vectors $\mathbf{x}(m)$ and $\mathbf{x}(m-1)$
int_l	$l-th$ Interference
$\mathbf{int}_l$	$l-th$ vector of interferences
P_l	Power of the $l-th$ signal.

Chapter 1
Introduction

1.1 Motivation

The research work described in this thesis was motivated by the desire to find an adaptive signal processing technique to measure the instantaneous frequencies of multiple non-stationary sinusoidal signals. This desire was driven by the necessity for an appropriate technique to measure the format frequency trajectories of speech resonances. These resonances are known to convey important phonetic information and measuring their frequencies has been the subject of many past and present research efforts.

After a solution to the problem of tracking multiple frequencies in the spatial domain was proposed (as summarised in Chapter 4), the idea of measuring the frequencies of superimposed exponentials was extended to the spatial domain. This extension was motivated by the success of the proposed solution in the temporal domain.

1.2 Original Contribution

Although the analysis of multiple exponential signals with time-varying characteristics has been subject of research in the past and the use of adaptive filters in the analysis of non-stationary signals is not new, explicit signal decomposition in conjunction with direct adaptive estimation of instantaneous frequency is introduced for first time in the area of signal processing with the research work described here. A contribution can be found in a better understanding of the applicability of adaptive filtering techniques to the analysis of non-stationary multiple exponential signals.

The first part of the research work has been oriented towards the development of an efficient technique to extract information from voiced segments of speech. Specifically, the task of tracking formant frequencies which has been of great interests to researchers in the field of speech processing. The second part focuses on the field of spatial processing applications.

Examples are presented by simulating discrete samples from the output of an array of sensors (antennas) with potential application in the development of radar surveillance systems.

1.3 Thesis organisation

The key work reported in the thesis can be divided in two main areas: The first part comprising chapters 2, 3 and 4 is focused on the analysis of non-stationary sinusoids oriented towards the task of tracking formant frequencies in voiced segments of speech: the second part (chapter 5) focuses on the analysis of complex exponentials obtained form the discrete spatial sampling of planar waves relying on the use on a linear array of sensors. The final aim in the second part is to track the directions at which the waves impinge on the array.

In Chapter 2, the concept of non-stationary exponential signals is defined in conjunction with a review of some of the many discrete-time signal processing techniques that have been used in the past to analyse this kind of signals. The techniques reviewed include:

- the Hilbert transform;
- energy Operators[8] [9] [10];
- time-localised linear prediction [15];
- time-dependent autoregressive modelling and difference equation representation [16] [17] [18] [19] [22];
- time-frequency representations [29].

This chapter is concluded with an overview of some of the potential areas where the multicomponent exponential model could be used including the area of speech processing where the task of *formant tracking* with its many practical applications has driven researchers to explore different approaches in recent years.

In Chapter 3, a detailed review is made of the theory of adaptive digital filters describing the different techniques that have been used in the task of analysing non-stationary exponential signals. Different structures, accompanied by their respective techniques are described including the cascade structure with its application in the analysis of speech signals.

In Chapter 4, the concepts which constitute the heart of this thesis are presented using an appropriate mathematical framework. There, a gradient-based technique is developed and analysed to directly adapt the phase of the zeros of a filter to enable the tracking of multiple non-stationary frequencies. Examples of the performance of the proposed approach are given in the task of tracking the instantaneous frequency of multiple non-stationary real-valued synthetic sinusoids as well as in tracking formant trajectories in a voiced segment of speech. After the non-stationary frequencies have been estimated a cascade of notch filters is used to isolate a given sinusoidal component before a two-sampled-based algorithm is used to estimate its instantaneous amplitude.

In Chapter 5, a review of the concepts of spatial frequency estimation using arrays of sensors is presented. For the problem of non-stationary waves, three approaches for tracking the angles of arrival were presented. These approaches have been grouped under the three general classes:

- adaptive subspace techniques [81] [82] [83];
- direct recursive update of the angles estimates [84] [85];
- adaptive null-steering [90] [89] [91] [92].

These illustrate the common goal of providing a way to recursively adapt the parameters of spatial filters to "track" information in non-stationary scenarios. This is followed with a description of a technique based on the ideas of directional signal separation and direct parameter estimation. The problem concentrated on is tracking the direction of arrival of rapidly moving non-stationary sources using relatively large arrays of sensors.

Chapter 6 concludes the thesis with a summary of the thesis, a description of key contributions and suggestions for potential future directions of research.

Chapter 2
Analysis of non-stationary multi-component exponential signals: Time-domain case

In this chapter, a brief review of some of the many techniques that have been used to extract information form non-stationary multicomponent exponential (NSME) signals is presented. This review is made to provide the basis for the direct estimation approach that constitute the central idea of this thesis. As a result , only research work closely related to the main idea are included.

Adaptive techniques, providing the final connection of past research work with the approach summarised here, have been left to the third chapter where they are explained with more detail.

2.1 Definition of non-stationary multicomponent exponential signals

A single component time-varying complex exponential signal (cisoid) can be defined as:

$$s(t) = a(t)\ \exp(j\phi(t)) \tag{2.1}$$

where $a(t)$ represents the ***instantaneous amplitude*** and $\phi(t)$ the ***instantaneous phase*** of the signal. The real-valued equivalent of this signal is given by a sinusoidal signal:

$$s(t) = a(t)\ \cos(\phi(t)). \tag{2.2}$$

For these signals, we can define their ***instantaneous frequency*** $\omega(t)$ as the derivative of the phase :

$$\omega(t) = \frac{d\phi(t)}{dt}. \tag{2.3}$$

These concepts can be extended to the case of multicomponent non-stationary exponential signals which can be defined as:

$$s(t) = \sum_{l=1}^{L} a_l(t)\ \exp(j\phi_l(t)) \tag{2.4}$$

in the *complex signal* case, and

$$s(t) = \sum_{l=1}^{L} a_l(t)\ \cos(\phi_l(t)) \tag{2.5}$$

in the *real-valued signal* case.

Whether these are models of real-world signals or they are the actual representations of man-made signals, there is a need to devise signal processing techniques to estimate the instantaneous parameters of the representation from noisy measurements of the signal.

2.2 The analytic signal

In order to be analysed using discrete-time processors, the above mentioned signals need to be sampled. From these samples, their instantaneous amplitude and fequency can be estimated as:

$$\hat{a}(n) = \sqrt{Re[s(n)]^2 + Im[s(n)]^2} \tag{2.6}$$

$$\hat{\phi}(n) = \arctan(\frac{Im[s(n)]}{Re[s(n)]}) \tag{2.7}$$

where n represents the discrete time index.

An instantaneous frequency estimate can obtained form the phase estimates by performing the phase differencing operation in discrete-time [26]:

$$\hat{\omega}_f(n) = (\hat{\phi}(n+1) - \hat{\phi}(n)) \tag{2.8}$$

$$\hat{\omega}_b(n) = (\hat{\phi}(n) - \hat{\phi}(n-1)) \tag{2.9}$$

$$\hat{\omega}_c(n) = (\hat{\phi}(n+1) - \hat{\phi}(n-1)) \tag{2.10}$$

where the sub-indexes f, b and c stand for forward, backward and central finite differences. The lack of a similar method to estimate the instantaneous parameters $a(n)$ and $\phi(n)$ from real-valued mono-component signals motivated the search for techniques to perform real-to-complex transformation. Gabor [4] proposed a transformation based on the suppression of all the negative frequency components of the signal to create the ***analytical signal***.

In the frequency domain we can define the analytical signal of $s(n)$ as:

$$\hat{S}_a(\Omega) = \begin{cases} 2\hat{S}(\Omega) & \text{if } \Omega \geq 0 \\ 0 & \text{if } \Omega < 0 \end{cases} \tag{2.11}$$

where $\hat{S}(\Omega)$ represents the Fourier transform of $s(n)$. The resulting complex signal is expressed as :

$$s_a(n) = a(n)\exp(j\phi(n)), \tag{2.12}$$

from which $s(n)$ will be given by:

$$s(n) = \text{Re}[s_a(n)] = a(n)\cos\phi(n). \tag{2.13}$$

As a result of this transformation, $a(n)$ and $\phi(n)$ (known as the analytic instantaneous amplitude and phase) are uniquely defined.

A related way to define the *analytical signal* in the time domain is by using the ***Hilbert transform*** which in continuous time can be defined as:

$$s_h(t) = H(s(t)) = s(t) * \frac{1}{\pi t} = \frac{1}{\pi}\int_{-\infty}^{\infty} \frac{s(t)}{t-u} d(u) \tag{2.14}$$

which can be expressed in the frequency-domain as:

$$S_h(\Omega) = H(\Omega)S(\Omega) \tag{2.15}$$

where

$$H(\Omega) = -j\ \text{sgn}(\Omega). \tag{2.16}$$

The *analytic signal* will then be given by:

$$s_a(t) = s(t) + j s_h(t). \tag{2.17}$$

For discrete-time signals $s(n)$ their *Hilbert transform* can be defined in the time domain as the convolution of $s(n)$ with a *Hilbert filter*:

$$s_h(n) = s(n) * h(n), \tag{2.18}$$

where $h(n)$ is an infinite impulse response (IIR) filter defined by:

$$h(n) = \begin{cases} \frac{2}{\pi}\frac{sin^2(\pi n/2)}{n} & n \neq 0, \\ 0 & n = 0. \end{cases} \tag{2.19}$$

In practice this IIR filter can be approximated by a finite impulse response filter (FIR) [5].

The *Hilbert-transformed* signal can be used to obtain the instantaneous amplitude and frequency estimates according to the following expressions:

$$\hat{a}(n) = \sqrt{s^2(n) + s_h^2(n)} \tag{2.20}$$

$$\hat{\phi}(n) = \arctan(\frac{s_h(n)}{s(n)}). \tag{2.21}$$

From the instantaneous phase $\hat{\phi}(n)$ we can get the instantaneous frequency estimate by differentiation (forward, backward or symmetric) in discrete time.

2.3 Teager-Kaiser energy operators for instantaneous amplitude envelope a frequency separation.

Another way to estimate the instantaneous amplitude envelope and frequency of sinusoidal signals is by using ***energy operators*** which can be defined as:

$$\Psi_c[s(t)] = s(t)^2 - s(t)\ddot{s}(t), \tag{2.22}$$

for continuous-time signals $s(t)$ with $\dot{s}(t) = ds/dt$ and as:

$$\Psi_d[s(n)] = \dot{s}(n)^2 - s(n-1)s(n+1), \tag{2.23}$$

for discrete-time signals $s(n)$.

These operators, first proposed by Teager and subsequently studied by Kaiser [8] [9], provide a way to obtain estimates of the squared product amplitude-frequency of sinusoidal signals. These ideas are briefly explained bellow.

An energy operator Ψ_c applied to a sinusoid $s(t) = A\cos(\omega(t) + \theta)$, can be used to obtain an estimate of the squared product amplitude-frequency [13]:

$$\Psi_c[A\cos(\omega_c t + \theta)] = (A\omega_c)^2 \tag{2.24}$$

for any constants A and ω_c.

The reason way this operator has been denominated *energy operator* is because if the signal $s(t)$ is used to represent the displacement produced by a mass-spring linear oscillator, the squared product amplitude frequency will equal the total energy (per half-unit mass) of the oscillator. These ideas have been extended to the analysis of sinusoidal signals with time-varying amplitude envelope and frequency in [10] where it was shown that for a sampled sinusoid $s(n) = a(n)\cos(\phi(n))$, the energy operator provides an instantaneous estimate of the square product amplitude-frequency:

$$\Psi_d[s(n)] \cong (a(n)\omega(n))^2. \tag{2.25}$$

This allows the estimation of one of the instantaneous parameters ($a(n)$ or $\omega(n)$) when the other is constant by a simple scaling of $\sqrt{\Psi[s(n)]}$. When both amplitude and frequency modulations are present, several algorithms proposed in [10] provide separate estimates of $a(n)$ and $\omega(n)$. These algorithms were denominated energy separation algorithms (DESA) and we cite here one of them (DESA1) for the purpose of illustration.

For a sinusoidal signal $s(n)$ whose first difference is defined as:

$$s_{1d}(n) = s(n) - s(n-1), \tag{2.26}$$

the DESA1 algorithm give estimates of the signals instantaneous amplitude and frequency:

$$\hat{\omega}(n) = \arccos(1 - \frac{\Psi[s_{1d}(n)] + \Psi[s_{1d}(n+1)]}{4\Psi[s(n)]}), \tag{2.27}$$

$$|\hat{a}(n)| = \sqrt{\frac{\Psi[s(n)]}{1 - (1 - \frac{\Psi[s_{1d}(n)]+\Psi[s_{1d}(n+1)]}{4\Psi[s(n)]})^2}} \tag{2.28}$$

for $0 \leq \omega(n) \leq \pi$.

This approach has been used to model speech resonances in [11] where in order to face the multicomponent nature of speech, resonances were isolated using band-pass filtering relying on Gabor filters [4].

2.4 Instantaneous frequency estimation using time-localised linear prediction

Another computationally efficient approach proposed in [15] to estimate an unknown mono-component signal's instantaneous frequency consists of computing the coefficients of a second-order predictor filter from a small number of samples. Once that the predictor filter coefficients have been estimated, the frequency estimate is obtained by evaluating the roots of the predictor polynomial. This approach yields an accurate estimate of the frequency for real-valued signals in high SNR environments.

For a signal modelled as:

$$s(n) = A\rho^n \cos(\omega(n)n + \theta), \tag{2.29}$$

where A represents the amplitude of the signal and ρ its damping factor; the second order error predictor filter can be defined as :

$$e(n) = s(n) - c_1 s(n-1) - c_2 s(n-2) \tag{2.30}$$

$$= s(n)(1 - c_1 q^{-1} + c_2 q^{-2}), \tag{2.31}$$

where q^{-1} represents the delay operator.

The two coefficients c_1 and c_2 can be computed by using a modified covariance method [15] :

$$\begin{bmatrix} r_{1,1} & r_{1,2} \\ r_{2,1} & r_{2,2} \end{bmatrix} \begin{bmatrix} c_1 \\ c_2 \end{bmatrix} = - \begin{bmatrix} r_{1,0} \\ r_{2,0} \end{bmatrix}$$

where the correlation estimates are computed from N data samples as:

$$r_{j,k} = \frac{1}{2(N-2)} \left(\sum_{n=2}^{N-1} s(n-j)s(n-k) + \sum_{n=2}^{N-3} s(n-j)s(n-k) \right).$$

An estimate of the unknown signal's instantaneous frequency is then obtained from the root of the predictor polynomial $(1 - c_1 q^{-1} + c_2 q^{-2})$ yielding:

$$\hat{\omega}_{LP} \approx \arccos\left(\frac{-c_1}{2\sqrt{c_2}}\right). \tag{2.32}$$

Using four and five data samples to obtain a highly time-localised frequency estimate, equation (2.32) has been shown to yield [15] :

$$\hat{\omega}_{LP4}(n) \approx \arccos\left(\frac{s(n-2)s(n-1) + 2s(n-1)s(n) + s(n)s(n+1)}{2(s(n-1)^2 + s(n)^2)} \right) \tag{2.33}$$

$$\hat{\omega}_{LP5}(n) \approx \arccos\left(\frac{s(n-2)s(n-1) + 2s(n-1)s(n) + 2s(n)s(n+1) + s(n+1)s(n+2)}{2(s(n-1)^2 + s(n)^2 + s(n+1)^2)} \right). \tag{2.34}$$

Using Prony's method instead of the covariance method, the frequency estimate has been found to be :

$$\hat{\omega}_{P4}(n) \approx \frac{\Upsilon(s(n))}{\Psi(s(n-1) + \Psi(s_n))} \tag{2.35}$$

where

$$\Psi(s(n)) \equiv s(n)^2 - s(n-1)s(n+1)$$

is the energy operator (2.23), and

$$\Upsilon(s(n)) \equiv s(n-1)s(n) - s(n-2)s(n+1)$$

a new operator. This technique has been compared with discrete energy operators in the task of estimating instantaneous frequency of amplitude and frequency modulated sinusoids showing that it constitutes a more efficient algorithm in terms of computational complexity while providing similar estimation performance.

2.5 Time-dependent autoregressive modelling and difference equation representation of chirp signals

Time-dependent autoregressive models have been used in the past to analyse non-stationary signals (e.g. [16] [17] [18] [19]). In this approach, the time-dependent parameters of the model are expressed as linear combinations of basic functions to allow their estimation by solving a set of linear equations. Recently, this approach has been used to estimate the instantaneous parameters of signals consisting of one sinusoid [21] or several superimposed sinusoids [22] with time varying amplitudes and frequencies . This is achieved by using a second stage once the time-dependent parameters have been estimated. These ideas are briefly introduced next.

Consider a time-dependent autoregressive (TDAR) process given by:

$$s(n) + \sum_{k=1}^{K} c_k(n)s(n-k) = w(n) \tag{2.36}$$

where $c_k(n)$ represent the time-dependent autoregressive parameters, $w(n)$ a zero mean decorrelated input and $s(n)$ the output signal.

When this model is used to represent non-stationary sinusoids at high signal-to-noise ratios, equation (2.36) can be simplified as a time-dependent difference equation equation of the form [22]:

$$s(n) = \sum_{k=1}^{K} c_k(n)s(n-k) \tag{2.37}$$

where the time-dependent parameters parameters $c_k(n)$ can be estimated by expanding them

with some known functions $\beta_i(n)$:

$$c_k(n) = \sum_{i=0}^{P-1} c_{ki}\beta_i(n), \tag{2.38}$$

assuming that the parameters vary slowly in the analysis interval.

Substituting (2.38) into (2.37) we get:

$$s(n) = \sum_{k=1}^{K}\sum_{i=0}^{P-1} c_{ki}\beta_i(n)s(n-k) \tag{2.39}$$

and the resulting time-independent coefficients c_{ki} can be obtained by solving a set of linear equations [16] [17] [18] [23]:

$$\mathbf{Rc} = \mathbf{r}, \tag{2.40}$$

where the elements of $\mathbf{R}$ and $\mathbf{r}$ are given by:

$$\mathbf{R}_{u,v} = \sum_n \beta_i(n)\beta_j^*(n)s(n-k)s^*(n-l) \tag{2.41}$$

$$\mathbf{r}_{u,l} = \sum_n \beta_j(n)s(n)s^*(n-l) \tag{2.42}$$

for $u = (l-1)P + j$ and $v = (k-1)P + i$.

Once the time-dependent autoregressive parameters have been estimated, a second stage will be needed to obtain instantaneous amplitude and frequency estimates from sampled amplitude and frequency modulated sinusoids by extracting the time-varying roots of the difference equation.

This approach was used in [22] in conjunction with skew-shift operators [24] [25] to estimate the instantaneous amplitude and frequency of superimposed real-valued chirps. In [21], this approach has been used to estimate instantaneous amplitude envelope and frequency of modulated sinusoids and a classification of non-stationary signals was introduced as a function of the movement of the time-varying poles of their associated first order autoregressive model.

This classification can be obtained by expressing the differential equation used to model a

sinusoid as:

$$s(n) = p(n)s(n-1), \tag{2.43}$$

then different kind of non-stationary signals can be studied and grouped according to the movement of the pole $p(n)$ in the *z-plane* [21]. The resulting models are explained below.

2.5.1 Damped sinusoidal model

For a complex-valued damped sinusoid of the form:

$$s(n) = \rho^n \exp(j\omega_c n), \;\; \rho < 1 \tag{2.44}$$

the ratio of two successive samples or instantaneous pole will be given by:

$$p(n) = \frac{s(n)}{s(n-1)} = \rho \exp(j\omega_c). \tag{2.45}$$

2.5.2 Amplitude modulated sinusoidal model

For a complex-valued damped sinusoid with amplitude modulated with a discrete-time real-valued signal $u_1(n)$:

$$s(n) = u_1(n) \exp(j\omega_c n) \tag{2.46}$$

the ratio of two successive samples or instantaneous pole will be given by:

$$p(n) = \frac{s(n)}{s(n-1)} = \frac{u_1(n)}{u_1(n-1)} \exp(j\omega_c). \tag{2.47}$$

In this case it is worth noting that the time-varying part of the pole $p(n)$ is real, which results in a time variation of the magnitude of the pole while its angle remains constant.

2.5.3 Frequency modulated sinusoidal model

For a complex-valued damped sinusoid with frequency modulated with a discrete-time real-valued signal $u_2(n)$:

$$s(n) = A\exp(j(\omega_c n + \alpha u_2(n))), \tag{2.48}$$

the ratio of two successive samples or instantaneous pole will be given by:

$$p(n) = \frac{s(n)}{s(n-1)} = \exp(j\omega_c + \alpha \dot{u}_2(n)), \tag{2.49}$$

where $\dot{u}_2(n)$ is the first other backward difference of $u_2(n)$. In this case it is worth noting that the time-varying part of the pole $p(n)$ is complex, which results in a time variation of the angle of the pole while its amplitude remains constant.

2.5.4 Amplitude and frequency modulated sinusoidal model

In the case of a complex-valued damped sinusoid with amplitude and frequency modulated with discrete-time real-valued signals $u_1(n)$ and $u_2(n)$:

$$s(n) = u_1(n)\exp(j(\omega_c n + \alpha u_2(n))), \tag{2.50}$$

the ratio of two successive samples or instantaneous pole will be given by:

$$p(n) = \frac{s(n)}{s(n-1)} = \frac{u_1(n)}{u_1(n-1)}\exp(j\omega_c + \alpha \dot{u}_2(n)) \tag{2.51}$$

where $\dot{u}_2(n)$ is the first other backward difference of $u_2(n)$. In this case it is worth noting that the time-varying part of the pole $p(n)$ is complex, which results in a time variation of the angle of the pole while its amplitude remains constant.

2.6 Time frequency representations

Time-frequency representations allow displaying the energy distribution of non-stationary signals in the *time-frequency plane*. As will be explained in the following, time-frequency representations provide an indirect mean to extract information from time-varying exponential signals

with a limited practical applicability that can be attributed to its high computational complexity, limited resolution and the appearance of spurious components in some of the representations types.

Once a representation of a multicomponent signal has been obtained in the *time-frequency plane*, the instantaneous frequencies of each exponential component can be obtained by determining local maxima (picking the peaks) in the representation. A detailed review of this approach was presented in [26], [27].

2.6.1 Short Time Fourier Transform

The Fourier transform can be used to analyse non-stationary signals by decomposing them into segments where its characteristics are considered to be stationary. This results in the *short-time Fourier transform* (STFT) [28]:

$$F_s(t,\Omega) = \int_{-\infty}^{+\infty} s(t)h(u-t)e^{-j\Omega u}du \tag{2.52}$$

where $h(t)$ represents the window introduced to obtain time-localised spectral estimates. The time resolution of the STFT is determined by the duration of the window $h(t)$ while its frequency resolution is proportional to the bandwidth of the window. Increasing the resolution in the time domain would imply decreasing the duration of the window while increasing frequency resolution would imply decreasing its duration. This trade-off implies that no infinite resolution can be obtained simultaneously in both domains.

The STFT belongs to a class of representations known as linear time-frequency representations which include the Gabor and Wavelet transform [28].

The discrete-time discrete-frequency STFT can be expressed taking into account sampling considerations [28] as:

$$F_s(n,m) = \sum_k s(t)h(n-k)e^{-j2\pi mk} \quad for \quad \frac{-1}{2} \leq m \leq \frac{1}{2} \tag{2.53}$$

where $n \in \mathcal{N}$.

The squared magnitude of the STFT is known as the *spectrogram*:

$$|F_s(t,\Omega)|^2 = |\int_{-\infty}^{+\infty} s(t)h(u-t)e^{-j\Omega u}du|^2 \tag{2.54}$$

which measures the energy of the signal around the point (t,ω). And the discrete time discrete frequency squared magnitude of the STFT will the be defined by:

$$F_s(n,m) = |\sum_k s(t)h(n-k)e^{-j2\pi mk}|^2 \quad for \quad \frac{-1}{2} \leq m \leq \frac{1}{2}, \tag{2.55}$$

where $n \in \mathcal{N}$.

Although not complying with some of their desired properties, the *spectrogram* belongs to a class of quadratic time-frequency representations known as time-frequency energy distributions that will be reviewed in the next section.

When used to analyse non-stationary exponential signals, the *ridges* of the *spectrogram* provide estimates of the instantaneous frequency trajectories of the components of the signal. This technique constitutes an indirect and computationally expensive approach to obtaining instantaneous frequency estimates that is also affected by the limited resolution achievable with the *spectrogram.*

2.6.2 Time frequency distributions

The purpose of these distributions is to provide an expression of the energy of the signal as a function of time and frequency. The total summation in time and frequency of a joint time and frequency density $P_s(t,\omega)$ would provide the total energy of the signal:

$$E = \int_{-\infty}^{\infty}\int_{-\infty}^{\infty} P_s(t,\Omega)dt\, d\Omega \tag{2.56}$$

which is known as the energy conservation property. Also the temporal $|s(t)|^2$ and $|S(\omega)|^2$ spectral densities should be derived from the joint density as:

$$|s(t)|^2 = \int_{-\infty}^{\infty} P_s(t,\Omega)d\Omega. \tag{2.57}$$

$$|S(\Omega)|^2 = \int_{-\infty}^{\infty} P_s(t,\Omega)dt \tag{2.58}$$

which are known as the marginal properties.

Two other important properties satisfied by some TFD's are *invariance by translation in time and frequency* which means that a translation of the signal in time and frequency (frequency modulation) should be reflected as the translation of the signal's distribution with equal amounts in the time-frequency plane [29]. Time-frequency representations satisfying this property can be grouped under the ***Cohen's Class*** [29] which will be defined by exploiting the concept of the ***local autocorrelation function*** (LAF).

The LAF of a signal $s(t)$ can be defined as [30]:

$$R(t,\tau) = s(t+\tau/2)s^*(t-\tau/2). \tag{2.59}$$

This function can be filtered in time and frequency by convolving it with a "kernel" function $\kappa(t,\tau)$ to obtain a ***generalised local autocorrelation function*** (GLAF) :

$$GR(t,\tau) = \kappa(t,\tau) * R(t,\tau). \tag{2.60}$$

where $\kappa(t,\tau)$ is the time-lag expression of the kernel that can be obtained as the inverse Fourier transform of the frequency-lag expression $\zeta(\omega,\tau)$:

$$\kappa(t,\tau) = \frac{1}{2\pi}\int_{-\infty}^{+\infty} \zeta(\Omega,\tau)e^{\Omega t}d\Omega. \tag{2.61}$$

Finally the ***Cohen's Class*** of TFD's can be defined as the Fourier transform of the GLAF :

$$P_c(t,\Omega) = \int_{-\infty}^{+\infty} GR(t,\tau)e^{-j\Omega\tau}d\tau. \tag{2.62}$$

Two distributions belonging to this class are the Wigner-Ville [31] (WV) and the Choi-Williams [32] distributions whose kernels are given by:

$$\zeta_{wv}(\Omega,\tau) = 1 \tag{2.63}$$

for the Wigner-Ville distribution, and

$$\zeta_{cw}(\Omega,\tau) = e^{-\Omega^2\tau^2/\sigma}; \tag{2.64}$$

for the Choi-Williams distribution.

The WV distribution was formulated in [31] in the context of quantum mechanics and re-introduced by Ville [33], motivated by the desire to perform instantaneous frequency measurements. The first moment of this distribution provides the instantaneous frequency of a mono-component signal [28]:

$$\hat{\omega}(t) = \frac{\int_{-\infty}^{+\infty} \Omega P_{wv}(t,\Omega)d\Omega}{\int_{-\infty}^{+\infty} P_{wv}(t,\Omega)d\Omega}. \tag{2.65}$$

Given its quadratic nature the WV distribution leads to the appearance of spurious peaks in the distribution when multicomponent signals are analysed [29]. This fact motivated the work of Choi and Williams [32] to devise a representation with reduced spurious peaks by convolving the *local autocorrelation function* with a Gaussian kernel.

These time-frequency distributions can be used to analyse multicomponent exponential signals showing a higher concentration of energy along the instantaneous frequency of each component of the signal when compared with the *spectrogram*. They can be used to obtain instantaneous frequency estimates from the peaks of the representations but still constitute an indirect and computationally complex way to perform instantaneous frequency measurements.

As an illustrative example, several time-frequency representations are presented for a signal composed of two superimposed chirps (Fig. 2.1). These representations are: the spectrogram (Fig. 2.2), Wigner-Ville (Fig. 2.3) and Choi-Williams (Fig. 2.3) distributions. It can be observed in these figures that the WV distribution presents an increased resolution in comparison with the Spectrogram but this improvement is obscured with the appearance of spurious cross terms.

Finally, the CW distribution which is equivalent to the WV distribution convolved in time and frequency with a Gaussian kernel, shows a representation with degraded resolution compared to the WD distribution.

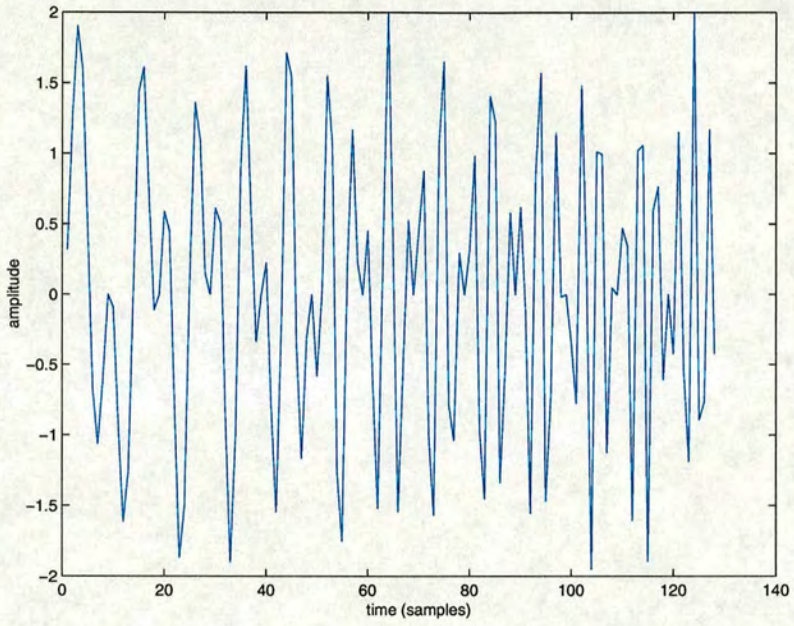

Figure 2.1: *Two superimposed chirps with linearly increasing frequency.*

Taking into account important sampling considerations [28] to avoid aliasing in the frequency domain, the ***Cohen class*** can be expressed in discrete time as:

$$P(n,\Omega) = \sum_{l=-L/2}^{L/2} GR(n,l)e^{-j\Omega l}, \tag{2.66}$$

$$GR(n,l) = \sum_{m=-L/2}^{L/2} \kappa(n-m,l)s(m+l)s^*(m-l), \tag{2.67}$$

where l represents the lag with maximum value L.

For the discrete-time Wigner-Ville distribution, the kernel will be defined as :

$$\kappa_{wv}(n,l) = \delta(n),$$

whereas for discrete-tine Choi-Williams distribution, will be:

$$\kappa(n,l)_{cw} = (1/\sqrt{4\pi l^2/\sigma}) \exp(-n^2/(4l^2/\sigma)),$$

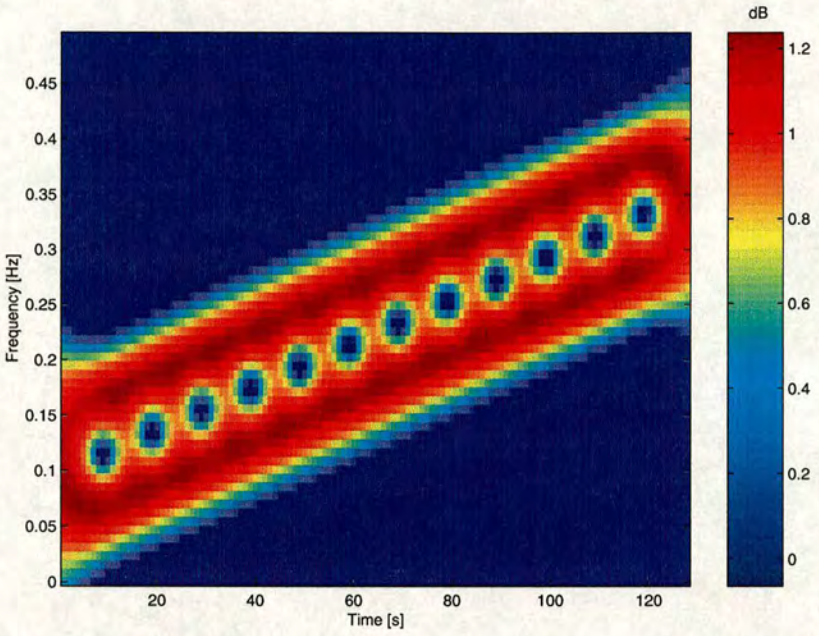

Figure 2.2: *Spectrogram of two superimposed chirps with linearly increasing frequency .*

2.7 Other approaches to the analysis of non-stationary multi-component signals

In the folowing, two other approaches which nave been used to analyse NSME signals are briefly described.

Residual signal analysis

This technique is based on signal decomposition and parameter tracking [36]. A given component is isolated by subtracting the rest of the components. Then the isolated signal is analysed with a "tracker". This technique has been reintroduced recently in [38] [39].

Signal Transduction

Motivated by the possibility that the human auditory system exploits FM-to-AM transduction using the spectral shapes of auditory filters, some researchers have proposed an approach to AM-FM estimation of a single-component sinusoidal signals using discrete-time filters with a non-flat frequency response. When the FM signal passes through the filter, the instantaneous frequency of the signal moves across the filter's non-flat passband and a change in the output amplitude envelope occurs. The modulated amplitude and frequency of a single component

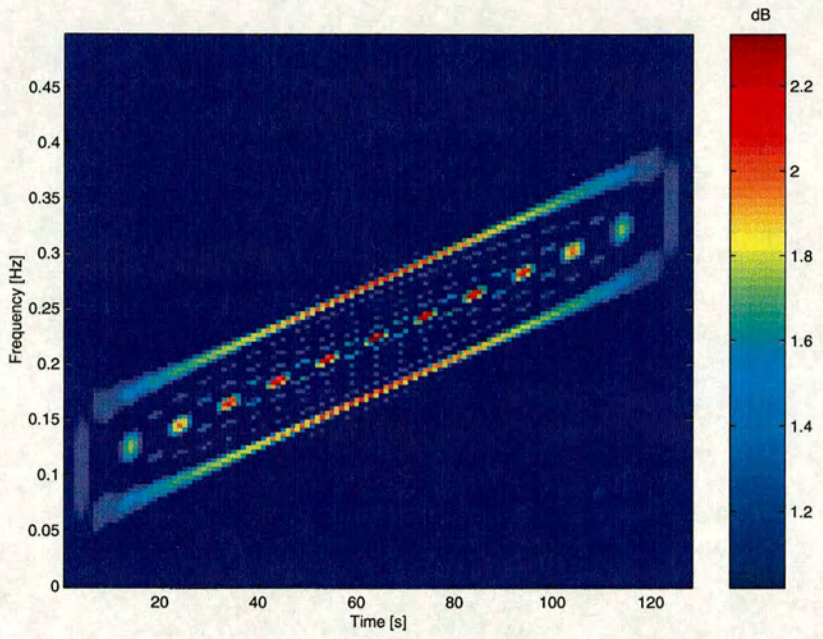

Figure 2.3: *Wigner-Ville distribution of two superimposed chirps with linearly increasing frequency.*

sinusoidal signal can be estimated by using two overlapping transduction filters and processing the amplitude envelopes of the filter outputs [40]. This approach has been further generalised to signals that consist of two AM-FM sinusoids in [42].

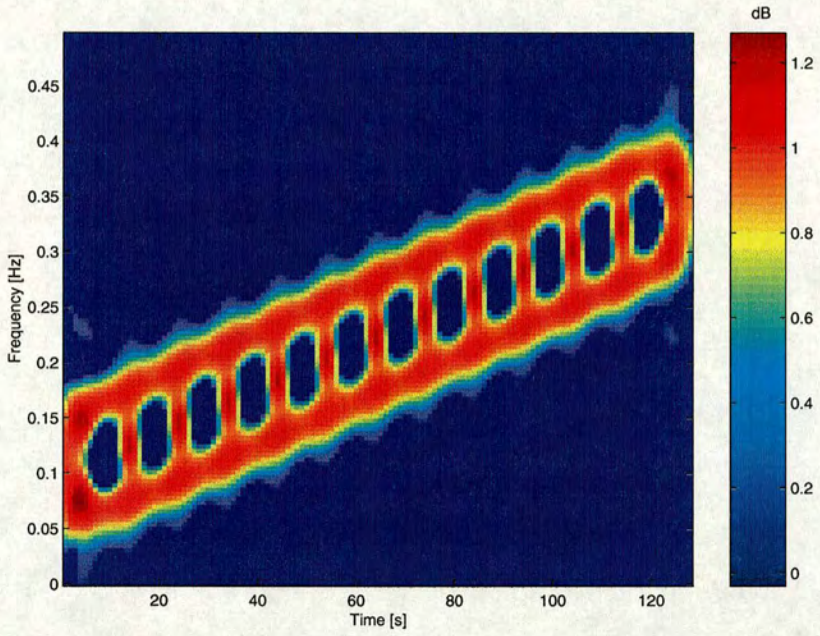

Figure 2.4: *Choi-Williams distributions of two superimposed chirps with linearly increasing frequency .*

2.8 Applications

2.8.1 Analysis of communication signals

Sinusoidal signals are used as conveyers of information in communication systems by modulating the sinusoid's amplitude and frequency with *information signals* [47] [48]. These ideas, introduced in the research works of Carson [49], Vander Pol [50] and Armstrong [51], are still being used in the development of of current communication systems.

With the advent of discrete-time signal processors which have recently been incorporated into these systems, it is necessary to develop new discrete-time techniques to extract information (demodulate) single and multiple sinusoidal carriers of information as substitutes to previous analog techniques such as those relying on phase locked loops (PLL's) [48].

2.8.2 Analysis of speech and music

Traditionally the speech production system has been modelled as a linear time-invariant (LTI) filter excited by periodic or random excitations depending on whether modelling voiced or unvoiced utterances [48]. This model is depicted in Fig. 2.5 where the glottal, vocal tract and radiation sections are approximated by discrete time (LTI) filters. In this approach there is an implicit representation of vocal tract resonances (commonly known as ***formants***) in the poles of the filters [48]. Although this model has been successfully used to represent speech utterances and constitutes the basic structure in the design of many schemes for speech coding a synthesis, a more realistic representation should incorporate the time variant features of speech.

As a result of their importance as phonetic features, *formants* have been explicitly used in the development of systems for speech synthesis and recognition, and the necessity to measure these features has motivated the search for appropriate signal processing techniques to perform this task. Despite many efforts made within the speech processing community, measuring *formant* frequencies still constitutes an unsolved problem.

In the discrete models described above, speech resonances are implicitly represented as the impulse response of time-invariant one-pole systems:

$$R_{tin}(n) = a \exp(-\sigma n) \cos(\omega n + \theta), \tag{2.68}$$

where σ and ω represent the damping factor and frequency of the decaying sinusoid and n is the discrete-time index.
These model should be extended to obtain a more realistic representation by making its parameters time-variant:

$$R_{tva}(n) = a(n)\cos(\omega(n)n + \theta), \tag{2.69}$$

where $a(n)$ and $\omega(n)$ represent the instantaneous amplitude and frequency of the resonance model.

This mathematical representation of a speech resonance is implicitly supported in the observations made by Teager [52] indicating rapid changes in the amplitude and frequency of resonances within short period of time in voiced segments of speech. This fact has motivated the search for signal processing techniques to provide instantaneous measurements of amplitude envelope and frequency of single [11] and multiple superimposed sinusoidal signals.

Musical waveforms have also been modelled as superposition of non-stationary sinusoids and techniques relying on time-frequency representations [43] and signal transduction [42] have been used to estimate the parameters of the model.

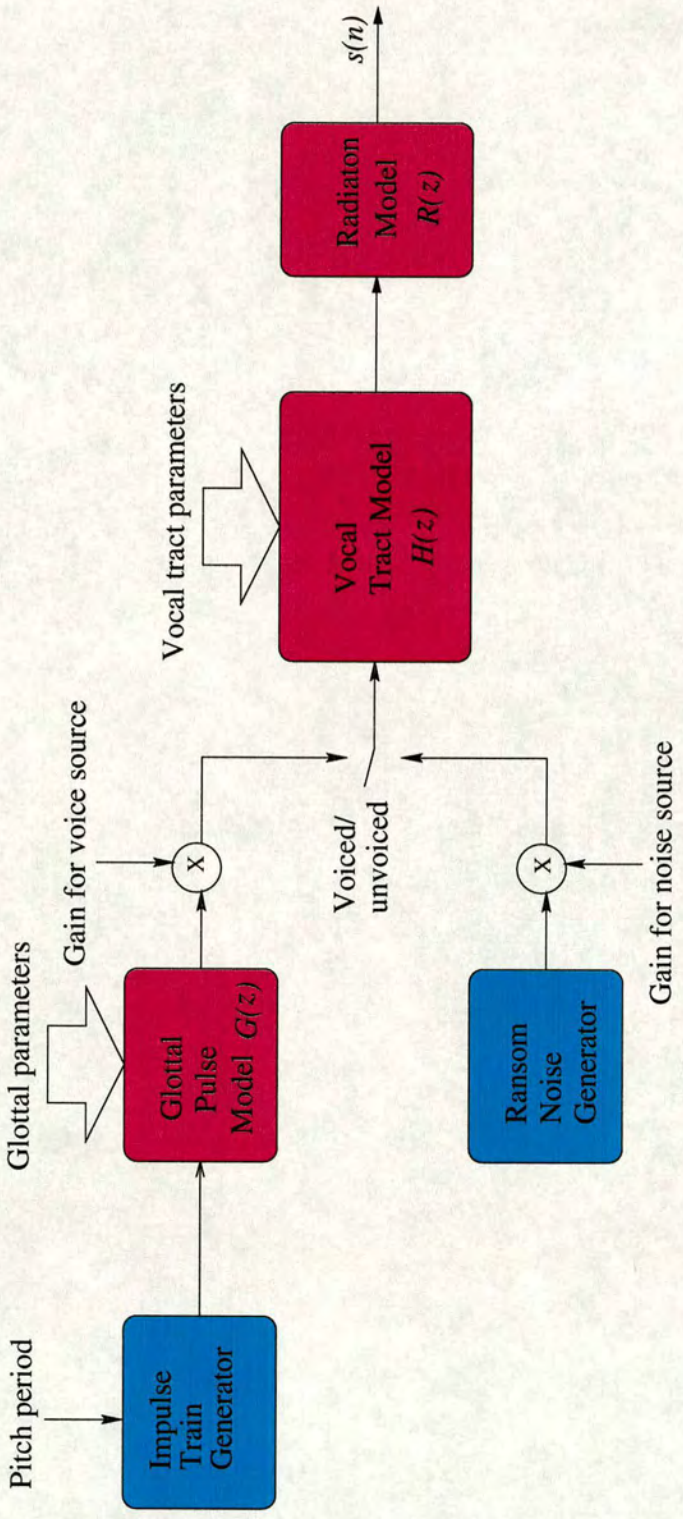

Figure 2.5: *Discrete-time model of the speech production system. After Rabiner and Schafer [1].*

2.9 Summary

In this chapter, non-stationary multicomponent exponential (NSME) signals were defined in conjunction with a brief review of some of the many techniques that have been proposed to extract information from this kind of signals.

While estimates of the parameters of complex mono-component exponential signals can be directly extracted from their discrete-time samples, applying this approach to real-valued exponentials (sinusoids) requires the use of a real-to-complex transformation such as the Hilbert transform. Other techniques that can be used to extract information from non-stationary sinusoidal signals include energy operators and time-localised linear prediction. Extension of these techniques to the analysis of multicomponent signals requires the use of band-pass filtering preprocessing to separate the components.

For the estimation of amplitude and frequency of non-stationary multicomponent signals, several approaches such as time-dependent differential equations and time-frequency representations have been proposed. A brief description of these techniques has also been included in this chapter.

The extraction of information from time-dependent differential equations requires two-steps: first, the parameters of the equation have to be estimated from the non-stationary signal by using a parameter expansion relying on a set of basis functions to transform the nonlinear problem into a linear one; secondly, the parameters of interest have to be estimated by extracting the roots of the differential equation. This technique has recently been successfully used to demodulate amplitude and frequency modulated signals and to separate multicomponent signals into its components [11].

Instantaneous amplitude and frequency estimates for NSME signals can also be obtained from time-frequency representations which allow displaying the energy contents of signals in the *time-frequency plane*. This is also an indirect way to obtain the estimates since a first step must be used to compute the representation while a second step is required to extract the desired parameters from the representations by requiring to moment estimation or peak-picking.

Chapter 3
Adaptive FIR filters to analyse non-stationary multi-component signals

This chapter describes some of the adaptive filtering structures and algorithms that have been used in the past to analyse non-stationary multicomponent exponential signals. This is done with the purpose of introducing the adaptive approach that has been the subject of the research work summarised in this thesis.

Finite impulse response filters (FIR) structured in transversal, lattice and cascade forms have been used in the past to analyse non-stationary multi-component exponential signals (NSME) signals. As the adaptive FIR filtering theory is based on finding the optimal values for the filter parameters, the description of these algorithms is started by describing the closed optimal solution known as Wiener-Hopf equation.

Order-recursive techniques implemented in the form of FIR filters structured in lattice form are also described as a means for obtaining the optimal parameters. Adaptive implementation of these structures which has been used in the past to analyse NSME signals are subsequently described highlighting its use in the analysis of non-stationary multicomponent signals.

Finally adaptive FIR filters structured in cascade form are presented providing the ultimate link with the approach proposed in chapter 4.

3.1 Optimum transversal FIR

The linear estimation technique by which a given signal $d(n)$ is estimated by passing a signal $s(n)$ through a Finite Impulse Response (FIR) filter is shown in figure (3.1). The optimal parameters of this filter can be found as those that minimise the absolute squared differences between $d(n)$ and its estimate $\hat{d}(n)$ at the output of the filter.

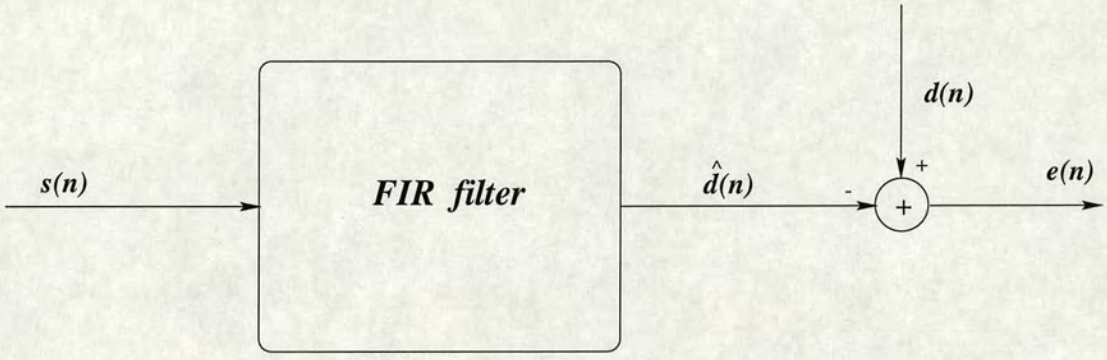

Figure 3.1: *FIR filter for signal estimation.*

If the output of the filter $\hat{d}(n)$ can be found as the convolution of the unit sample response $c(n)$ of the filter with the signal $s(n)$:

$$\hat{d}(n) = s(n) * c(n). \tag{3.1}$$

which can be expressed in vector form for a filter with p weights as:

$$\hat{d}(n) = \mathbf{c}^T \mathbf{s}(n) \tag{3.2}$$

where $\mathbf{s}(n) = [s(n), s(n-1), ..., s(n-p+1)]^T$ and $\mathbf{c} = [c(0), c(1), ..., c(p-1)]^T$.

The optimum FIR filter filter coefficients , $\mathbf{c}$, can be found as those that minimise the summed square errors (SSE):

$$\xi = \sum_n |e(n)|^2 = \sum_n \{e(n)e^*(n)\} \tag{3.3}$$

where $n \in [0, N]$, N being the total number of data samples.

Substituting

$$e(n) = d(n) - \hat{d}(n) = [1 \ -\mathbf{c}^T] \begin{bmatrix} d(n) \\ \mathbf{s}(n) \end{bmatrix} \tag{3.4}$$

in equation (3.3) we obtain an expression of ξ as a function of $\mathbf{c}$:

$$\xi = \sum_n \left\{ \begin{bmatrix} 1 & -\mathbf{c}^T \end{bmatrix} \begin{bmatrix} d(n) \\ \mathbf{s}(n) \end{bmatrix} \begin{bmatrix} d^*(n) & \mathbf{s}^H(n) \end{bmatrix} \begin{bmatrix} 1 \\ -\mathbf{c}^* \end{bmatrix} \right\}$$

$$= \begin{bmatrix} 1 & -\mathbf{c}^T \end{bmatrix} \sum_n \left\{ \begin{bmatrix} d(n) \\ \mathbf{s}(n) \end{bmatrix} \begin{bmatrix} d^*(n) & \mathbf{s}^H(n) \end{bmatrix} \right\} \begin{bmatrix} 1 \\ -\mathbf{c}^* \end{bmatrix}$$

$$= \begin{bmatrix} 1 & -\mathbf{c}^T \end{bmatrix} \sum_n \left\{ \begin{bmatrix} d(n)d^*(n) & d(n)\mathbf{s}^H(n) \\ d^*(n)\mathbf{s}(n) & \mathbf{s}(n)\mathbf{s}^H(n) \end{bmatrix} \right\} \begin{bmatrix} 1 \\ -\mathbf{c}^* \end{bmatrix}$$

$$= \begin{bmatrix} 1 & -\mathbf{c}^T \end{bmatrix} \begin{bmatrix} r_d(0) & \mathbf{r}_{ds}^T \\ \mathbf{r}_{ds}^* & \mathbf{R}_\mathbf{s} \end{bmatrix} \begin{bmatrix} 1 \\ -\mathbf{c}^* \end{bmatrix}$$

$$= \begin{bmatrix} 1 & -\mathbf{c}^T \end{bmatrix} \mathbf{R}_{ds} \begin{bmatrix} 1 \\ -\mathbf{c}^* \end{bmatrix} \tag{3.5}$$

where $\mathbf{R}_\mathbf{s}$ represents the matrix of autocorrelation of the vector sequence $\mathbf{s}(n)$, and $\mathbf{R}_{ds}$ a matrix containing the autocorrelation of $d(n)$ and its cross-correlations with $\mathbf{s}(n)$ and $\mathbf{R}_\mathbf{s}$.

Assuming that both $d(n)$ and $s(n)$ are jointly wide-sense stationary processes [55], the correlation matrix $\mathbf{R}_{ds}$ becomes:

$$\mathbf{R}_{ds} = \lim_{n\to\infty} \frac{1}{N} \sum_{n=0}^{N-1} \left\{ \begin{bmatrix} d(n)d^*(n) & d(n)\mathbf{s}^H(n) \\ d^*(n)\mathbf{s}(n) & \mathbf{s}(n)\mathbf{s}^H(n) \end{bmatrix} \right\} = E \left\{ \begin{bmatrix} d(n)d^*(n) & d(n)\mathbf{s}^H(n) \\ d^*(n)\mathbf{s}(n) & \mathbf{s}(n)\mathbf{s}^H(n) \end{bmatrix} \right\} \tag{3.6}$$

which is known as a *stochastic correlation* measure.

In order to find a set of filter coefficients to minimise ξ, it is necessary and sufficient that the

derivative of ξ with respect to $\mathbf{c}$ be equal to zero [55]:

$$\nabla_{\mathbf{c}^*}\xi = 0 \tag{3.7}$$

from equation (3.5) we have that the gradient $\nabla_{\mathbf{c}^*}\xi$ can be computed as

$$\nabla_{\mathbf{c}^*}\xi = \nabla_{\mathbf{c}^*}\left\{ \begin{bmatrix} 1 & -\mathbf{c}^T \end{bmatrix} \mathbf{R}_{ds} \begin{bmatrix} 1 \\ -\mathbf{c}^* \end{bmatrix} \right\} = \begin{bmatrix} \mathbf{r}_{ds} & \mathbf{R}_{ds} \end{bmatrix} \begin{bmatrix} 1 \\ -\mathbf{c} \end{bmatrix}$$

or

$$\nabla_{\mathbf{c}^*}\xi = \mathbf{r}_{ds} - \mathbf{R}_{ds}\mathbf{c} \tag{3.8}$$

equalising it to zero we get the equation for the optimum filter parameters:

$$\mathbf{r}_{ds} - \mathbf{R}_{ds}\mathbf{c}_{opt} = 0 \tag{3.9}$$

which is known as ***Wiener Hopf equation*** [55].

One way to determine the optimal parameters in equation (3.9) is by finding the inverse of the autocorrelation matrix:

$$\mathbf{c}_{opt} = \mathbf{R}_{ds}^{-1}\mathbf{r}_{ds} \tag{3.10}$$

which results in a heavy computational operation for filters of large order.

The minimum sum of square errors associated with the optimal filter can be found by substituting the optimal filter parameters into equation (3.5) which results in:

$$\xi_{min} = \begin{bmatrix} 1 & -\mathbf{c}_{opt}^T \end{bmatrix} \mathbf{R}_{ds} \begin{bmatrix} 1 \\ -\mathbf{c}_{opt}^* \end{bmatrix}$$

$$= \begin{bmatrix} 1 & -\mathbf{c}_{opt}^H \end{bmatrix} \mathbf{R}_{ds}^H \begin{bmatrix} 1 \\ -\mathbf{c}_{opt} \end{bmatrix}. \tag{3.11}$$

Taking into account that:

$$\mathbf{R}_{ds}^H \begin{bmatrix} 1 \\ -\mathbf{c}_{opt} \end{bmatrix} = \begin{bmatrix} r_d(0) & \mathbf{r}_{ds}^H \\ \mathbf{r}_{ds} & \mathbf{R}_s \end{bmatrix} \begin{bmatrix} 1 \\ -\mathbf{c}_{opt} \end{bmatrix} = \begin{bmatrix} r_d(0) - \mathbf{r}_{ds}^T \mathbf{c}_{opt} \\ \mathbf{0} \end{bmatrix} \tag{3.12}$$

and substituting into (3.11)

$$\xi_{min} = r_d(0) - \mathbf{r}_{ds}^H \mathbf{c}_{opt} \tag{3.13}$$

which in conjunction with equation (3.9) is known as the ***extended Wiener-Hopf equation*** :

$$\mathbf{R}_{ds}^H \begin{bmatrix} 1 \\ -\mathbf{c}_{opt} \end{bmatrix} = \begin{bmatrix} \xi_{min} \\ \mathbf{0} \end{bmatrix} \tag{3.14}$$

3.1.1 Linear prediction

Wiener filtering can be restated as linear prediction if the desired signal is taken to be a "future" sample of the signal

$$d(n) = s(n+1) \tag{3.15}$$

estimated from previous "past" samples:

$$\mathbf{s}(n) = [s(n), s(n-1), ..., s(n-(p-1))]^T. \tag{3.16}$$

Consequently, the cross-correlation $\mathbf{r}_{ds}$ will be transformed into the auto-correlation:

$$\mathbf{r}_{ds} = E[s(n+1)\mathbf{s}(n)] = \mathbf{r}_{s_{+1}s} \tag{3.17}$$

The extended Wiener-Hopf equation can then be rewritten as:

$$\begin{bmatrix} r_s(0) & r_{s+1s}^H \\ r_{s+1s} & \mathbf{R}_s \end{bmatrix} \begin{bmatrix} 1 \\ -\mathbf{c}_{opt} \end{bmatrix} = \begin{bmatrix} \xi_{min} \\ \mathbf{0} \end{bmatrix}$$

$$\mathbf{R}_s^{(+1)} \begin{bmatrix} 1 \\ -\mathbf{c}_{opt} \end{bmatrix} = \begin{bmatrix} \xi_{min} \\ \mathbf{0} \end{bmatrix} \tag{3.18}$$

where $\mathbf{R}_s^{(+1)}$ is a $(p+1) \times (p+1)$ autocorrelation matrix.

The optimal parameters in this case are known as linear prediction or autoregressive parameters.

3.1.2 Spectral estimation based on the autoregressive model

The autoregressive vector of optimal coefficients $\mathbf{c}_{opt}$ can be used to obtain an estimate of the spectrum of the signal [55] as:

$$\hat{P}_s[\exp(j\Omega)] = \left| \frac{1}{\sum_{k=0}^{p} c_{opt}(k) \exp(-j\Omega k)} \right|^2 . \tag{3.19}$$

In the case of multiple sinusoids in noise, the frequencies of each component can be found by searching for local maxima in this spectrum estimate. This approach implies that the signal is stationary within the segment used to estimate the coefficients and may therefore be unsuitable for the estimation of of non-stationary frequencies.

Another way to estimate the frequencies of the noisy sinusoids at high signal-to-noise ratios would be extracting the roots of the linear prediction polynomial:

$$C(q^{-1}) = \sum_{k=0}^{p} c_{opt}(k) q^{-1} \tag{3.20}$$

where q^{-1} represents the delay operator, and selecting those roots located nearest to the unitary radius circumference on the $z - plane$.

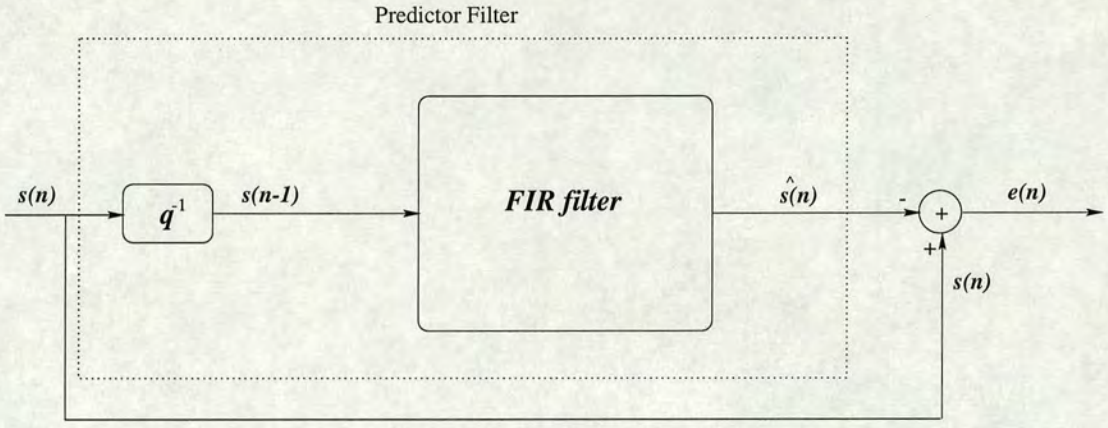

Figure 3.2: *FIR filtering for linear prediction.*

3.2 FIR filter structured in lattice form

Order-recursive techniques [56] [55] that can be used to obtain the optimal auto-regressive or predictive parameters, have lead to the implementation of FIR filters in lattice form which represents a modular easy implementable structure as shown in figures (3.4) and (3.3).

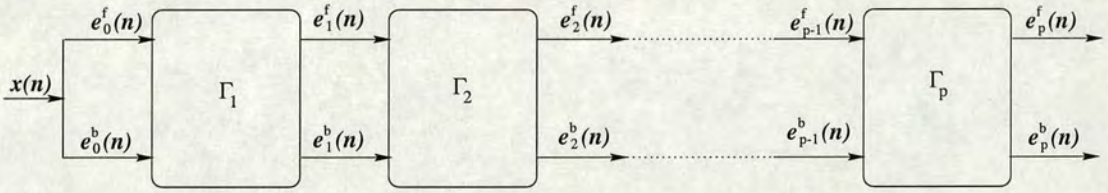

Figure 3.3: *Lattice filter structure.*

The inputs of each section are the forward $e_{i-1}^{f}(n)$ and backward $e_{i-1}^{b}(n)$ errors of the previous section which are decorrelated to get a the output errors $e_{i}^{f}(n)$ and $e_{i}^{f}(n)$:

$$e_{i}^{f}(n) = e_{i-1}^{f}(n) - \Gamma_i e_{i-1}^{b}(n-1) \tag{3.21}$$

$$e_{i}^{b}(n) = e_{i-1}^{b}(n-1) - \Gamma_i^{*} e_{i-1}^{f}(n) \tag{3.22}$$

where Γ_i represents the reflection coefficients of the $i-th$ section. Optimal filter parameters Γ_i^{*} are obtained to minimise the variance of the output error:

$$\xi_i^{f} = E[|e_i^{f}(n)|^2] = E[e_i^{f}(n) e_i^{f*}(n)] = E[e_i^{f}(n)(e_{i-1}^{f*}(n) - \Gamma_i^{*} e_{i-1}^{b*}(n-1))] \tag{3.23}$$

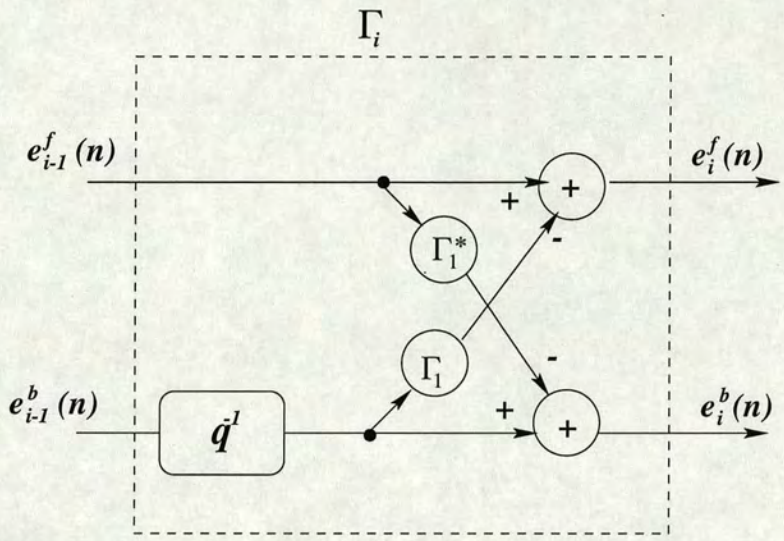

Figure 3.4: *Section of lattice filter.*

Deriving ξ_i^f with respect to the filter parameters results in :

$$\nabla_{\Gamma_i^*}\xi_i^f = E[e_i^f(n)e_{i-1}^{b*}(n-1)] = E[(e_{i-1}^f(n) - \Gamma_i e_{i-1}^b(n-1))e_{i-1}^{b*}(n-1)] \tag{3.24}$$

$$= E[(e_{i-1}^f(n)e_{i-1}^{b*}(n-1)] - \Gamma_i E[e_{i-1}^b(n-1))e_{i-1}^{b*}(n-1)]. \tag{3.25}$$

Equalising this gradient to zero

$$\nabla_{\Gamma_i^*}\xi_i^f = 0 \tag{3.26}$$

the optimal paramters are found to be:

$$\Gamma_i = \frac{E[(e_{i-1}^f(n)e_{i-1}^{b*}(n-1)]}{E[e_{i-1}^b(n-1))e_{i-1}^{b*}(n-1)]}$$

$$= \frac{E[e_{i-1}^f(n)e_{i-1}^{b*}(n-1)]}{E[|e_{i-1}^f(n-1)|^2]} \tag{3.27}$$

This approach can also be used to estimate the frequencies of multiple sinusoids in noise by

first transforming the reflection coefficients into autoregressive coefficients and then using the autoregressive spectrum or the root extraction procedure to estimate the desired frequencies.

3.3 Adaptive FIR filters

The techniques studied before allow the estimation of the filter parameters based on the assumption that the analysed signals are stationary. In the case of non-stationary signals there is a need to make the estimation techniques and therefore the filters adaptive in order to track non-stationary characteristics.

In the specific case of multiple non-stationary sinusoids in noise, this necessity is evident and although the estimation of transversal and lattice structure is in principle unsuitable for the analysis of such signals, these techniques have been used in the past and will be presented here as a "summary of the evolution" of a adaptive filtering techniques designed to analyse NSME signals.

3.4 Adaptive transversal FIR filters

FIR filters structured in transversal form can be made adaptive by using algorithms that ideally will minimise the residual error on a sample-by-sample basis. Two adaptive procedures are presented in the following lines aiming at this goal.

3.4.1 Steepest Descent Algorithm

For the case of non-stationary signals equation (3.9) will be time-dependent:

$$\begin{bmatrix} r_d(0,n) & \mathbf{r}_{ds}^H(n) \\ \mathbf{r}_{ds}(n) & \mathbf{R}_s(n) \end{bmatrix} \begin{bmatrix} 1 \\ -\mathbf{c}_{opt}(n) \end{bmatrix} = \begin{bmatrix} \xi_{min}(n) \\ \mathbf{0} \end{bmatrix}. \tag{3.28}$$

This implies that an appropriate estimation technique should take into account these time-varying statistics which has motivated the search for ***adaptive techniques*** to *track* the non-stationary nature of the analysed signal. One way to do this is by using adaptive techniques

based on ***gradient descent methods*** in which the vector of filter parameters are iteratively estimated by following the direction of ***steepest descent*** over the mean square error (MSE) surface determined by the negative of the gradient of this surface respect to the parameters space.

Using the *steepest descent method* the parameters of the optimal filter can be estimated recursively as:

$$\mathbf{c}(n+1) = \mathbf{c}(n) + \mu \nabla_{\mathbf{c}^*} \xi(n), \tag{3.29}$$

where the parameter μ, often referred as *step size*, determines the convergence characteristics of the algorithm (rate and stability). Choosing "too large" a step size would cause divergence while a "too small " step size would guarantee convergence but at a slow rate.

Extending equation (3.8) to the non-stationary case we have the gradient of the MSE for the non-stationary case:

$$\nabla_{\mathbf{c}^*} \xi(n) = \mathbf{r}_{d\mathbf{s}(n)} - \mathbf{R}(n)\mathbf{c}(n). \tag{3.30}$$

Substituting equation(3.30) in equation(3.29) the steepest descent algorithm becomes

$$\mathbf{c}(n+1) = \mathbf{c}(n) + \mu(\mathbf{r}_{d\mathbf{s}}(n) - \mathbf{R}(n)\mathbf{c}(n)). \tag{3.31}$$

This equation has limited applicability in practice since the estimation of the gradient requires a-priori knowledge of the signal statistics. This fact has motivated its simplification to what is known as the ***least mean square algorithm*** (LMS).

In order to derive this algorithm, the gradient $\nabla_{\mathbf{c}^*} \xi(n)$ can also be expressed as

$$\nabla_{\mathbf{c}^*} \xi(n) = \nabla_{\mathbf{c}^*} E[e(n)e^*(n)] = \nabla_{\mathbf{c}^*} E[e(n)(d^*(n) - \mathbf{c}\mathbf{s}^*(n)] \tag{3.32}$$

$$= -E[e(n)\mathbf{s}^*(n)] \tag{3.33}$$

Substituting in equation (3.29) we have:

$$\mathbf{c}(n+1) = \mathbf{c}(n) + \mu E[e(n)\mathbf{s}^*(n)]. \tag{3.34}$$

In practical scenarios an instantaneous estimate of the expectation $E[e(n)\mathbf{s}^*(n)]$:

$$\hat{E}[e(n)\mathbf{s}^*(n)] = e(n)\mathbf{s}^*(n) \tag{3.35}$$

can be used, leading to the LMS algorithm:

$$\mathbf{c}(n+1) = \mathbf{c}(n) + \mu e(n)\mathbf{s}^*(n). \tag{3.36}$$

which has a computational complexity of $O(N)$, where N represents the length of the signal in samples.

As stated before, the convergence of this algorithm is determined by the value of the step size which means that some criteria should be used to determine an appropriate value to guarantee convergence while avoiding instability. Using an analysis technique based on the eigen-decomposition of the autocorrelation matrix [57], the boundaries for the value of μ can be found as :

$$0 \leq \mu \leq \frac{1}{\lambda_{max}}, \tag{3.37}$$

where λ_{max} is the maximum eigenvalue of the autocorrelation matrix.

A more practical bound [56] is given by:

$$0 \leq \mu \leq \frac{1}{POW(s)} \tag{3.38}$$

where $POW(s)$ represents the signal power.

The LMS algorithm has been used in the past to estimate the frequency trajectories of non-stationary sinusoids by finding time-localised spectral estimated and searching for maxima [58] or minima [61] in these functions.

Figure 3.5 illustrates the adaptive spectrum estimation procedure proposed in [58] by which an adaptive spectrum is obtained from the LMS-estimated autoregressive coefficients.

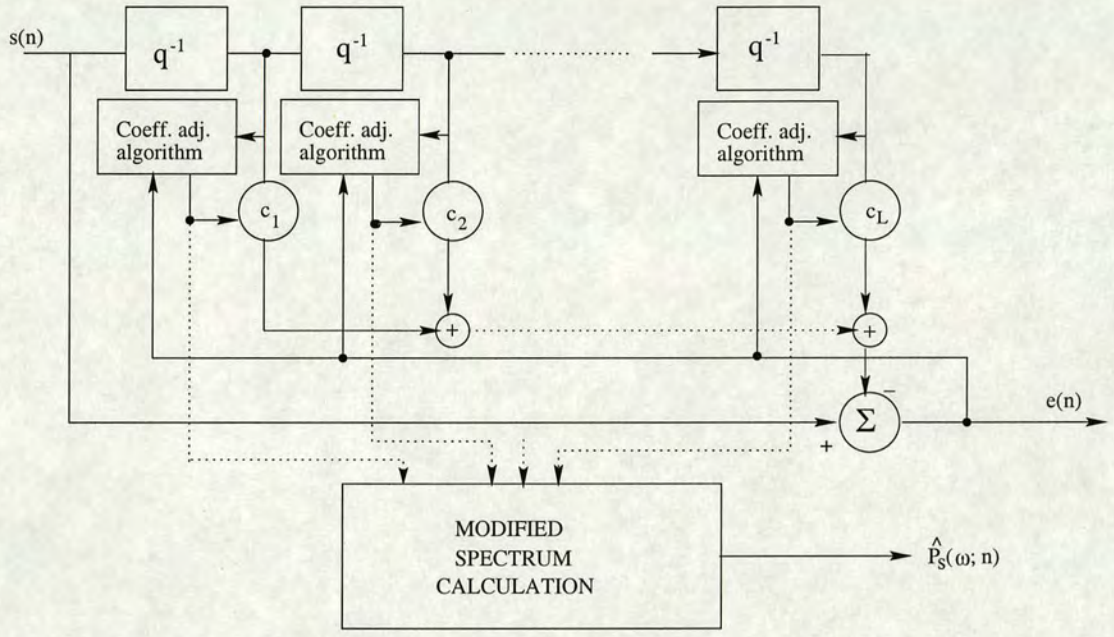

Figure 3.5: *Adaptive spectrum calculation proposed by Griffiths [58].*

3.4.2 Recursive least squares algorithm

In the LMS adaptive filter the ensemble average $\hat{E}[e(n)s^*(n-k)]$ is estimated using instantaneous values:

$$\hat{E}[e(n)s^*(n-k)] = e(n)s^*(n-k). \tag{3.39}$$

This approach is useful in many applications but in others cases leads to slow convergence due to the eigenvalue spread of the autocorrelation matrix [55] [56]. An alternative approach consists on using a minimisation technique not relying on expectation operators but in measures directly computed from the available signal. For example, the ***least square error*** computed from N samples of the signal could be used:

$$\epsilon(n) = \sum_{i=n-N}^{n} |e(i)|^2 \tag{3.40}$$

This measure can be estimated recursively as

$$\epsilon(n) = \lambda\epsilon(n-1) + |e(n)|^2 = \sum_{i=n-N}^{n} \lambda^{n-i}|e(n)|^2 \tag{3.41}$$

where a forgetting factor λ has been introduced to give more "weight" to recently acquired samples. This equation can be expanded as

$$\epsilon(n) = \sum \lambda^{n-i} \{e(n)e^*(n)\} \tag{3.42}$$

$$= \begin{bmatrix} 1 & -\mathbf{c}^T \end{bmatrix} \sum \lambda^{n-i} \left\{ \begin{bmatrix} d(n) \\ \mathbf{s}(n) \end{bmatrix} \begin{bmatrix} d^*(n) & \mathbf{s}^*(n) \end{bmatrix} \right\} \begin{bmatrix} 1 \\ -\mathbf{c} \end{bmatrix}$$

$$= \begin{bmatrix} 1 & -\mathbf{c}^T \end{bmatrix} \sum \lambda^{n-i} \left\{ \begin{bmatrix} d(n)d^*(n) & d(n)\mathbf{s}^*(n) \\ d^*(n)\mathbf{s}(n) & \mathbf{s}(n)\mathbf{s}^*(n) \end{bmatrix} \right\} \begin{bmatrix} 1 \\ -\mathbf{c} \end{bmatrix}$$

$$= \begin{bmatrix} 1 & -\mathbf{c}^T \end{bmatrix} \mathbf{R}_{ds}(n) \begin{bmatrix} 1 \\ -\mathbf{c} \end{bmatrix}$$

where $\mathbf{R}_{ds}(n)$ can be found recursively as:

$$\mathbf{R}_{ds}(n) = \lambda \mathbf{R}_{ds}(n-1) + \begin{bmatrix} d(n) \\ \mathbf{s}(n) \end{bmatrix} \begin{bmatrix} d^*(n) & \mathbf{s}^*(n) \end{bmatrix} \tag{3.43}$$

$$\mathbf{R}_{\mathbf{s}}(n) = \lambda \mathbf{R}_{\mathbf{s}}(n-1) + \mathbf{s}(n)\mathbf{s}^H(n) \tag{3.44}$$

and $\mathbf{r}_{ds}(n)$ as:

$$\mathbf{r}_{ds}(n) = \lambda \mathbf{r}_{ds}(n-1) + d^*(n)\mathbf{s}(n) \tag{3.45}$$

Substituting the optimal solution (3.9) (reproduced here for convenience):

$$\mathbf{r}_{ds}(n) - \mathbf{R}_{\mathbf{s}}(n)\mathbf{c}_{opt} = 0 \tag{3.46}$$

in equation (3.45) we get after arranging terms, a recursive method to estimate the parameters of the filter:

$$\mathbf{R_s}(n)\mathbf{c}_{opt}(n) = \lambda\mathbf{R_s}(n-1)\mathbf{c}_{opt}(n-1) + d^*(n)\mathbf{s}(n) \tag{3.47}$$

Replacing equation (3.44) in (3.47) we get:

$$\mathbf{R_s}(n)\mathbf{c}_{opt}(n) = (\mathbf{R_s}(n) - \mathbf{s}(n)\mathbf{s}^H(n))\mathbf{c}_{opt}(n-1) + d^*(n)\mathbf{s}(n), \tag{3.48}$$

which, after pre-multiplying by $\mathbf{R_s}^{-1}$ and some arrangements, can be written as:

$$\mathbf{c}_{opt}(n) = \mathbf{c}_{opt}(n-1) + \mathbf{R_s}^{-1}(n)\mathbf{s}(n)e^*(n) \tag{3.49}$$

In order to avoid an explicit matrix inversion to estimate the optimal parameters, the inverse can be computed recursively by relying on the matrix inversion lemma [56]:

$$\mathbf{R_s}^{-1}(n) = \lambda^{-1}\mathbf{R_s}^{-1}(n-1) - \frac{\lambda^{-2}\mathbf{R_s}^{-1}(n-1)\mathbf{s}(n)\mathbf{s}^H(n)\mathbf{R_s}^{-1}(n-1)}{1+\lambda^{-1}\mathbf{s}^T(n)\mathbf{R_s}^{-1}(n-1)\mathbf{s}^*(n)} \tag{3.50}$$

If $\mathbf{P}(n)$ is defined as the inverse of the autocorrelation matrix:

$$\mathbf{P}(n) = \mathbf{R_s}^{-1}(n), \tag{3.51}$$

and the gain factor $\mathbf{k}(n)$:

$$\mathbf{k}(n) = \frac{\lambda^{-1}\mathbf{R_s}^{-1}(n-1)\mathbf{s}(n)}{1+\lambda^{-1}\mathbf{s}^T(n)\mathbf{R_s}^{-1}(n-1)\mathbf{s}^*(n)} \tag{3.52}$$

which after some arrangements can be written as :

$$\mathbf{k}(n) = \mathbf{P}(n)\mathbf{s}(n), \tag{3.53}$$

equation (3.49) can be rewritten as:

$$\mathbf{c}_{opt}(n) = \mathbf{c}_{opt}(n-1) + \mathbf{k}(n)e^*(n) \tag{3.54}$$

The RLS algorithm has been used in [62] to detect the formants of voiced speech through *instantaneous frequency* estimation. There, a hierarchical approach was used to recursively

estimate and remove the predominant resonant component.

3.5 Adaptive FIR filters in a lattice structure

Implicit in the lattice structure there is an orthogonalisation process that can be interpreted as a decoupling process. This has motivated the research for an adaptive version of this structure [63] [64] to overcome the convergence dependence on eigenvalue spread which limits the performance of adaptive transversal filters based on stochastic gradient.
The adaptive version of the lattice filter is based on the use of the gradient estimate in equation (3.24) to estimate the reflection coefficients through:

$$\Gamma_i(n+1) = \Gamma_i(n) - \mu_i \nabla_{\Gamma_i^*} \xi_i^f \tag{3.55}$$

$$\Gamma_i(n+1) = \Gamma_i(n) - \mu_i E[e_i^f(n) e_{i-1}^{b*}(n-1)]. \tag{3.56}$$

The practical use of equation (3.56) is limmited by the *a priori requisite* of the second order statistics of the forward and backward prediction errors. However as in the case of the transversal LMS algorithm the expected values can be substituted by instantaneous estimates leading to the *Gradient Adaptive Lattice (GAL) filter* [55].

$$\Gamma_i(n+1) = \Gamma_i(n) - \mu_i [e_i^f(n) e_{i-1}^{b*}(n-1)] \tag{3.57}$$

In the case of multiple non-stationary exponentials in noise this algorithm can be used to estimate the frequency track of each component by first obtaining the coefficients of the equivalent transversal filter and the picking the peaks of the corresponding autoregressive spectral estimate or extracting the roots of the corresponding autoregressive polynomial. This idea was used in [65] to track multiple narrow-band components whose power levels are widely separated including a formant tracking example of real speech.

3.6 Adaptive FIR filters structured in cascade form.

This is the structure that has been the centre of study in the research work reported in this thesis. The key point is the design of an appropriate technique to estimate the parameters of

each section of the cascade. Intuitively it provides the possibility of independently tracking the parameters of multicomponent signals and if appropriately designed the algorithm could provide a highly time localised estimate with low computational load.

The use of adaptive FIR filters structured in cascade form and its application to the analysis of speech was first explored in [67]. Subsequently this structure was studied by other researchers in [69] [71] [72] [73] [74] [75].

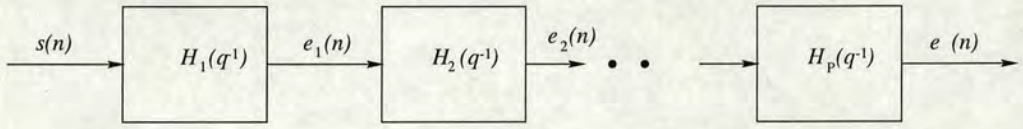

Figure 3.6: *Structure of a FIR filter in cascade.*

In [74] a subsection adaptation scheme based on the RLS algorithm was proposed to estimate a linear predictive model for speech coding purposes. A brief description of this algorithm is presented here as an introduction to the problem of estimating the parameters of the cascade structure.

3.6.1 Recursive least-squares adaptation

In order to estimate the parameters of the filter, it is necessary to find the gradient of the error with respect to the coefficients of each section [67] [69]:

$$\Phi_k(n) = \nabla_{\mathbf{c}_k} e(n) \tag{3.58}$$

where $\Phi_k(n)$ and $\mathbf{c}_k(n)$ represent the gradient and the coefficients of the $k-th$ section respectively. The output of the total error predictor filter is $e(n)$. This gradient can be computed by filtering the output $e(n)$ with $C_k^{-1}(n)$, which represent the inverse of the $k-th$ section. The autocorrelation matrix of the cascade RLS will be defined as the autocorrelation of the output gradient :

$$\Phi(n) = [\Phi_1^T(n), \Phi_2^T(n), ..., \Phi_{1/N/2}^T(n)]^T \tag{3.59}$$

where N represents the order of the filter. Stated in this way, the cascade RLS algorithm requires the computation of an $N \times N$ matrix autocorrelation matrix. However this task can be simplified by realising that in the linear prediction case the computation of $\Phi_k(n)$ is

equivalent to computing the output after removing all the poles except those belonging to the $k-th$ section. This leads to an autocorrelation matrix in the form of a nearly block diagonal matrix with blocks $\mathbf{R}_k$ representing the 2×2 autocorrelation of the $k-th$ section.

Based on the assumption that the resulting autocorrelation matrix has this topology, the parameters of each section can be computed independently by using the RLS algorithm. The coefficients of the $k-th$ section, $\mathbf{c}_k(n)$, are adapted as follows:

$$\mathbf{c}_k(n) = R_k^{-1}(n)\mathbf{pc}_k(n) \tag{3.60}$$

where $\mathbf{pc}_k(n)$ represents the cross-correlation between the input and the desired signal. The computation of the coefficients can be simplified using the matrix inversion lemma [56], which leads to to the cascade recursive least squares subsection adaptation (CRLS-SA) algorithm [74]:

$$\Phi_{k,1}(n) = C_k^{-1}(q^{-1})e_{N/2}(n) \tag{3.61}$$

$$\Phi_{k,2}(n) = \Phi_{k,1}(n-1) \tag{3.62}$$

$$\Phi_k(n) = [\Phi_{k,1}(n)\Phi_{k,2}(n)]^T \tag{3.63}$$

$$\boldsymbol{\kappa}_k(n) = \frac{\lambda P_k(n-1)\Phi_k(n)}{1+\Phi_k^H(n)P_k(n-1)\Phi_k(n)} \tag{3.64}$$

$$P_k(n) = \lambda^{-1}P_k(n-1) - \lambda^{-1}\boldsymbol{\kappa}_k(n)\Phi_k(n)P_k(n-1) \tag{3.65}$$

$$e_k(n) = s_k(n) - \mathbf{c}_k^H(n-1)\mathbf{s}_k(n) \tag{3.66}$$

$$\mathbf{c}_k(n) = \mathbf{c}_k(n-1) + \boldsymbol{\kappa}_k(n)e_k(n) \tag{3.67}$$

where $e_{N/2}$ represents the final output of the predictor error filter, $e_k(n)$ the predictor error

output of the $k-th$ section and $\mathbf{s}_k(n)$ the input of the $k-th$ section.

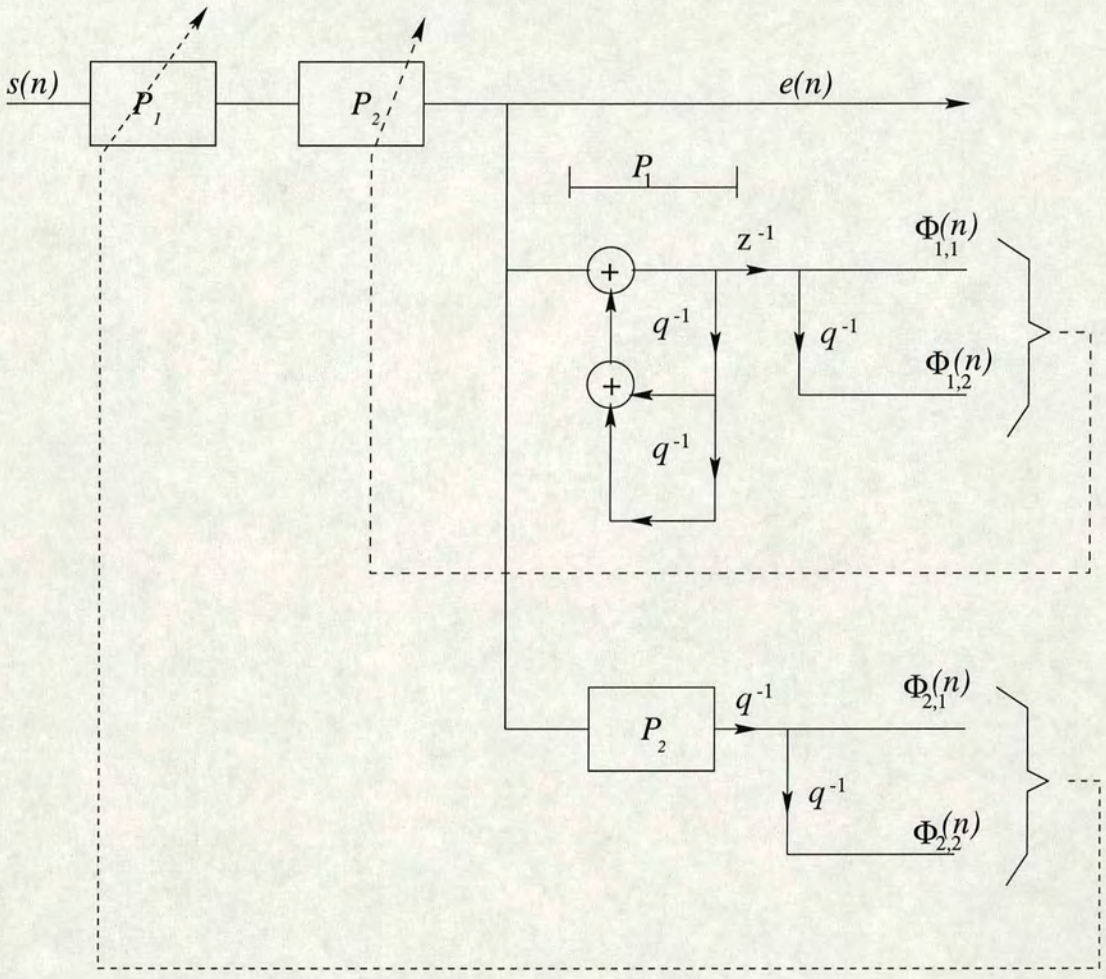

Figure 3.7: *Estimation of the parameters of the cascade structure using the cascade-RLS algorithm [74].*

3.7 Summary

In this chapter adaptive FIR filters have been reviewed in the context of the analysis of non-stationary multicomponent signals. The chapter started with a review of the theory behind FIR filters, describing transversal and lattice structures using statistical concepts. After that adaptive FIR filters were introduced as a means to analyse non-stationary signals highlighting their use in the past in the analysis of nonstationary sinuoids in noise. There, it was explained how this task was achieved by relying on autoregressive spectral estimates or root extraction procedures in conjunction with adaptive filters structured in transversal and lattice form.

In the final part of the chapter, the cascade structure was presented in conjunction with the most recently proposed algorithm to estimate its parameters. This structure constitutes the basic analysis tool of the work summarised in Chaper 4 and the review made here is intended to reinforce the ideas behind this approach.

Chapter 4
Adaptive zeros for direct multi-frequency tracking: Time domain case

The techniques described so far provide indirect ways to estimate the instantaneous frequency of each exponential component of the composite signal in the sense that several stages, consuming computation effort and increasing the overall complexity of the procedure, are required. This fact has motivated the search for a *direct approach* to estimate the non-stationary frequency trajectories of time-varying multicomponent exponential signals.

The approach introduced in this chapter can be briefly condensed into the following: provided that the amplitude of each exponential component is slowly varying (relatively speaking), which implies an associated time-varying pole with near to unitary radius and time-varying angle; a filter composed by a cascade of zeros with constant unitary radii and adaptive angle can be used to simultaneously cancel all but one component and estimate the residual signal's instantaneous frequency.

In order to guarantee the estimation accuracy, the adapted parameters should be the instantaneous angles of the zeros which will be - after convergence of the adaptive algorithm - estimates of the instantaneous frequencies of the exponential components.

4.1 Analysis of mono-component signals

As described in the previous chapters, deterministic signals with time varying features can be represented using a basic complex exponential signal with time-varying amplitude and frequency:

$$s(n) = a(n)\exp(j\phi(n)) \tag{4.1}$$

where $a(n)$ and $\phi(n)$ represent the instantaneous amplitude and phase of the signal respectively.

This signal can also be defined as a function of the ***complex phase*** $\varphi(n)$:

$$s(n) = \exp(\varphi(n)) \tag{4.2}$$

where $\varphi(n) = (\ln[a(n)] + j\phi(n)) \in \mathcal{C}$ (set of complex numbers).

For this signal we can define its ***pole track*** as:

$$p(n) = \frac{s(n)}{s(n-1)} = \frac{a(n)}{a(n-1)} \exp(j\phi(n) - j\phi(n-1)) \tag{4.3}$$

$$= \rho(n)exp(j\omega(n)) = \exp(\varphi(n) - \varphi(n-1)) = \exp(\varpi(n))$$

where $\rho(n), \omega(n)$and $\varpi(n)$ represent the instantaneous damping factor, frequency and complex frequency of the signal. The pole track defined as the ratio of two successive complex-valued samples conveys information about the frequency of the signal and the estimation of its parameters will be performed relying on a filter with adaptive zeros.

In order to estimate the parameters of this signal we can use a time-varying *predictor filter* for which the ***filter signal*** can be defined as:

$$\psi(n) = \hat{s}(n) = \hat{a}(n) \exp(j\hat{\phi}(n)) = \exp(\hat{\varphi}(n)) \tag{4.4}$$

and its associated ***zero track***:

$$z(n) = \frac{\psi(n)}{\psi(n-1)} = \frac{\hat{a}(n)}{\hat{a}(n-1)} \exp(j\hat{\phi}(n) - j\hat{\phi}(n-1)) \tag{4.5}$$

$$\exp(\hat{\varphi}(n) - \hat{\varphi}(n-1)) = \exp(\hat{\varpi}(n)).$$

The *filter signal*, which is defined as an estimate of $s(n)$, is introduced here to define the *zero track*. This *filter signal* conceptually permits the suppression of $s(n)$ by a simple subtraction and a time-varying *predictor filter* which, with the corresponding *zero track*, would allow cancellation of $s(n)$. The technique presented in the sequel is focussed on the estimation of the

zero track by using a gradient-descent technique to minimise the output of the filter. The *filter signal* is never explicitly calculated, rather the estimated zero track provides the mechanism for instantaneous frequency estimation.

The *pole-track* of the basic signal as defined in (4.3) can be estimated using a gradient-descent technique to minimise the instantaneous residual energy:

$$\xi(m) = |e(m)|^2 = |s(m) - z(m)s(m-1)|^2 \tag{4.6}$$

$$= |s(m-1)^2(p(m) - z(m))|^2$$

where the time index m represents an *expanded-time index* introduced to appropriately model the adaptation process that will be characterised by *approaching* and *locked* periods.

Equation (4.6) which describes a quadratic function of the distance between the instantaneous location of the signals pole and the filters zero can be interpreted as the free energy of an adaptation process with gradient-type dynamics. From this perspective, a *vector field* originated at the signal's pole attracts the filter's zero with velocity:

$$\Delta z(m) = f_z(z(m)) = -\mu_z \nabla \xi(z(m)); \tag{4.7}$$

where $\frac{1}{\mu_z}$ represents the *inertia* of the system. If the location of the attractor (pole) is represented in the plane defined by $\hat{\varpi}$, the free-energy ξ induces a velocity of attraction:

$$\Delta\hat{\varpi}(n) = f_{\hat{\varpi}}(\hat{\varpi}(m)) = -\mu_{\hat{\varpi}} \nabla \xi(\hat{\varpi}(m)) \tag{4.8}$$

$$= -\mu_{\hat{\varpi}} J_{z/\hat{\varpi}} \nabla \xi(z(m)),$$

where $J_{z/\hat{\varpi}}$ represents the Jacobian of the transformation.
It is interesting to note that

$$\frac{1}{\mu_{\hat{\varpi}}}.\Delta\hat{\varpi}(m) = -\nabla \xi(\hat{\varpi}(m))$$

$$\Delta^2\hat{\varphi}(m) = -\mu_{\hat{\varpi}}.\nabla \xi(\hat{\varpi}(m)) \tag{4.9}$$

which means that the induced phase acceleration $\Delta^2\hat{\varphi}(m)$ is directly proportional to the gradient of the free-energy at the corresponding filter's instantaneous frequency and inversely proportional to the inertia of the adaptation process.

4.2 Analysis of multicomponent signals

Having presented the ideas involved in the analysis of mono-component signals, we now proceed to extend the concepts to the case of real-valued multi-component signals. These signals can be modelled as a superposition of the basic mono-component signals defined in (4.2):

$$s(n) = \sum_{k=1}^{K} sr_k(n) = \sum_{k=1}^{K} (s_k(n) + s_k^*(n)) \tag{4.10}$$

where

$$s_k(n) = \exp(\varphi_k(n)).$$

Related to these signals there will be a set of poles or *super-pole*:

$$\text{sup}(n) = \bigcup_{k=1}^{K} \{p_k(n), p_k^*(n)\} \tag{4.11}$$

where

$$p_k(n) = \exp(\varpi_k(n)).$$

In order to estimate the parameters of K components, a filter of the same order can be used defined by the *super-zero*:

$$\text{suz}(n) = \bigcup_{k=1}^{K} \{z_k(n), z_k^*(n)\} \tag{4.12}$$

where

$$z_k(n) = \exp(\hat{\varpi}_k(n))$$

And the free-energy of a given pair signal-predictor can be re-defined as:

$$\xi(m) = |e(m)|^2 \tag{4.13}$$

$$= |\tilde{s}_k(m)(\tilde{p}_k(m) - z_k(m)) + \tilde{s}_k^*(m)(\tilde{p}_k(m) - z_k^*(m))|^2$$

where

$$\tilde{s}_k(m) = (1 - z_k^*(m)q^{-1}) \cdot$$

$$\prod_{\substack{l=1 \\ l \neq k}}^{K} s(m)(1 - z_l(m)q^{-1})(1 - z_l^*(m)q^{-1})$$

$$= e(m)(1 - z_l(m)q^{-1})^{-1} \tag{4.14}$$

represents the *k-th semi-residual signal* and $\tilde{p}_k(m)$ its time-varying pole.

A general structure for the signal separation procedure in the case of real-valued signals is represented in Fig. 4.1, and a close look at the structure on each second-order section is given in Fig. 4.2. As each second-order section is composed of two zeros, it will also be referred to here as a *zero pair* to remark on the fact that the parameters that are actually being estimated are the angle and the phase of a pair of complex conjugate zeros.

The free-energy at the output of the cascade can be expressed as a function of the filter parameters as:

$$\xi(m) = (\tilde{sr}_k(m) P_k(\mathbf{c}, q^{-1}))^2 \tag{4.15}$$

where $\tilde{sr}_k(m)$ represents the $k - th$ *real-valued semi-residual signal*,

$$P_k(\mathbf{c}_k, q^{-1}) = (1 + c_{k1}(m)q^{-1} + c_{k2}(m)q^{-2}) \tag{4.16}$$

its associated predictor or zero pair filter, and

$$\mathbf{c}_k(m) = [c_{k1}(m), c_{k2}(m)] \tag{4.17}$$

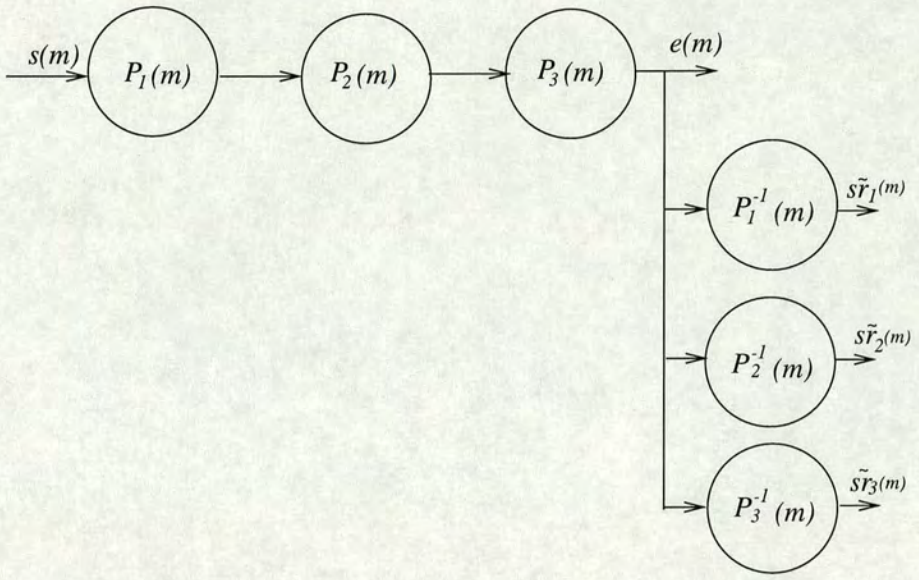

Figure 4.1: *Structure of a third-order predictor-estimator filter.*

$$= [-2\mathrm{Re}(z_k(m)), (\mathrm{mod}(z_k(m)))^2]$$

$$= [-2\hat{\rho}_k(m)\cos(\hat{\omega}_k(m)), \hat{\rho}_k^2(m)]$$

represents the vector of time-varying parameters.

In this case the *induced velocity* will be defined by :

$$\Delta\theta_k(m) = \mu_\theta J^t_{\mathbf{c}_k/\theta_k}|_m \bar{\tilde{s}r}_k(m) \tag{4.18}$$

where

$$\theta_k(m) = [\hat{\omega}_k, \hat{\rho}_k]^t$$

represent the parameters (angle and radius) of the $k-th$ zero,

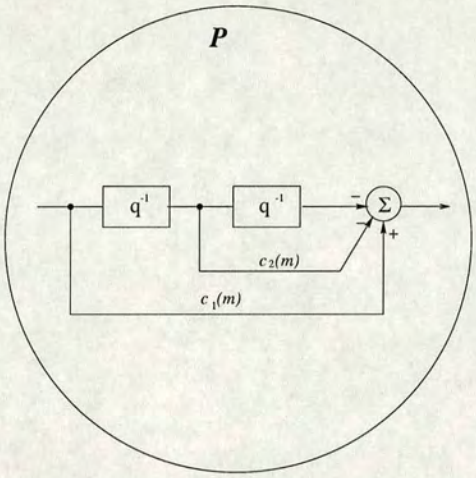

Figure 4.2: *One section of the cascade (second-order predictor filter or zero pair).*

$$\mu_\theta = \begin{bmatrix} \mu_{\hat{\omega}} & 0 \\ 0 & \mu_{\hat{\rho}} \end{bmatrix}$$

a constant representing the inverse of the *inertia* of the adaptation process,

$$J^t_{\bar{a_k}/\theta_k}|_m = \begin{bmatrix} -\hat{\rho}_k \sin(\hat{\omega}_k) & 0 \\ \cos(\hat{\omega}_k) & -\hat{\rho}_k \end{bmatrix}|_m$$

the Jacobian of the transformation from the space defined by the parameters of the filter to the space defined by the parameters of its zeros, and

$$\bar{\bar{sr}}_k(m) = \vec{U}(\nabla_c \xi(m))$$

the direction of adaptation defined by a unitary vector in the direction of $\nabla_{\bar{a}}\xi(m)$.

4.3 Convergence analysis

In order to prove that the adaptation process described in the previous section converges to the optimal value, we can define the error estimate for a complex mono-component signal as:

$$zv = z - p \tag{4.19}$$

where z represents the adaptive zero and p the pole of the signal. From (4.6) we have:

$$\frac{\Delta\xi}{\Delta|zv|} \geq 0 \quad \forall\, zv \;\in\; z \text{ plane} \tag{4.20}$$

which means that the residual energy is a concave function of $|zv|$ with a minimum at:

$$zv = 0. \tag{4.21}$$

In a similar way, if the definitions:

$$\omega v = \hat{\omega} - \omega \tag{4.22}$$

and

$$\rho v = \hat{\rho} - \rho \tag{4.23}$$

are used, it is clear that:

$$\frac{\Delta|zv|}{\Delta|\omega v|} \geq 0 \text{ for } \hat{\rho} = constant \tag{4.24}$$

$$\frac{\Delta|zv|}{\Delta|\rho v|} \geq 0 \text{ for } \hat{\omega} = constant \tag{4.25}$$

In other words, ξ is a concave function of ωv and ρv. From (4.22) and (4.23), it can be seen that ξ is a concave function of $\hat{\omega}$ and $\hat{\rho}$ with a minimum at $[\hat{\omega}, \hat{\rho}] = [\omega, \rho]$, guaranteeing convergence for a large enough inertia.

For the case of real-valued mono-component signals the existence of a unique minimum can be visualised by interpreting the problem as the estimation of the instantaneous values of two complex mono-component signals with a cascade of two complex first-order filters adapted in

parallel.

The convergence of equation (4.18) can then be achieved by complying with the constraints

$$\mu_{\hat{\omega}}|\nabla_{\hat{\omega}}\xi| < |\omega v| \quad \forall\, \omega v \in [0, \pi]$$

and

$$\mu_{\hat{\rho}}|\nabla_{\hat{\rho}}\xi| < |\rho v| \quad \forall\, \rho v \in [0, 1].$$

If the magnitudes $|\nabla_{\hat{\rho}}\xi|$ and $|\nabla_{\hat{\rho}}\xi|$ are scaled to $|e|$ while the input signals are normalised to have magnitude less than one, then the constraints can be shown to be (Appendix 1):

$$\mu_{\hat{\omega}} < \frac{1}{2} \quad for\ \hat{\rho} = \rho.$$

and

$$\mu_{\hat{\rho}} < \frac{\rho}{2} \quad .$$

If a slow adaptation process is desired, the values of the $\mu_{\hat{\omega}}$ and $\mu_{\hat{\rho}}$ must be selected well below its upper limits.

In the case of multi-component real-valued signals, finding the optimal zeros of the filter can be interpreted as simultaneously finding the optimal values of first-order sections whose inputs are scaled and delayed versions of each component of the input signal plus *"interference"* . As the zeros approach the biased poles (due to the interference) of the signal, the amplitude of the *"interference"* will be smaller in relation to the component being estimated, and the proof of convergence for the complex mono-component signal case can be extended to the real and multicomponent cases. Once the zeroes are locked to the poles, any variation in a component's frequency will be independently tracked by its respective zero.

4.4 Computational complexity

The computational complexity of the proposed algorithm is of order $O(KM)$, where K represents the number of components being tracked and M represents the total number iterations

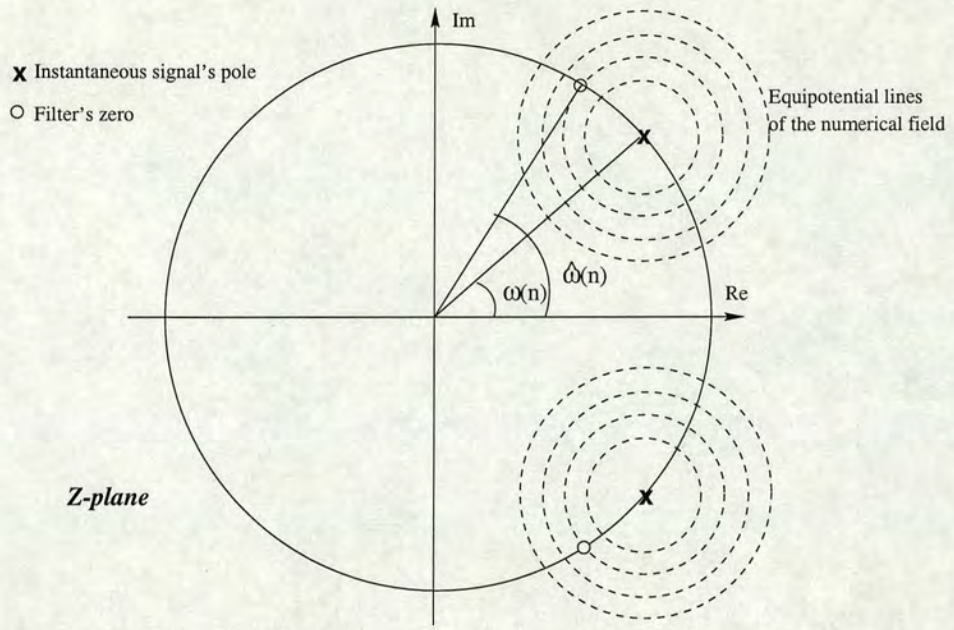

Figure 4.3: *Diagram showing the an "snap-shot" of the position in the z-plane of the instantaneous signals poles and their filtering zeros.*

required by the algorithm to converge to the optimal values. This can be understood by observing updating equation (4.18). In the case of *locked* periods when the zeros of the filter are locked to the poles of the signal, the computational complexity will be of order $O(KN)$, where N represents the total number of samples. This represents an advantage when compared with frequency tracking techniques based on the use of time-frequency representations which require algorithms with computational complexity of higher order to obtain the required transforms. For example, the computational complexity of just computing the spectrogram would amount (not considering data storage requirements) to an order of $O(N_W\ W_L\ N_F)$ where W_L represents the length of the window used to compute the short-time Fourier transform, N_W the number of windows and N_F the number of frequency bins. In addition a second stage incrementing the computational load is required to track K ridges.

4.5 Signal separation

Once the trajectory of the signal parameters have been estimated, a time-varying notch filter of the form [76]:

$$N_k(n, q^{-1}) = \frac{P_k(\mathbf{c}_k(n), q^{-1})}{P_k(\mathbf{c}_k(n), rq^{-1})} \tag{4.26}$$

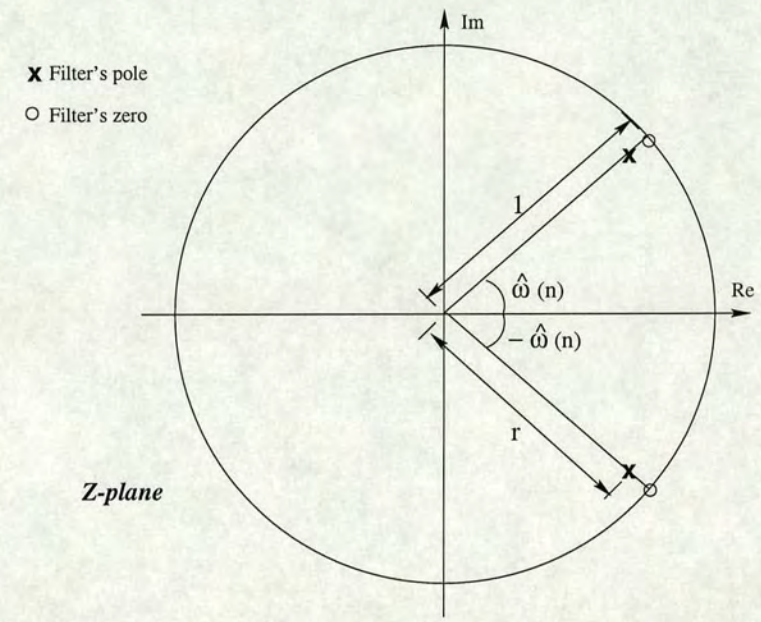

Figure 4.4: *Diagram showing the an "snap-shot" of the position in the z-plane of the time-varying poles and zeros for a notch filter (pole-zero pair).*

can be used to cancel the $k-th$ component of the composite signal. The notch filter will be denominated here as a *pole-zero* pair because it is defined by two complex conjugate poles and two complex conjugate zeros each having a pole at the same angle as a zero but with a radius scaled by the factor r (see Fig. 4.4).

Since each pole-zero pair tuned to the frequency trajectory of a component will cancel it, a cascade of pole-zero pairs defined as:

$$NC_k(n, q^{-1}) = \prod_{\substack{l=1 \\ l \neq k}}^{K} N_l(n) \tag{4.27}$$

will allow the isolation of the $k-th$ component of a composite signal with K components.

Once that a given component has been isolated it can be treated as a mono-component signal and its amplitude envelope can be estimated using a technique described in the next section.

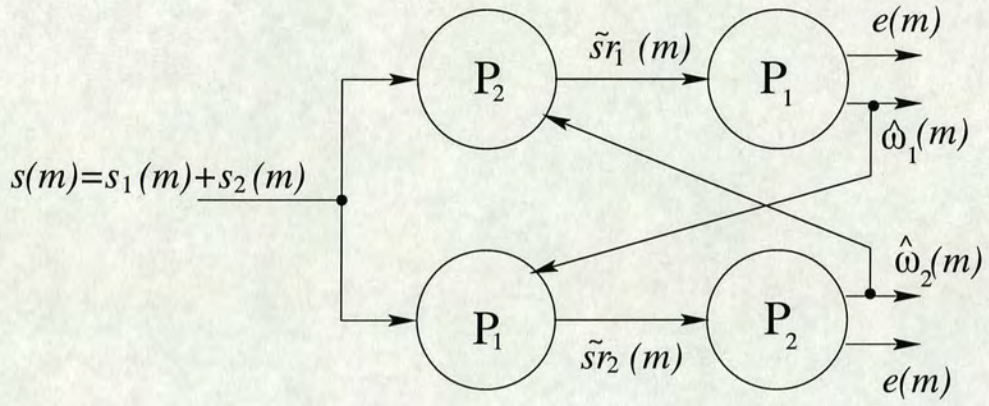

Figure 4.5: *Cascade of two zero pairs for tracking the instantaneous frequency of two superimposed sinusoids.*

4.6 Amplitude envelope estimation

In addition to the task of tracking the instantaneous frequency of each component of the composite signal, it is necessary to estimate the instantaneous amplitude of each component in order to fully characterise it.

The estimation technique proposed here is based on two samples. Specifically we have that two consecutive samples for an amplitude and frequency modulated sinusoid will be given by:

$$s(n) = a(n)\cos(\phi(n)), \tag{4.28}$$

and

$$s(n+1) = a(n)\cos(\phi(n) + \omega(n)). \tag{4.29}$$

Assuming a small variation of the signals amplitude envelope for two consecutive samples, the ratio of this samples will be given by:

$$\frac{s(n+1)}{s(n)} = \frac{\cos(\phi(n) + \omega(n))}{\cos(\phi(n))}. \tag{4.30}$$

Using trigonometric properties, the instantaneous phase can be expressed as:

$$\phi(n) = \arctan\left[\frac{\cos(\omega(n)) - \frac{s(n+1)}{s(n)}}{\sin(\omega(n))}\right]. \tag{4.31}$$

Based on an estimate $\hat{\omega}(n)$ of the instantaneous frequency, an estimate of the instantaneous phase can be obtained as:

$$\hat{\phi}(n) = \arctan\left[\frac{\cos(\hat{\omega}(n)) - \frac{s(n+1)}{s(n)}}{\sin(\hat{\omega}(n))}\right]. \tag{4.32}$$

Substituting Equ. (4.32) in Equ. (4.28) an estimate of the signal instantaneous amplitude envelope can be finally obtained as:

$$\hat{a}(n) = \frac{s(n)}{\cos\left\{\arctan\left[\frac{\cos(\hat{\omega}(n)) - \frac{s(n+1)}{s(n)}}{\sin(\hat{\omega}(n))}\right]\right\}}. \tag{4.33}$$

This is a two-samples estimate of the signals amplitude envelope that will be tested with computer simulations in the following section.

4.7 Computer simulations

Although the proposed algorithm allows the separation of damping and frequency related information, the signals studied here are analysed with filters whose zeros are constrained to be on a circumference with unitary radius in the $z - plane$. This is done to take advantage of the narrow-band nature of each component of the analysed signals. Additionally the inertia of the adaptive process (inverse of the adaptation constant μ_ω) is adjusted empirically to suit the dynamics of the analysed signals.

In order to estimate the amplitude envelope of a given component of the composite signal, the desired component is first isolated using a time-varying notch filter (pole-zero pair) and then the amplitude envelope estimate is obtained using the approach introduced in section 4.6.

4.7.1 Mono-component signals signals

CASE A. AM-FM demodulation of a real-valued synthetic mono-component signals

Figures 4.6, 4.7 , 4.8 and 4.9 show the performance of the proposed and energy separation approaches in the task of tracking the amplitude and frequency of a sinusoid with sinusoidally

modulated amplitude and frequency (SNR=20 $log_{10}(\frac{total\ signal\ power}{noise\ power}) = 35dB$):

$$s(n) = [1.2\cos(0.4n) + 2]\sin[\frac{\pi}{2} + 0.8\sin(0.4n)]. \tag{4.34}$$

In those figures, it can be observed how the proposed algorithm provides an overall more accurate instantaneous frequency estimate for the signal analysed. Particularly around the regions with higher rate of frequency change the absolute estimation error obtained with the energy separation algorithm is slightly larger than that obtained with the proposed algorithm. Although this fact is not enough to claim superiority of the proposed algorithm over the energy separation approach, the ultimate intention of the comparison is to present an alternate approach to perform amplitude and frequency demodulation with estimation errors that are comparable to those of previously proposed techniques.

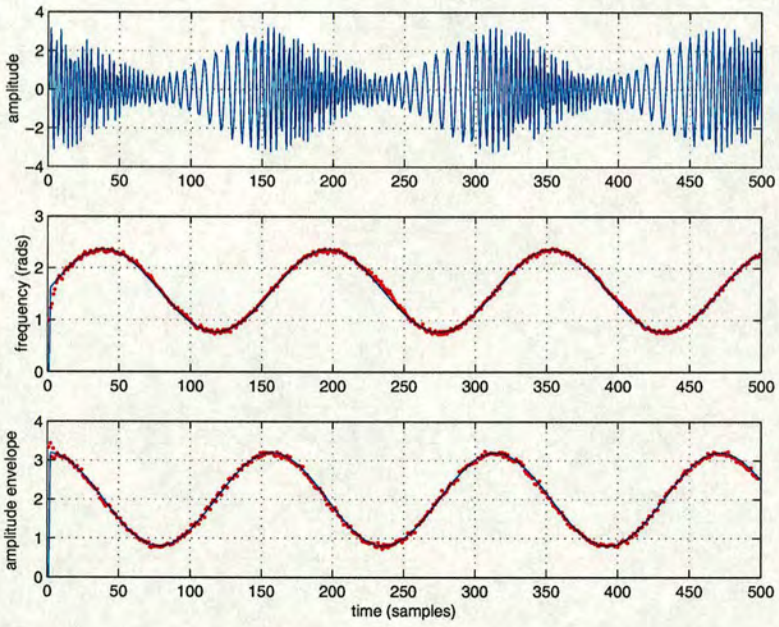

Figure 4.6: *Estimates of the instantaneous frequency and amplitude envelope (red dots) obtained with the proposed approach ($\mu_{\hat{\omega}} = 0.1$, $\hat{\rho} = 1$) for a synthetic sinusoid with sinusoidally modulated amplitude and frequency ($SNR = 35dB$).*

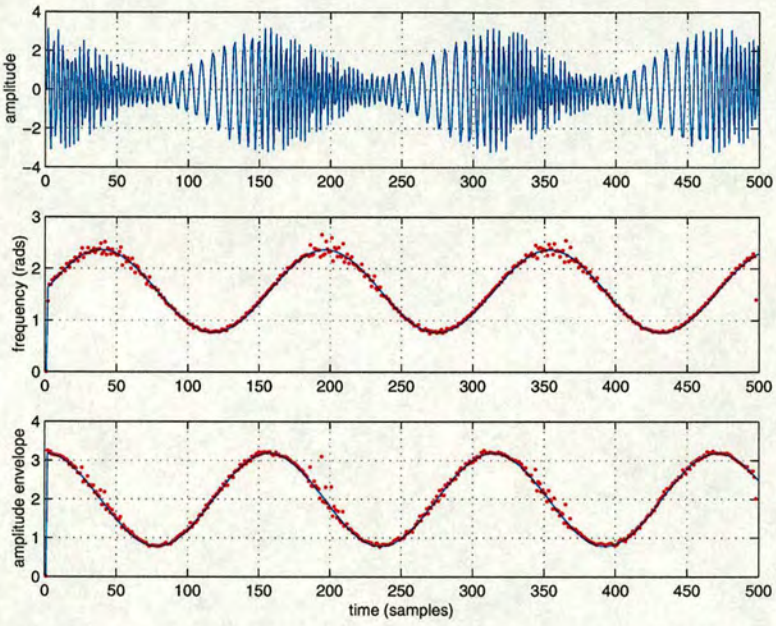

Figure 4.7: *Estimates of the instantaneous frequency and amplitude envelope (red dots) obtained with the DESA1 algorithm for a synthetic sinusoid with sinusoidally modulated amplitude and frequency ($SNR = 35dB$).*

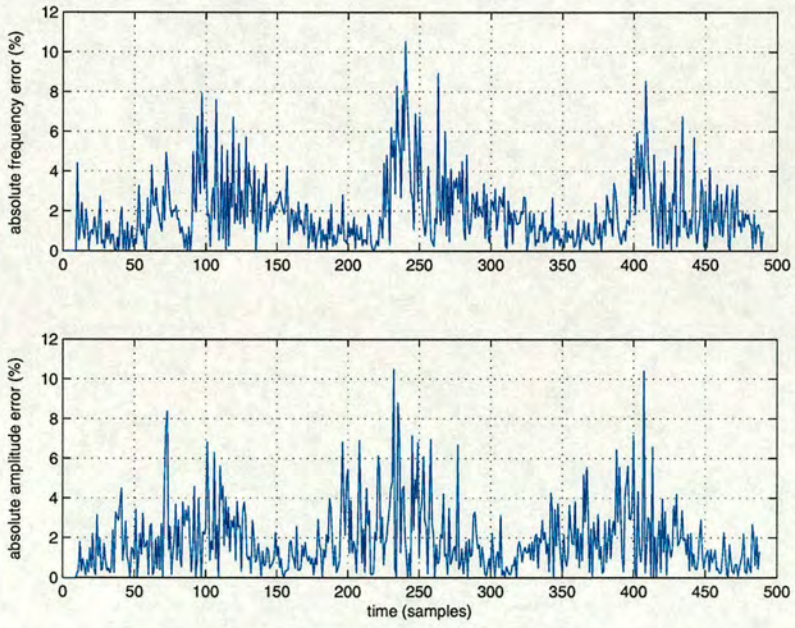

Figure 4.8: *Absolute error for the instantaneous frequency and amplitude envelope obtained with the proposed approach.*

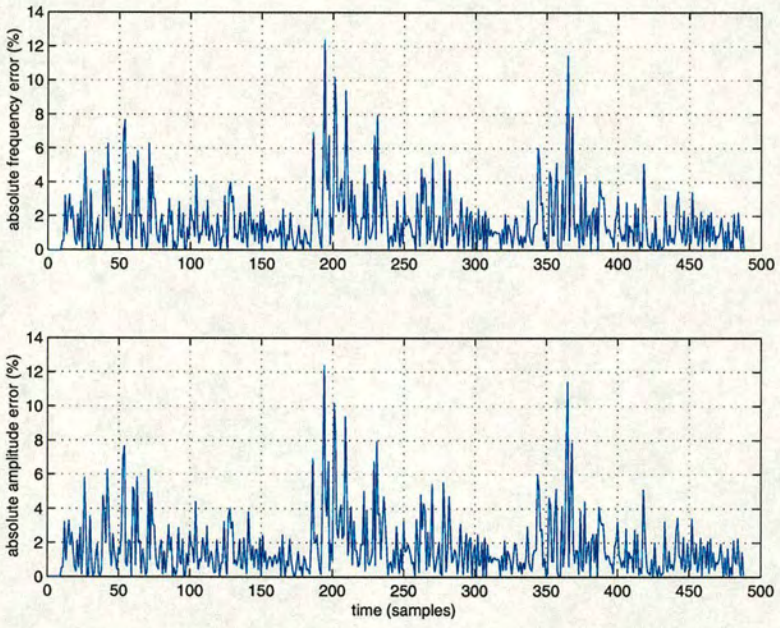

Figure 4.9: *Absolute error for the instantaneous frequency and amplitude envelope obtained with the the DESA1 algorithm.*

CASE B. A chirp with linear frequency rate and sinusoidal amplitude envelope

A second example for AM-FM demodulation consists on a chirp with linearly modulated frequency and sinusoidal amplitude envelope:

$$s(n) = [0.7\cos(\frac{\pi n}{200}) + 2]\cos(\frac{2.88n^2}{2000} + 0.12n). \tag{4.35}$$

The instantaneous frequency and amplitude envelope estimated obtained with the proposed approach is shown in Fig. 4.10 and the corresponding absolute instantaneous error are displayed in Fig. 4.11.

The performance of the algorithm has also been tested and compared with other approaches for a noisy version of this signal. The other approaches used were: energy operators based estimation and the Hilbert transform. For the energy operators approach the discrete energy separation algorithm (DESA1)[10] was used and the Hilbert transform was performed by using the DFT of the signal.

Figs. 4.12, 4.13 and 4.14 display the performance of the algorithms for SNR=30dB. And Figs. 4.15 and 4.16 display the mean absolute perceptual errors for different signal-to-noise ratios. In Fig. 4.15 it can be observed how the proposed approach outperforms both the energy separation an Hilbert transform based algorithms in the task of estimating the instantaneous frequency of the analysed signal for SNR's between 30 and $47dB$.

In the task of estimating the amplitude envelope of the analysed signal (Fig. 4.16), the performance of the proposed approach lies between those of the energy operator and Hilbert transform based algorithms for SNR's between 30 and $50dB$.

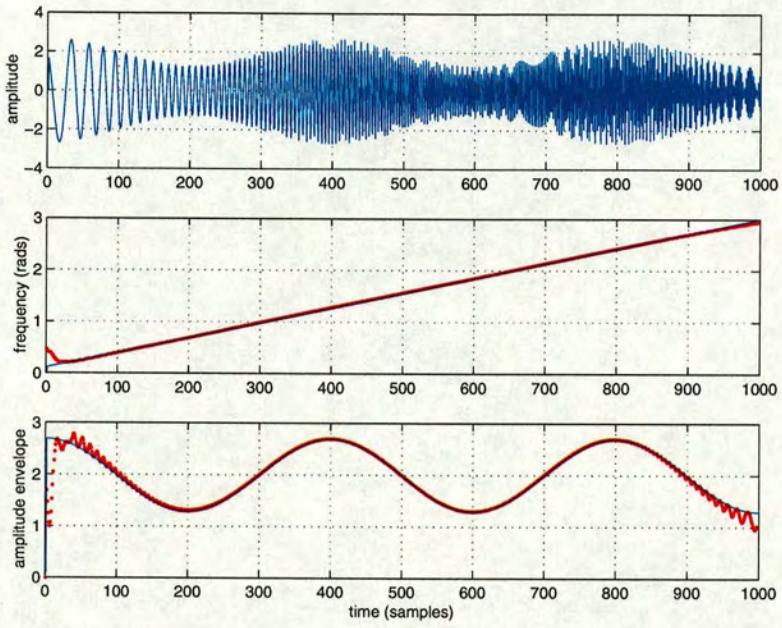

Figure 4.10: *Estimates of the instantaneous frequency and amplitude envelope (red dots) obtained with the proposed approach ($\mu_{\hat{\omega}} = 0.2$, $\hat{\rho} = 1$) for a synthetic chirp with linearly increasing frequency and sinusoidally modulated amplitude.*

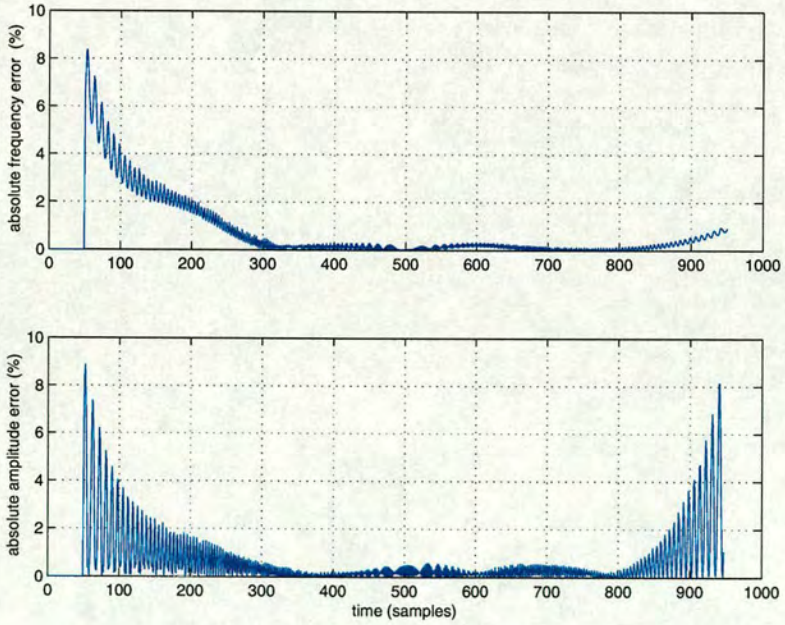

Figure 4.11: *Mean absolute errors for the simulation whose results are shown in Fig. (4.10)*

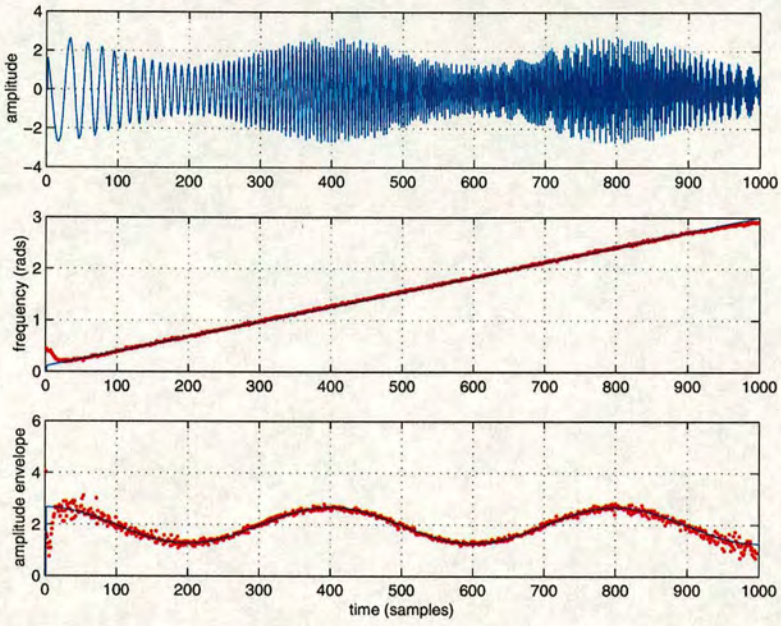

Figure 4.12: *Estimates of the instantaneous frequency and amplitude envelope (red dots) with the proposed approach ($\mu_{\hat{\omega}} = 0.1$, $\hat{\rho} = 1$, $SNR = 30dB$) for a synthetic chirp with linearly increasing frequency and sinusoidally modulated amplitude.*

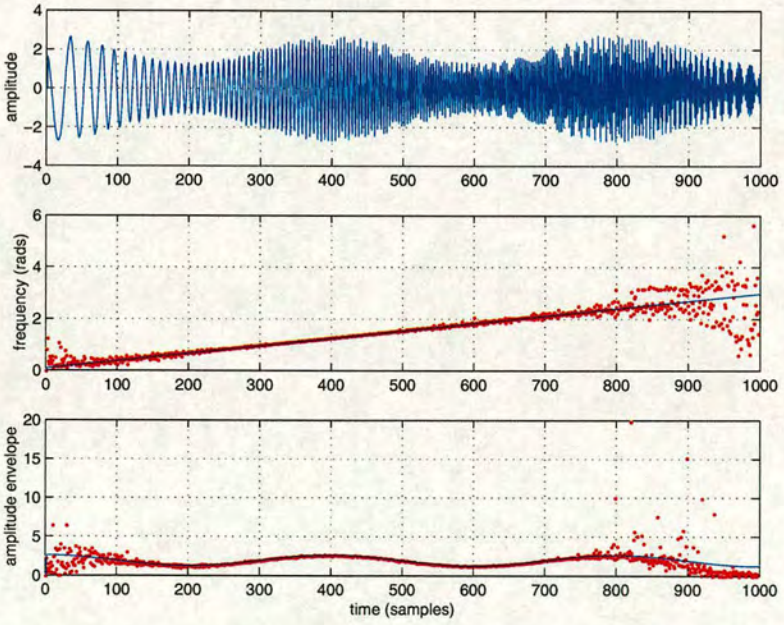

Figure 4.13: *Estimates of the instantaneous frequency and amplitude envelope (red dots) obtained with the DESA-1 algorithm for a synthetic chirp with linearly increasing frequency and sinusoidally modulated amplitude.*

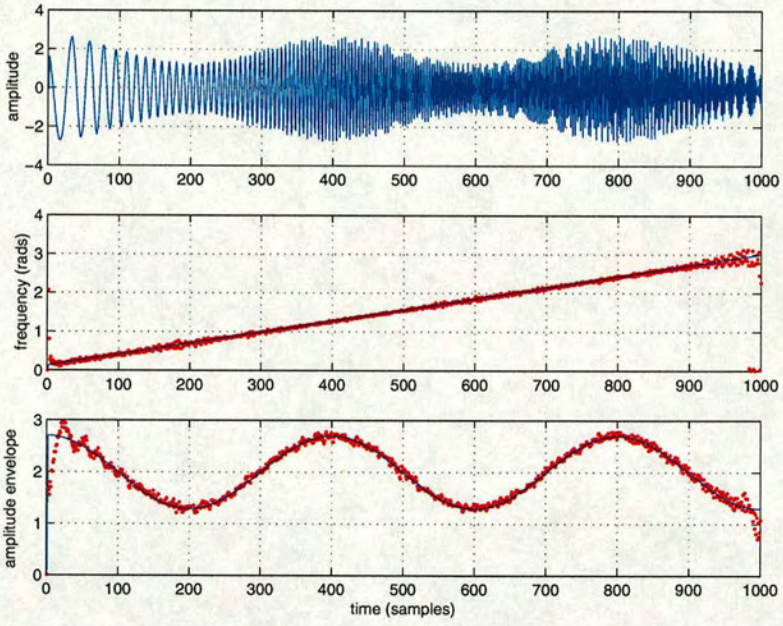

Figure 4.14: *Estimates of the instantaneous frequency and amplitude envelope (red dots) obtained with the Hilbert transform algorithm for a synthetic chirp with linearly increasing frequency and sinusoidally modulated amplitude.*

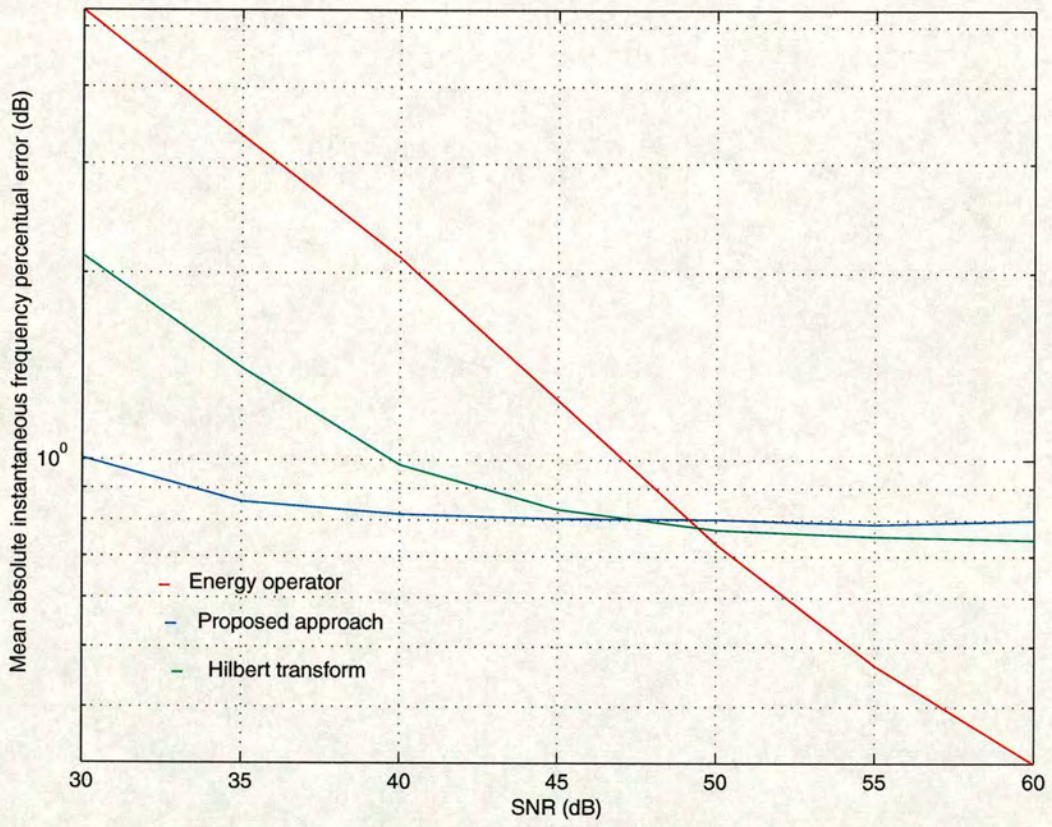

Figure 4.15: *Mean absolute instantaneous frequency error for a chirp signal with linearly modulated frequency and sinusoidally modulated amplitude corrupted by additive Gaussian noise.*

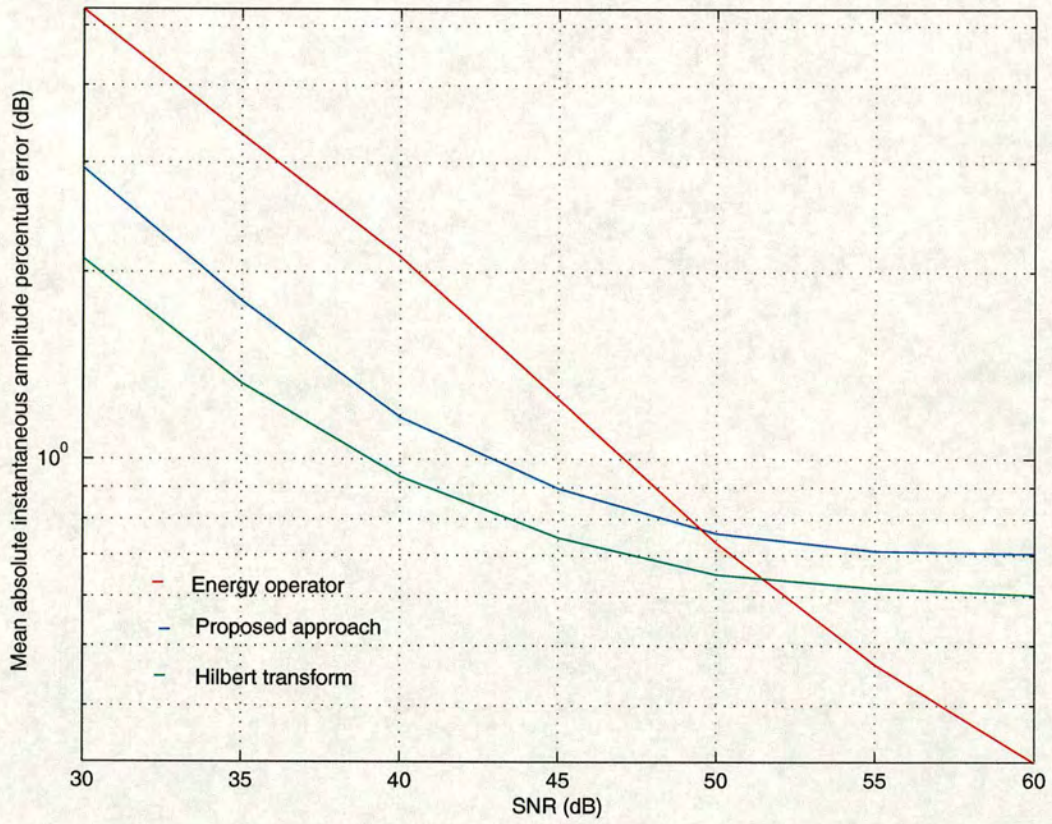

Figure 4.16: *Mean absolute instantaneous amplitude error for a chirp signal with linearly modulated frequency and sinusoidally modulated amplitude corrupted by additive Gaussian noise.*

CASE C. Analysis of a bat sonar signal

A bat sonar signal is analysed here as an example of a real mono-component signal. This signal, obtained from the Time-Frequency tool-box (http://iut-saint-nazaire.univ-nantes.fr/ auger/tftb.html), was sampled with a frequency of 230.4 Hz.

The Wigner-Ville distribution of a decimated $(7:1)$ segment of the bat sonar signal (illustrating its mono-component nature) is shown in Fig. 4.18 .

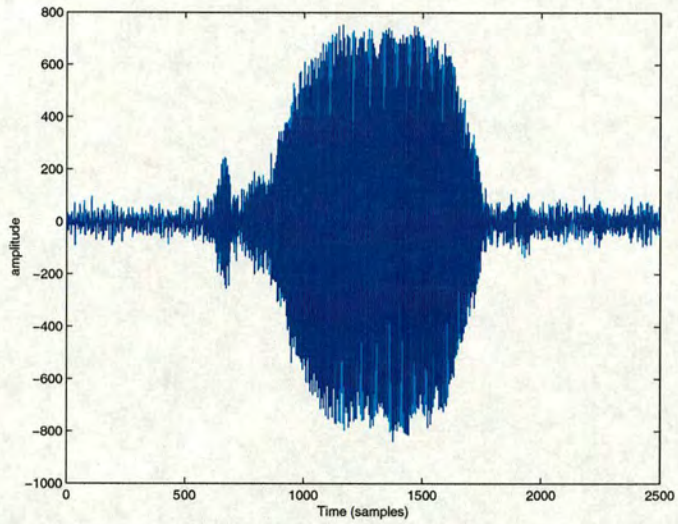

Figure 4.17: *Sonar signal of a bat*

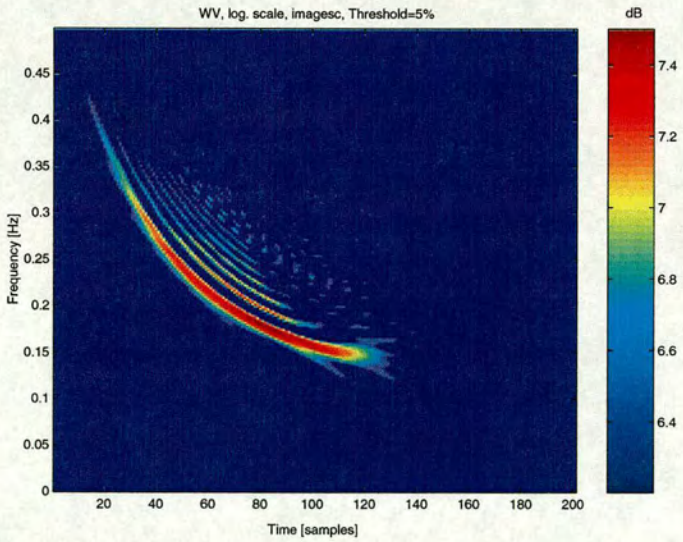

Figure 4.18: *Wigner-Ville distribution of the bat sonar signal*

Figures 4.19, 4.20 and 4.21 show the instantaneous frequency and amplitude envelope obtained with the proposed, energy separation and Hilbert transform approaches applied to the decimated segment of the bat sonar signal. The instantaneous frequency and amplitude estimates obtained with all the approaches are consistent in the sense that they follow the same trajectory, only the energy separation algorithm provides poor estimates in the segment with non-stationary frequency.

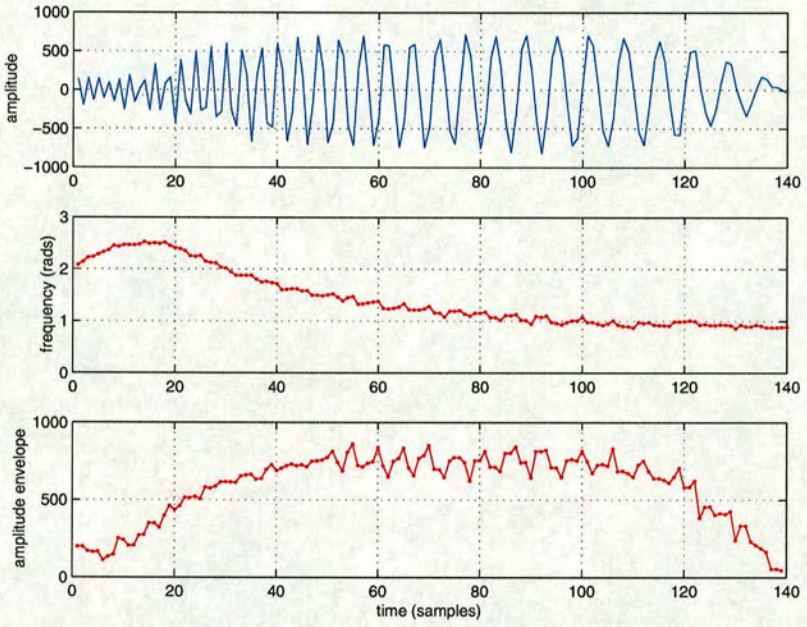

Figure 4.19: *Estimates of the instantaneous frequency and amplitude envelope (red line) obtained with the proposed approach ($\mu_{\hat{\omega}} = 0.1$, $\hat{\rho} = 1$) for the bat sonar signal.*

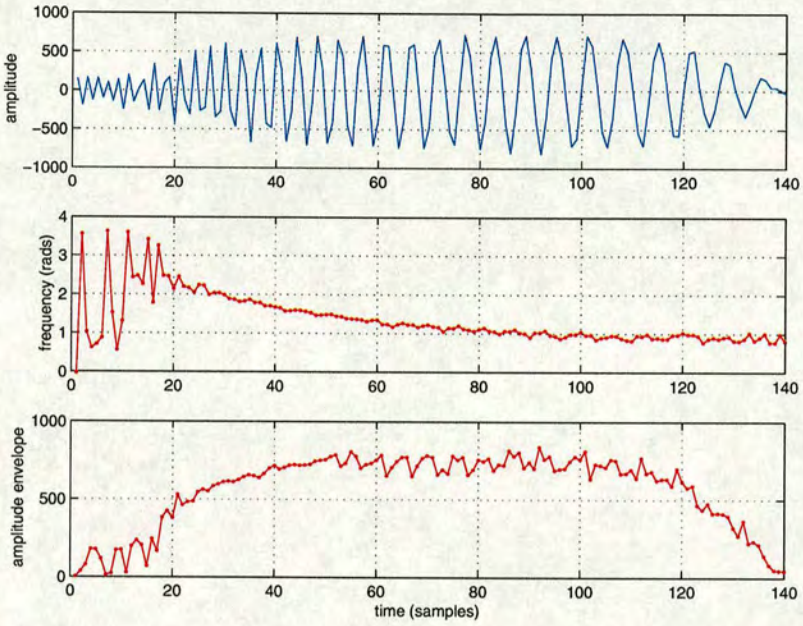

Figure 4.20: *Estimates of the instantaneous frequency and amplitude envelope (red line) obtained with DESA-1 algorithm for for the bat sonar signal.*

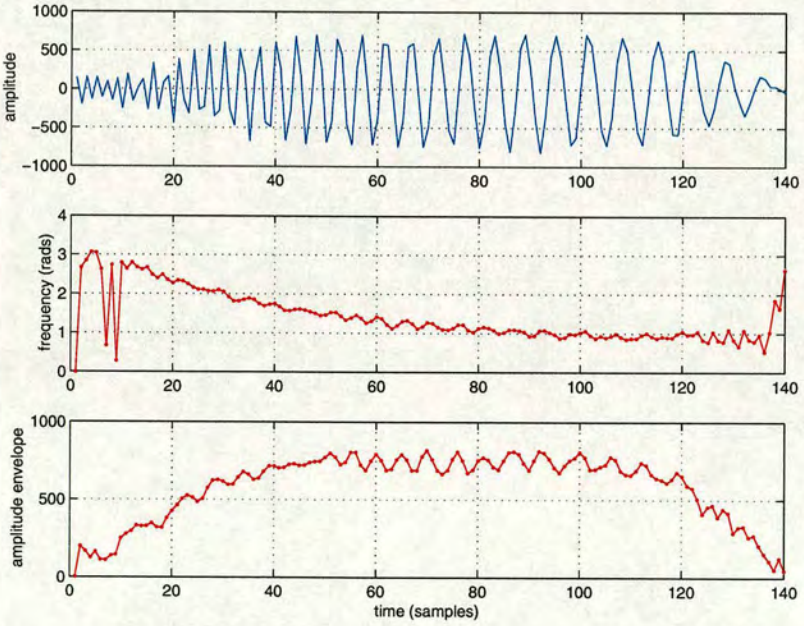

Figure 4.21: *Estimates of the instantaneous frequency and amplitude envelope (red line) obtained with Hilbert transform algorithm for for the bat sonar signal.*

4.7.2 Multicomponent signals

CASE D. Convergence of a cascade of two zero pairs

This example is intended to illustrate the convergence of a cascade of two zero pairs for the case of two stationary sinusoids with different amplitude corrupted by zero mean additive Gaussian noise (total SNR=30 dB):

$$s(n) = \cos(1.5n) + 3\cos(2n). \tag{4.36}$$

The convergence process is illustrated in Figs. 4.22, 4.23 and 4.24 where it can be observed how the algorithm converges to the optimal solution irrespective of the initial conditions.

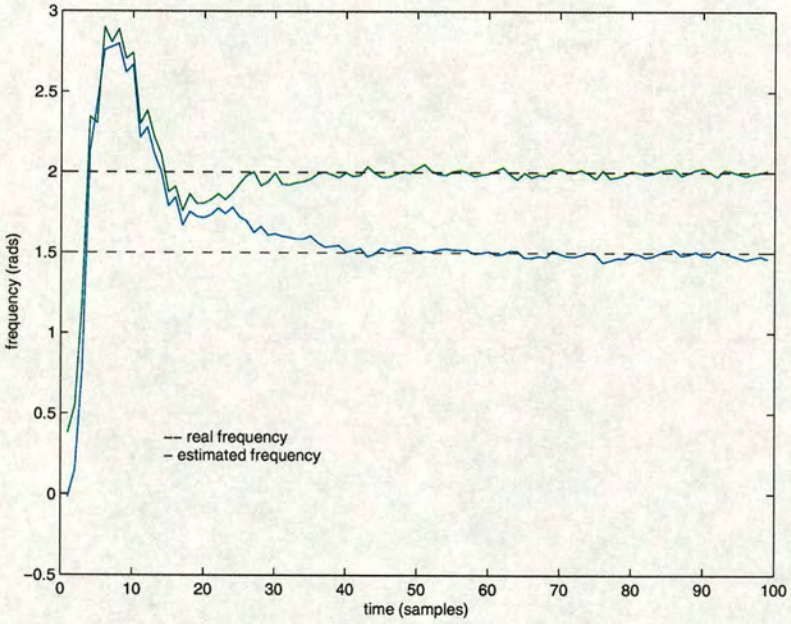

Figure 4.22: *Convergence to the frequencies of two tones with different amplitude (total SNR=30 dB) for a cascade of two second-order filters with initial values* $\omega_1(0) = 0.1\ rads$ *and* $\omega_2(0) = 0.5\ rads$ *(*$\mu_\omega = 0.4$ *and* $\rho = 1$*).*

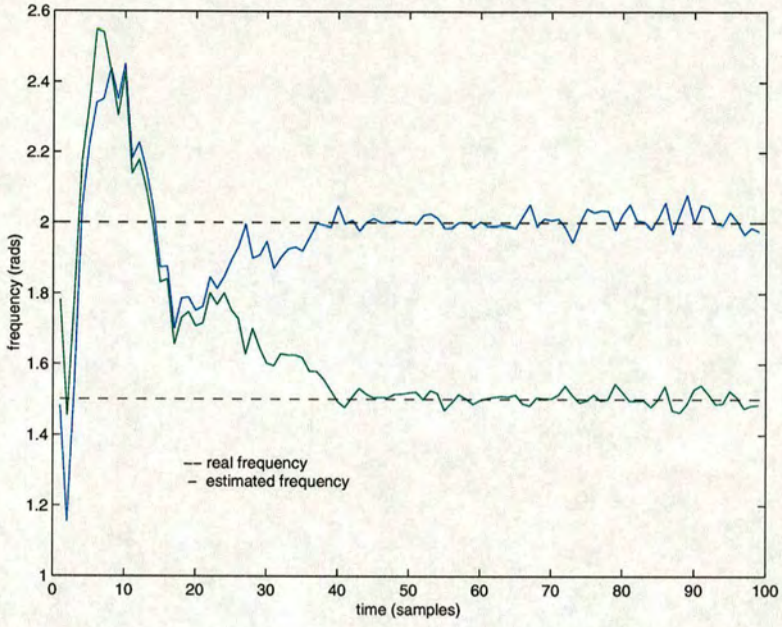

Figure 4.23: *Convergence to the frequencies of two tones with different amplitude (total SNR=30 dB) for a cascade of two second-order filters with initial values* $\omega_1(0) = 1.6$ *and* $\omega_2(0) = 1.9$ $rads$ *(*$\mu_\omega = 0.4$ $rads$ *and* $\rho = 1$*).*

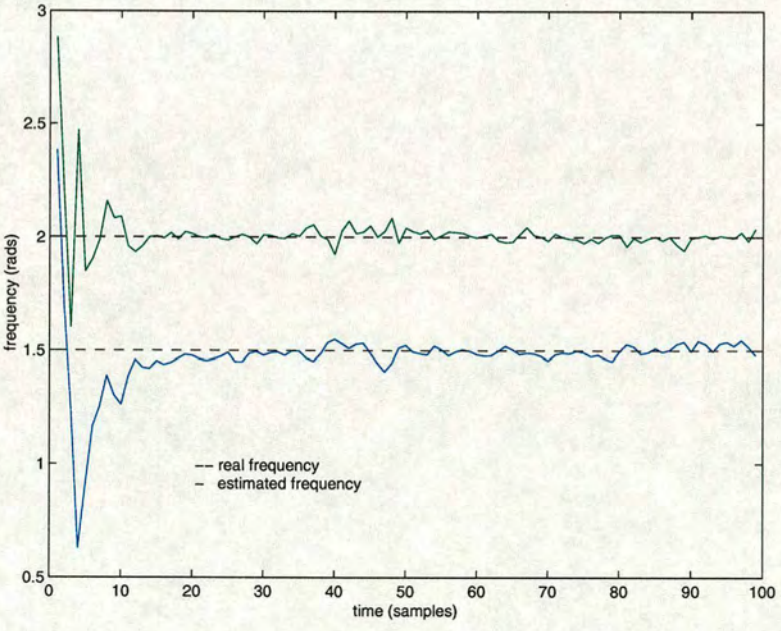

Figure 4.24: *Convergence to the frequencies of two tones with different amplitude (total SNR=30 dB) for a cascade of two second-order filters with initial values* $\omega_1(0) = 2.5$ *and* $\omega_2(0) = 3$ *(*$\mu_\omega = 0.4$ *and* $\rho = 1$*).*

Case E. Frequency hopping tones

This example is intended to show the performance of the algorithm in the task of tracking the frequencies of two tones with hopping frequencies embedded in additive Gaussian noise with a signal-to-noise ratio of 30 dB. The frequency tracks obtained with a cascade of two zero pairs with unitary radius and with an angle adaptation constant of $\mu_\omega = 0.2$ are shown in Fig. 4.25. The value of the adaptation constant was chosen empirically to achieve a relatively slow convergence time while producing a frequency track with relatively low tracking noise.

It can be observed in the figure how the proposed approach effectively tracks the instantaneous

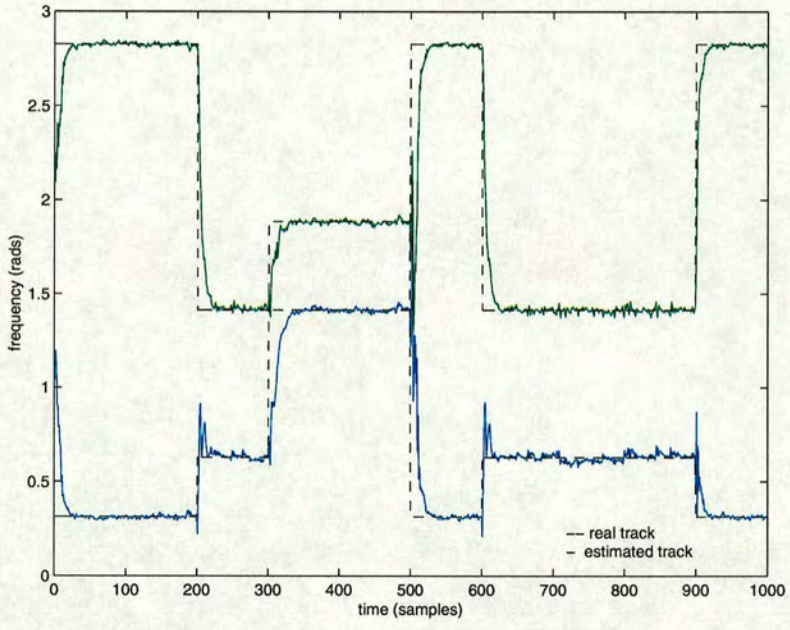

Figure 4.25: *Real and estimated frequency trajectories for a two superimposed tones with hopping frequency (SNR=30dB).*

frequency of each sinusoid. The adaptation constant chosen leads to transitory periods with a duration of around 30 samples after which the frequency tracks stabilise around the instantaneous frequency laws.

For illustration purposes, the Choi-Williams distribution of this signal is displayed in Fig. 4.26. This representation provides a high concentration of energy around the frequency laws of the signals but its estimation is computationally expensive which makes a ridge tracking algorithm based on this representation, a non practical solution.

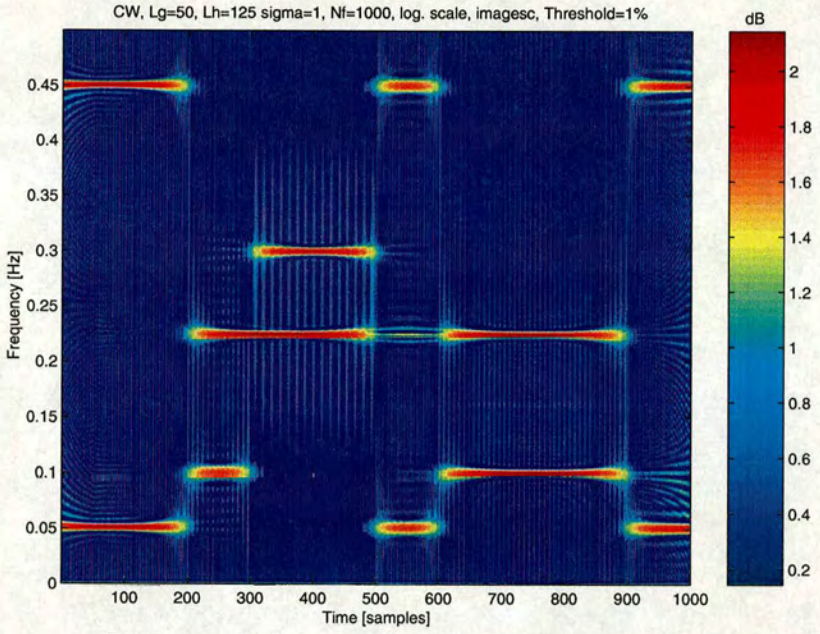

Figure 4.26: *Choi-Williams distribution of two superimposed tones with hopping frequency (SNR=30dB).*

Case F. Crossing chirp signals

In this example a multicomponent time-varying signal consisting of two chirps crossing in the time-frequency plane with constant but different amplitude is analysed:

$$s(n) = \cos(\frac{\pi n}{10} + \frac{4\pi n^2}{10000} + 3\cos(\frac{2n}{100}))$$

$$+3\cos(\frac{9\pi n}{10} - \frac{4\pi n^2}{10000} + 3\cos(\frac{2n}{100})). \tag{4.37}$$

Figure 5.8 shows the frequency trajectories estimated using two zero pairs with $\hat{\rho}(n) = 1$ and $\mu_{\hat{\omega}(n)} = 0.5$, and initial values for the angle of the zeros where set equally spaced over the constraining circumference ($\hat{\omega}_1(0) = \pi/3$ and $\hat{\omega}_2(0) = 2\pi/3$).

A conventional way to determine the frequency trajectory of these chirps would be using the *ridge tracking* algorithm [26], which consist of detecting and joining the peaks of a time-frequency representation such as the *spectrogram*. This would imply a great computational effort required for the estimation of the time-frequency distribution and pick-peaking on a representation with limited resolution.

Results obtained with ridge tracking over the spectrogram of the signal (computed with windows of 20 samples) are provided in Fig. 4.27. There it can be observed how the algorithm fails to provide good instantaneous frequency estimates near the crossing points due to the limited resolution of the spectrogram.

The proposed approach (Fig. 4.28), although yielding inaccurate frequency estimates near the crossing point, represent an advantage over the ridge tracking algorithm in terms of computational complexity, and for its ability to provide instantaneous frequency estimates on a sample-by-sample basis.

It must be noted that the real frequency trajectory of a given sinusoid (lost by a zero after the crossing point in the time-frequency plane) could be recovered by using a second stage to include additional information extracted form the instantaneous frequency estimates. The comparison of frequency estimates sampled at a low rate (in relation to the frequency at which the signal was sampled) can be used to detect changes in frequency trajectory that could be interpreted as the result of crossing in the time-frequency plane.

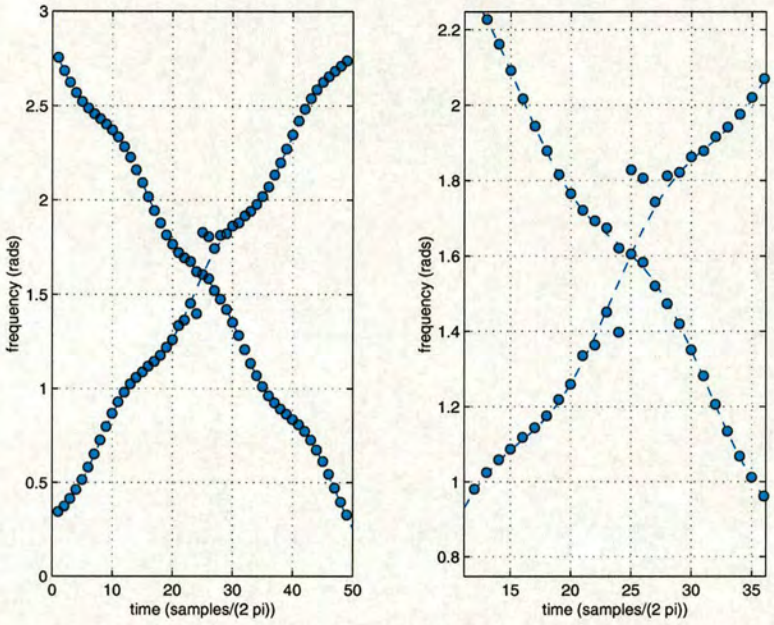

Figure 4.27: *Instantaneous frequency estimates of two chirps crossing in the time-frequency plane using ridge tracking over the spectrogram.*

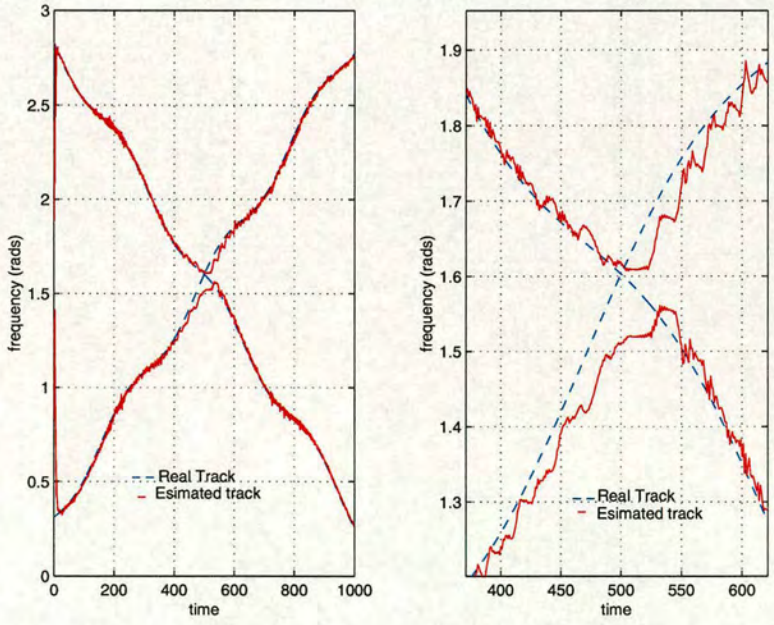

Figure 4.28: *Instantaneous frequency estimates of two chirps crossing in the time-frequency plane using a cascade of two zero pairs.*

Case G.

In this case a multicomponent time-varying signal consisting of two crossing chirp embedded in noise (SNR=15dB) is analysed:

$$s(n) = \cos(\frac{\pi n}{10} + \frac{4\pi n^2}{10000}) + \cos(\frac{9\pi n}{10} - \frac{4\pi n^2}{10000}), \tag{4.38}$$

for the purpose of showing the behaviour of the algorithm in more noisy environments. This signal was analysed with two zero pairs ($\hat{\rho}(n) = 1$ and $\mu_{\hat{\omega}(n)} = 0.3$). The results obtained are illustrated in Fig. 4.29. Despite the noise, the estimated frequency tracks are close to the real values with a mean square error (MSE) of the instantaneous frequency measure obtained after the transitory period was $2.08\ 10^{-3}$ (rads^2).

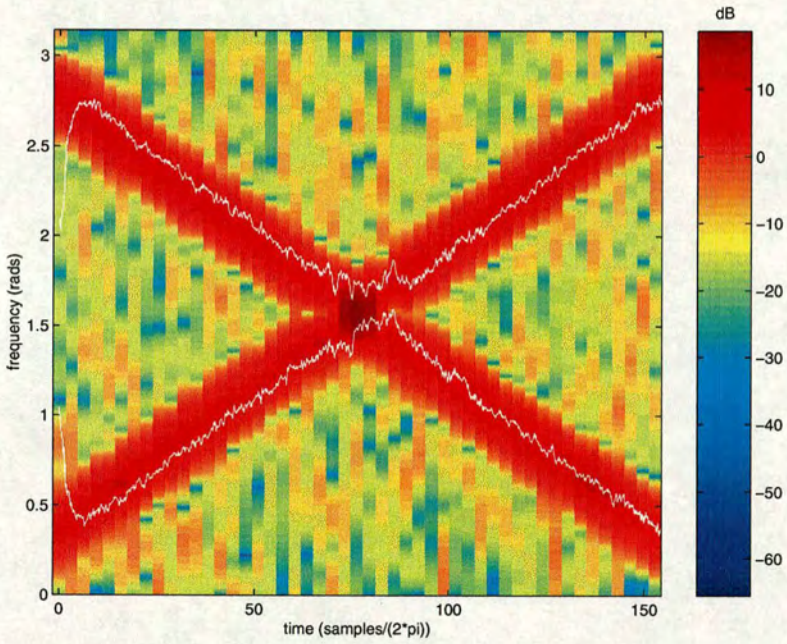

Figure 4.29: *Instantaneous frequency estimates (white lines) of two crossing chirps in noise (SNR=15 dB).*

In figure 4.30, the Wigner distribution of this signal is depicted for the purpose of illustrating that despite of the high resolution achievable with this approach tracking the peaks of this distribution would prove a computationally expensive procedure.

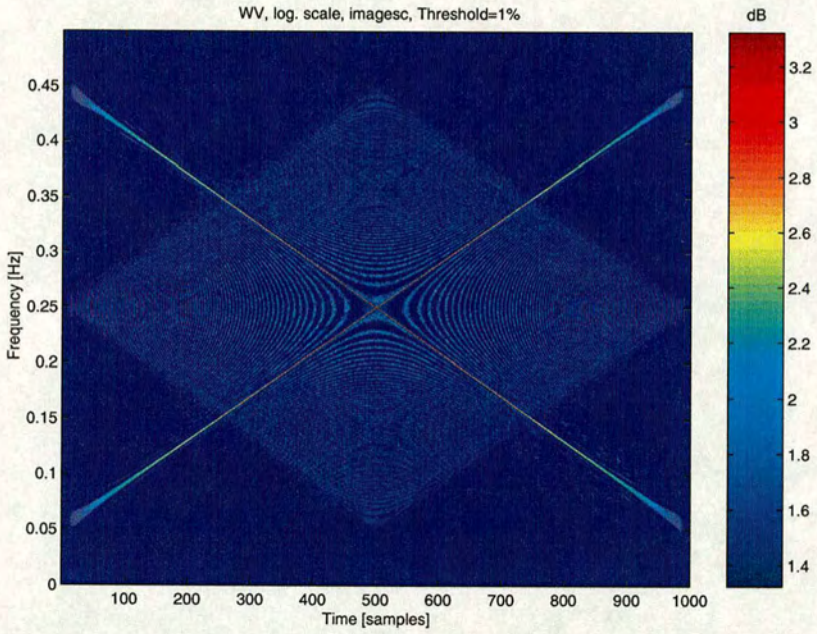

Figure 4.30: *Wigner distribution of two crossing chirps in noise (SNR=15 dB).*

Case H.

The following example is intended to illustrate the effect of using a number of zero pairs inferior to the number of analised sinusoids. The time-varying signal consisting of two crossing chirp embedded in noise (SNR=15dB):

$$s(n) = \cos(\frac{\pi n}{10} + \frac{4\pi n^2}{10000}) + 2\cos(\frac{9\pi n}{10} - \frac{4\pi n^2}{10000}), \tag{4.39}$$

analysed with one zero pair ($\hat{\rho}(n) = 1$,$\omega(0) = 0.5$,$\mu_{\hat{\omega}(n)} = 0.3$). The results obtained in Fig. 4.31 show how the the frequency track estimated is biased towards the frequency trayectory of the signal with greatest amplitude. This result should be expected since the "fuction" of the adaptive filter is to minimise its output energy.

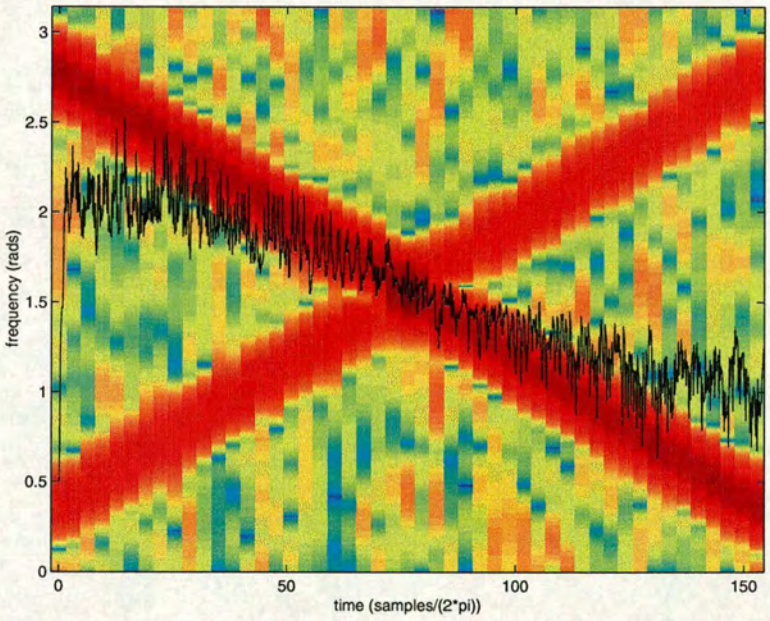

Figure 4.31: *Angle track of one zero-pair (black line) for two crossing chirps in noise (SNR=15 dB).*

Case I. Two tones with sinusoidally modulated frequency overlapping in the time-frequency plane

This example illustrates the flexibility of the proposed algorithm and its ability to track signals overlapping in the the time-frequency plane. The signal analysed is a multicomponent time-varying signal consisting of two sinusoids overlapping in the time-frequency plane :

$$s(n) = \sin[\frac{\pi}{8}\sum_{i=1}^{n}\cos(\frac{\pi i}{200} + \frac{\pi n}{3})] + \sin[\frac{\pi}{8}\sum_{i=1}^{n}\cos(\frac{\pi i}{200} + 0.5\pi n)]. \qquad (4.40)$$

This signal was analysed with two zero pairs ($\hat{\rho} = 1$ and $\mu_{\hat{\omega}} = 0.3$). The estimated frequency trajectories are displayed in Figure 4.32 superimposed over the spectrogram of the signal.

Figure 4.33 illustrates how a pole-zero pair ($r = 0.75$ tuned to the estimated frequency trajectory of one of the components can be used to suppress it.

Finally, the isolated component is treated as a mono-component signal to estimate its amplitude envelope (Fig. 4.34).

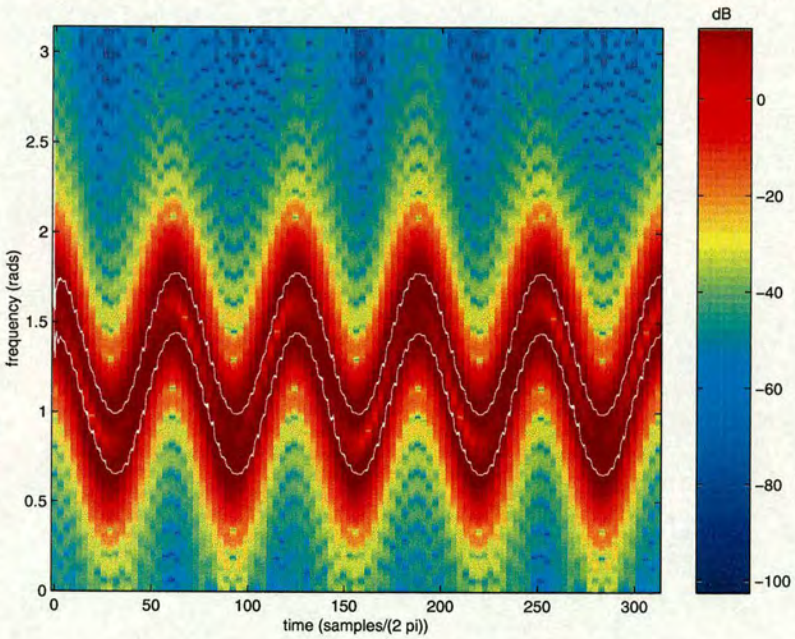

Figure 4.32: *Instantaneous frequency estimates (white lines) of two chirps with sinusoidally-modulated frequency overlapping in the time-frequency plane*

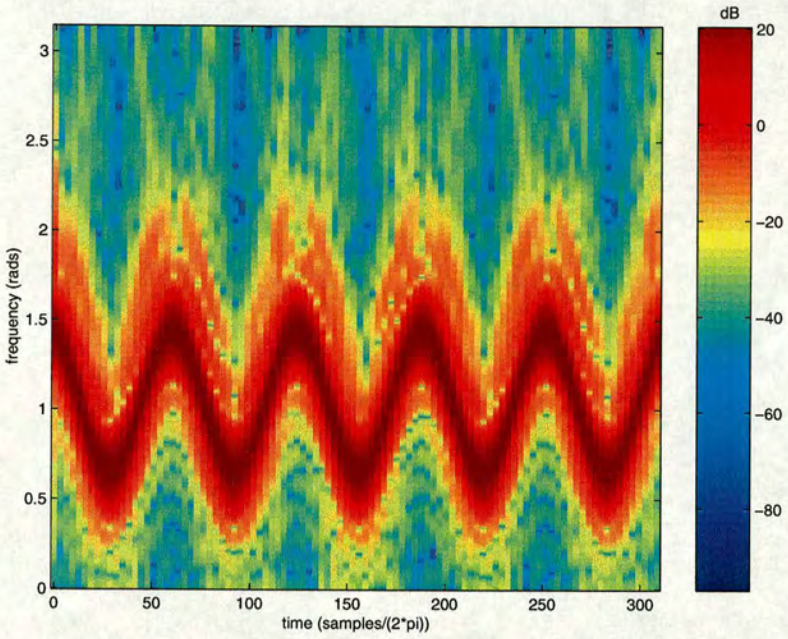

Figure 4.33: *Recovered chirp after notch-filtering the signal of fig. 4.34.*

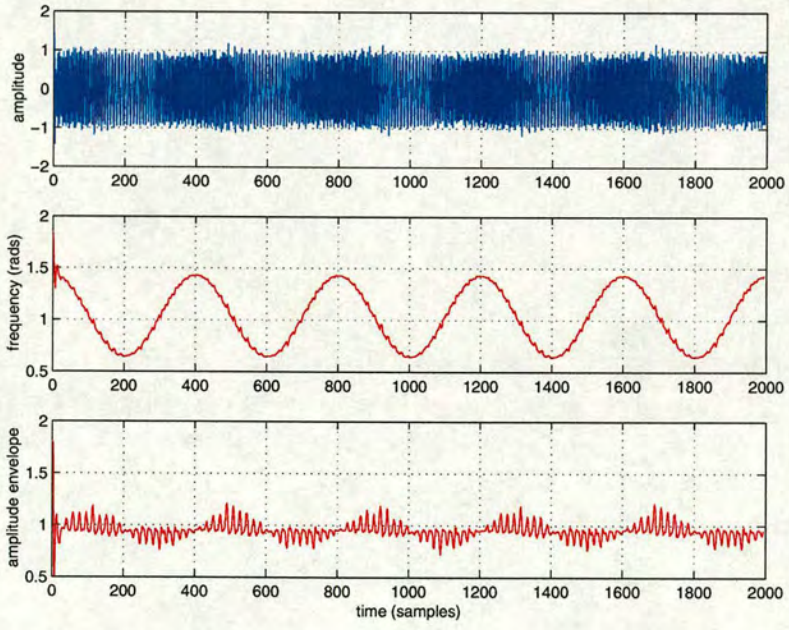

Figure 4.34: *Instantaneous frequency and amplitude envelope for the recovered chirp after notch-filtering the signal of fig. 4.34.*

Case J.

This example illustrates the performance of the proposed approach in the task of analysing a signal composed of three sinusoids with time-varying amplitude and frequency:

$$s(n) = [1 + 0.5\cos(\frac{\pi n}{200})][\sin(\frac{\pi n}{5} + \frac{\pi n^2}{20000})$$

$$+ \sin(\frac{2\pi n}{5} + \frac{\pi n^2}{20000}) + \sin(\frac{3\pi n}{5} + \frac{\pi n^2}{20000})] + \eta(n). \tag{4.41}$$

The additive noise $\eta(n)$ in this case is zero-mean Gaussian and the total SNR is 35dB.

In order to analyse this signal, the instantaneous frequency tracks of each sinusoid were estimated with a cascade of three zero pairs ($\hat{\rho} = 1$ and $\mu_{\hat{\omega}} = 0.3$). The results of this estimation are displayed in Fig. 4.35 where the estimated frequency trajectories are superimposed over the spectrogram of the signal. Subsequently, one component was isolated using a cascade of two pole-zero pairs ($r = 0.8$) as displayed in Fig. 4.36. Finally, the instantaneous amplitude envelope was estimated treating the isolated signal as a mono-component signal as displayed in Fig. 4.37.

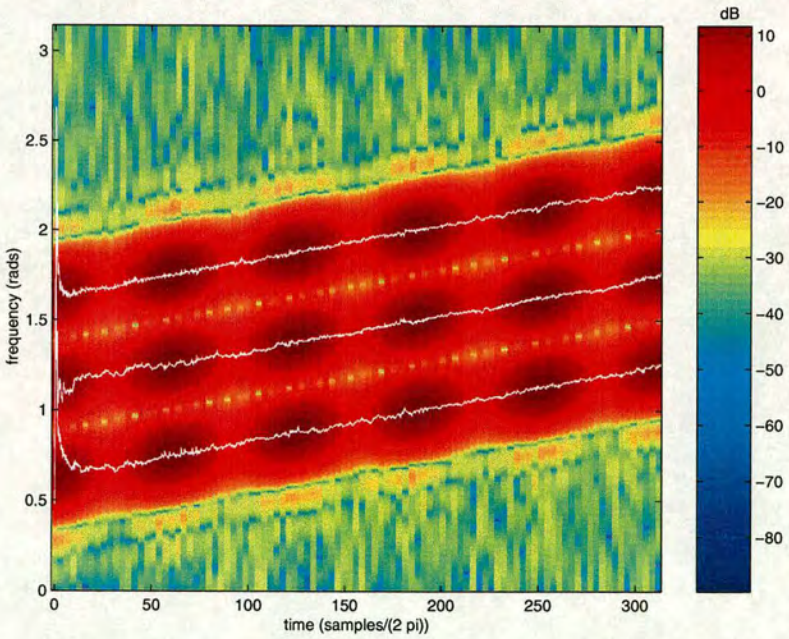

Figure 4.35: *Instantaneous frequency estimates (white lines) of three amplitude and frequency modulated sinusoids.*

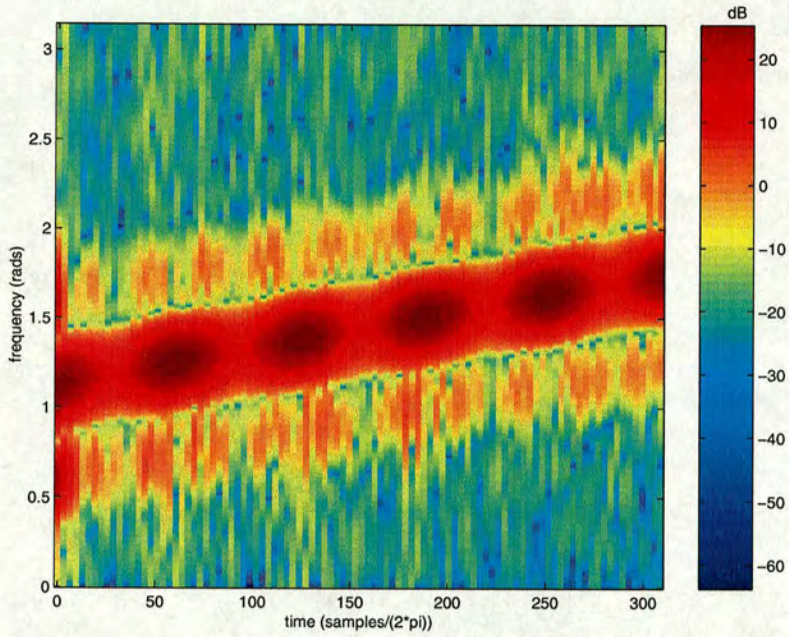

Figure 4.36: *Spectrogram of the sinusoid recovered after notch-filtering (cascade of two pole-zero pairs) the signal of fig. 4.35*

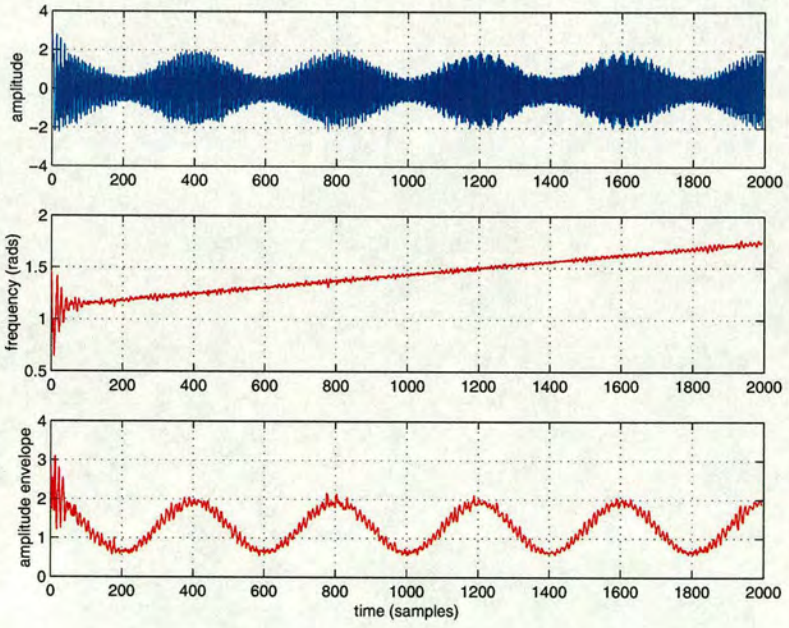

Figure 4.37: *Estimates of instantaneous frequency and amplitude envelope for the isolated sinusoid of fig. 4.35.*

CASE K. Voiced segment of speech

The performance of the proposed approach is finally evaluated in it's ability to estimate the trajectory of the formant frequencies of a voiced segment of speech. This segment of speech, uttered by a male speaker, was initially sampled at 16 kHz and then decimated to 8 kHz. After that, the resonant components of the signal were "preemphasised" using a first-order filter of the form:

$$H(q^{-1}) = 1 - 0.95q^{-1}. \tag{4.42}$$

In order to analyse this signal, the desired parameters are estimated using four zero pairs and the algorithm is locally iterated over windows of 100 samples with $\hat{\rho} = 1$ and $\mu_{\hat{\omega}} = 0.5$.
Fig. 4.38 shows how the estimated formant frequency trajectories match the ridges of the signal's spectrogram, and Fig. 4.39 displays the prediction residual which is characterised by a marked impulsive nature.

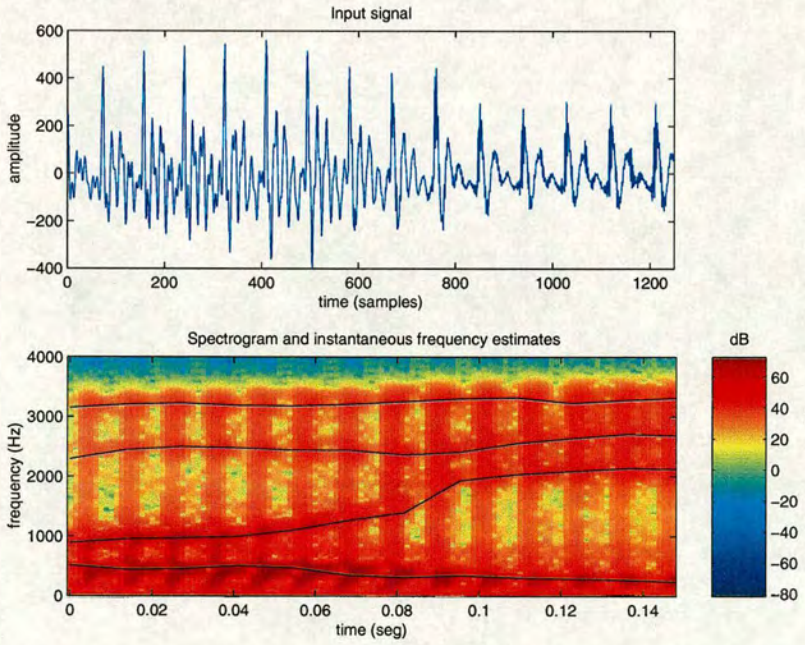

Figure 4.38: *Estimated trajectory of formant frequencies for a voiced segment of speech.*

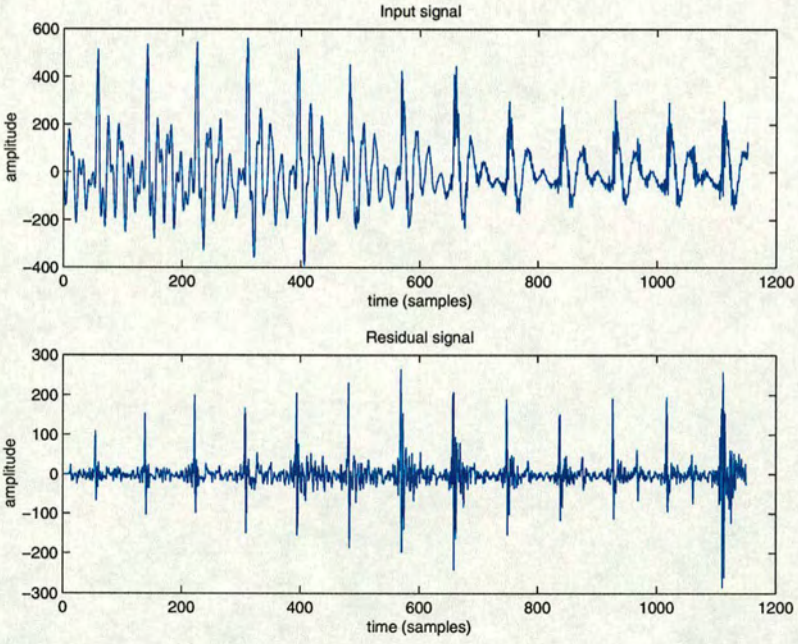

Figure 4.39: *Residual signal obtained after filtering speech with time-varying cascade of predictors.*

4.8 Conclusions

In this chapter, an adaptive technique was introduced to estimate the frequencies of multiple superimposed non-stationary sinusoids. This technique is based on the use of a filter composed by a cascade of *zero pairs* whose parameters are instantaneously estimated to minimise the output energy of the filter. For sinusoids with "slow-varying" amplitude, the *zero pairs* can be constrained to lie on a circle with unitary radius on the *z-plane*.

In addition to the technique proposed for the estimation of multiple instantaneous frequencies, another method was introduced to estimate the amplitude envelope of mono-component signals relying on two consecutive samples.

After the frequency trajectory of each sinusoid has been estimated, a given component of the composite signal can be isolated using a cascade of time-varying notch filters (also referred as *pole-zero pairs*) tuned to the appropriate frequency tracks to cancel all but the desired component. Once a given signal is isolated, its amplitude envelope can be estimated using the two-sample-based algorithm.

The proposed approaches were tested with computer simulations for synthetic and real signals. In the case of synthetic signals, it must be remarked that the proposed approaches was shown to provide instantaneous frequency and amplitude envelope estimates for signals with up to three sinusoidal components. The applicability of the the adaptive zeros approach was consolidated for real signals by estimating the amplitude envelope and instantaneous frequency of a mono-component bat sonar signal and by tracking the formant frequencies of a voiced segment of speech. .

Chapter 5
Adaptive zeros for direct multi-frequency tracking: Spatial domain case

The ideas proposed in Chapter 4 to estimate and track multiple frequencies in the temporal domain, will be extended to the spatial domain in the remaining part of the thesis. The present chapter is therefore intended as an introduction to the ideas involved behind this extension as well as a revision of some closely related approaches that have been explored in the past to estimate and track multiple spatial frequencies.

After the general background review, the approach of signal decomposition via direct parameter estimation and tracking, which is the subject of the research work summarised in this thesis, is explored for tracking the angle of arrival of multiple plane waves impinging on a distributed linear array of uniformly spaced sensors. The technique proposed is focused on the use of large arrays that avoid the necessity of collecting large number of data samples, therefore enabling the tracking of rapidly moving sources.

5.1 Non-stationary exponential signals as models for spatially sampled planar waves.

When a uniformly spaced linear array (ULA) of sensors (antennas) is used to sample a planar electromagnetic wave, the array's output signal can be modelled as an exponential function of the sensors index and therefore a function of a discretely measured space. As will be explained later, the frequency of this exponential signal conveys information about the direction from which this signal is arriving in the array. In the case of multiple planar waves, the array's output can be modelled as multiple exponential signals and the frequency of each of these signals conveys information about the direction of arrival of each planar component of the composite electromagnetic wave.

If the planar waves are produced or reflected by moving sources, the direction of arrivals will vary with time and this will be reflected as multiple sinusoids with non-stationary frequencies at the output of the array.

Among the most widely used techniques for angle of arrival estimation are those based on eigenvalue decomposition (ED) of the autocorrelation matrix of the sensors output measurements.

The preference for these techniques is due to their ability to resolve closely spaced spatial frequencies. Despite the success of these high resolution techniques in the task of estimating the direction of arrival of multiple plane waves impinging on an array of sensors, some problems remain unsolved:

- The computational complexity of these techniques is dramatically affected by the array size limiting their applicability in real-world scenarios. For instance, the problem availability of small numbers of data samples as in the task of tracking rapidilly moving sources, could be solved by using large arrays but this *advantage* cannot be exploited in ED-based algorithms due to their computational complexity dependence on the array's size.
- When relying on ED decomposition the angle of arrival of the different waves are accessed in an indirect way either by peak-picking on a pseudo-spectrum or by extracting the roots of a polynomial. This process of indirect estimation cannot fully exploit of track continuity in an angle-time space in the case of non-stationary sources.

In the following the concepts of narrow-band signals conveyed by planar waves and how this results in exponential signals at the output of a sampling array of sensors will be explained.

The general geometry of a plane wave impinging on a uniform linear array of electromagnetic sensors (antennas) consisting on M elements, is depicted in Fig. 5.1. Assuming that the plane wave is narrowband [77] with *carrier frequency* Ω_c, the noise-free output of the $m-th$ element of the array at time instant t can be modelled as:

$$X(m,t) = A(t)\cos[\Omega_c t + (m-1)\omega(t) + \alpha] \tag{5.1}$$

where

$A(t)$ is the amplitude of the signal

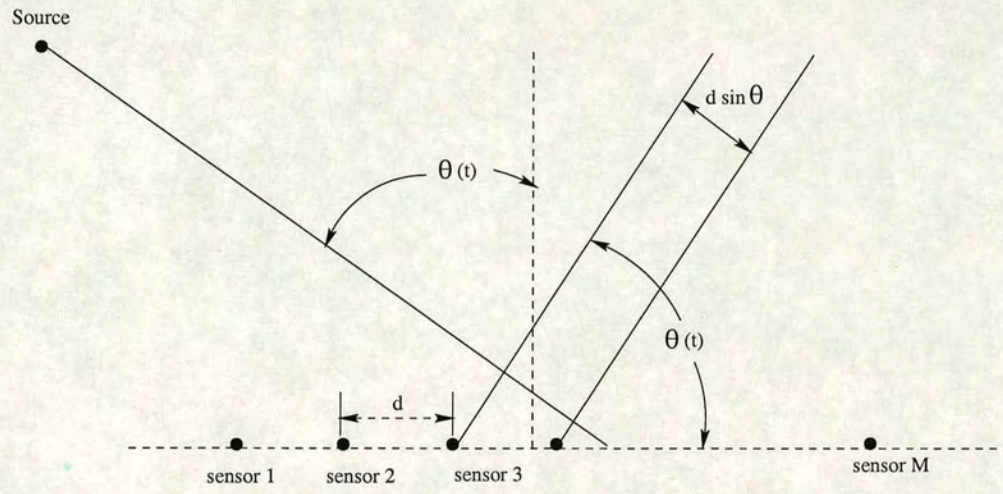

Figure 5.1: *Geommetry of the DOA scenario.*

Ω_c the carrier frequency and

$\omega(t)$ the electrical angle (inter-sensor phase shift) defined by:

$$\omega(t) = \frac{2\pi d}{\lambda} sin(\theta(t)), \tag{5.2}$$

where $\theta(t)$ is the angle of arrival, λ the wavelength and d the inter-sensor distance.

This signal can be demodulated and low-pass filtered (Fig. 5.2) to obtain a sampled complex baseband signal:

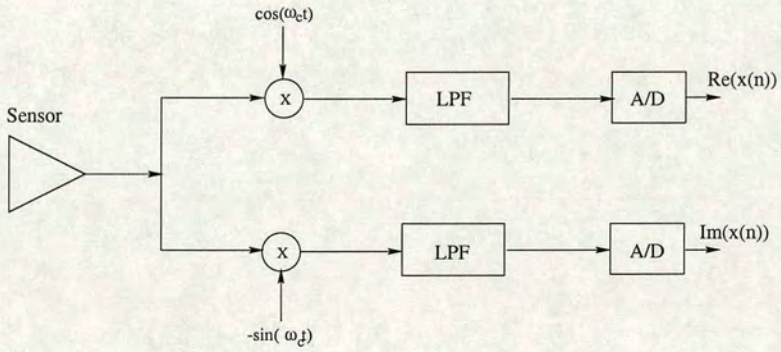

Figure 5.2: *Complex demodulation and low-pass filtering*

$$x(m,n) = s(m,n) + \eta_m(n) = a(n)\exp[j(m-1)\omega(n)] + \eta_m(n) \tag{5.3}$$

where

$a(n)$ represents the sampled amplitude of the signal

$\eta(m,n)$ the *m-th* sensor noise and

$\omega(n)$ the sampled electrical angle:

$$\omega(n) = \frac{2\pi d}{\lambda} \sin(\theta(n)), \tag{5.4}$$

where $\theta(n)$ is the sampled angle of arrival.

Equation (5.3) can be extended to model L plane waves, in which case the combined output of the $m-th$ element will be given by:

$$x(m,n) = \sum_{l=1}^{L} a_l(n) \exp(j(m-1)\omega_l(n)) + \eta(m,n). \tag{5.5}$$

This equation shows how the output of a linear array, upon which are impinging multiple non-stationary plane waves, can be modelled as a superposition of multiple exponential signals with time-varying *spatial frequency*. This fact has motivated the extension of direct multi-frequency estimation and tracking ideas introduced in the previous sections to the spatial domain. In this case the multiple frequencies that should be tracked convey information about the angles at which several plane waves impinge on a linear array with uniformly spaced elements.

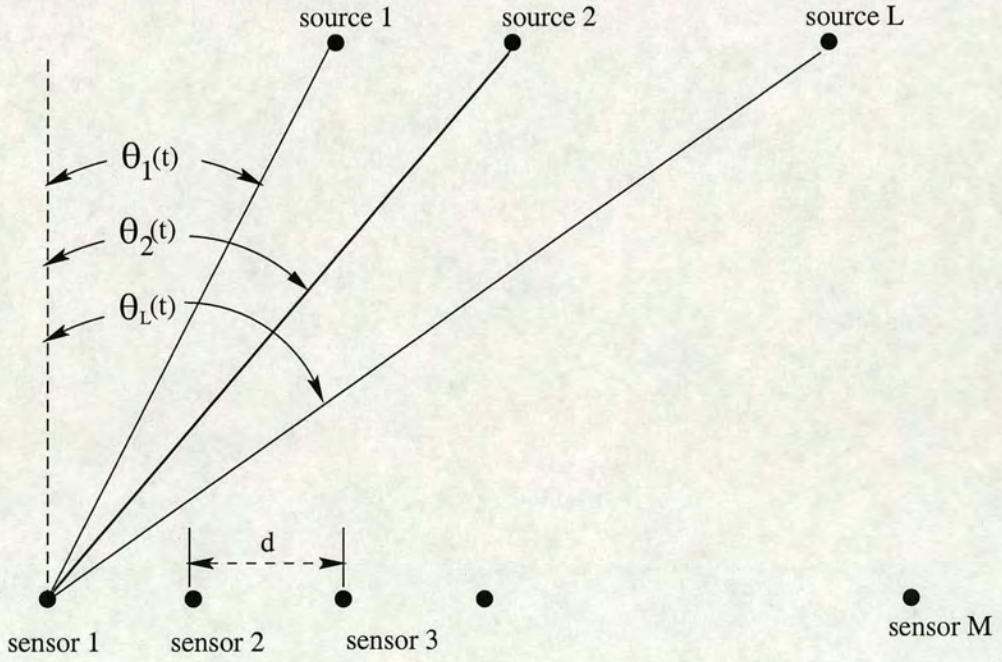

Figure 5.3: *Geometry of the multi-source case.*

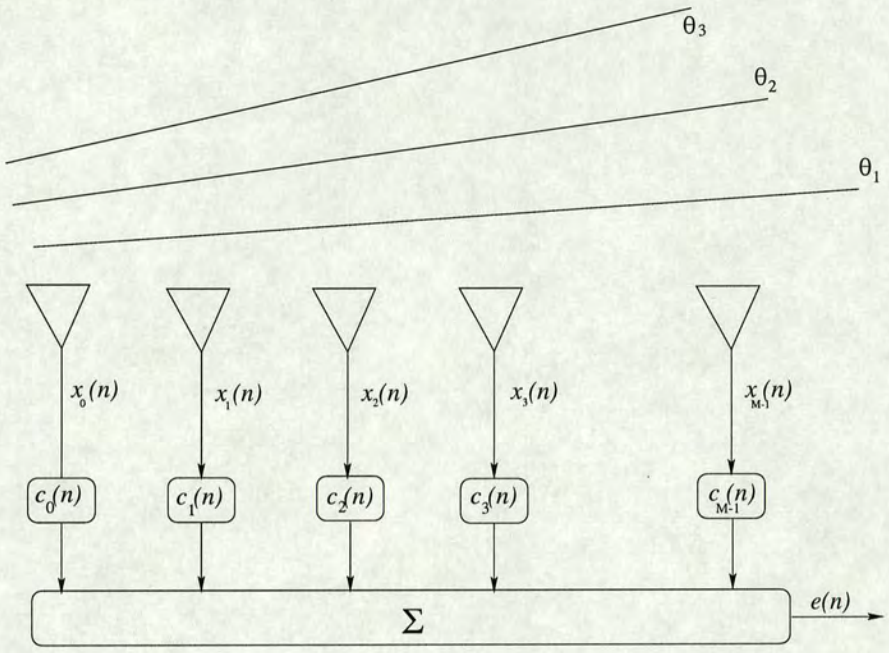

Figure 5.4: *Structure of an array of sensors for multiple angle of arrival estimation.*

5.2 Techniques for stationary direction of arrival estimation

In this section, eigen-decomposition-based approaches to estimate the angles of arrival of multiple stationary plane waves will be briefly described as an introduction to the non-stationary problem. Although other approaches have been explored in the past in the case of stationary scenarios, the high resolution achievable with eigen-decomposition techniques has made this approach one of the preferred solutions in recent years and efforts have been made to extend this approach to the non-stationary scenario.

Equation (5.5) can be expressed in matrix-vector form as:

$$\mathbf{x}(n) = \mathbf{B}(n)\mathbf{a}(n) + \vec{\eta}(n) \tag{5.6}$$

where:

$$\mathbf{x}(n) = [x(0,n)\ x(2,n)\ \ldots\ x(M-1,n)]^T \tag{5.7}$$

represents the sampled output of the array,

$$\mathbf{a}(n) = [a_1(n)\ a_2(n)\ \ldots\ a_L(n)]^T \tag{5.8}$$

the *amplitudes vector*,

$$\vec{\eta}(n) = [\eta(1,n)\ \eta(2,n) \ldots \eta(M,n)]^T \tag{5.9}$$

the noise vector, and

$$\mathbf{B}(n) = [\mathbf{b}_1(n)\ \mathbf{b}_2(n) \ldots \mathbf{b}_L(n)] \tag{5.10}$$

represents the *direction matrix* composed of *direction vectors*:

$$\mathbf{b}_l(n) = [1\ \exp(j\theta_l(n)) \ldots \exp(j(M-1)\theta_l(n))]^T. \tag{5.11}$$

The autocorrelation matrix of the arrays output can be written as:

$$\mathbf{R_x} = E[\mathbf{x}(n)\mathbf{x}(n)^H], \tag{5.12}$$

which can be expanded for *spatially incoherent* noise as:

$$\mathbf{R_x} = \sigma^2\mathbf{I} + \mathbf{B}\mathbf{R_s}\mathbf{B}^H \tag{5.13}$$

where σ^2 represents the noise power and:

$$\mathbf{R_s} = \mathbf{a}\mathbf{a}^H \tag{5.14}$$

the *signal autocorrelation matrix* also known as the *power matrix* .

5.2.1 Direction of arrival estimation using techniques based on eigenvalue decomposition

Assuming stationary exponential signals at the output of the array, the frequency of each component of the signal can be computed by decomposing the autocorrelation matrix $\mathbf{R_x}$ into its eigenvalues and eigenvectors:

$$\mathbf{R_x} = \mathbf{V_s}(\Lambda_s + \sigma^2\mathbf{I})\mathbf{V_s}^H + \mathbf{V}_\eta(\sigma^2\mathbf{I})\mathbf{V}_\eta^H \tag{5.15}$$

where

$$\mathbf{V_s} = [\mathbf{v}_1 \, \mathbf{v}_2 \, \ldots \, \mathbf{v}_p] \tag{5.16}$$

represents the $M \times p$ matrix of signal eigenvectors,

$$\mathbf{V}_\eta = [\mathbf{v}_{p+1} \, \mathbf{v}_{p+2} \, \ldots \, \mathbf{v}_M] \tag{5.17}$$

the $M \times (M-p)$ matrix of noise eigenvectors and $\Lambda_\mathbf{s}$ a diagonal matrix containing the eigenvalues of the signal.

The space spanned by the signal eigenvector is denominated *signal subspace* while the space spanned by the signal eigenvector is denominated *noise subspace*. It can be proven [55] that each of the signals vectors $\mathbf{b}_l$ lies in the *signal subspace* and therefore the frequencies of each exponential can be estimated by peak-picking on a pseudo-spectral function of the form:

$$PD(\exp(j\Omega)) = \frac{1}{\sum_{i=p+1}^{M} \alpha_i |\mathbf{b}^H \mathbf{v}_i|^2} \tag{5.18}$$

where

$$\mathbf{b} = [1 \; \exp(j\Omega) \ldots \exp(j(M-1)\Omega)]^T. \tag{5.19}$$

or by finding the roots of a filter of the form:

$$C(q^{-1}) = \sum_{i=p+1}^{M} \alpha_i V_i(q^{-1}) \tag{5.20}$$

where

$$V_i(q^{-1}) = \sum_{k=0}^{M-1} v_i(k) q^{-k} \tag{5.21}$$

is the *eigenfilter* associated with the $i-th$ eigenvector.

Several frequency estimation techniques encompassed under this approach are detailed below:

where

$$\mathbf{V_s} = [\mathbf{v}_1 \ \mathbf{v}_2 \ \ldots \ \mathbf{v}_p] \tag{5.16}$$

represents the $M \times p$ matrix of signal eigenvectors,

$$\mathbf{V}_\eta = [\mathbf{v}_{p+1} \ \mathbf{v}_{p+2} \ \ldots \ \mathbf{v}_M] \tag{5.17}$$

the $M \times (M-p)$ matrix of noise eigenvectors and $\Lambda_\mathbf{s}$ a diagonal matrix containing the eigenvalues of the signal.

The space spanned by the signal eigenvector is denominated *signal subspace* while the space spanned by the signal eigenvector is denominated *noise subspace*. It can be proven [55] that each of the signals vectors $\mathbf{b}_l$ lies in the *signal subspace* and therefore the frequencies of each exponential can be estimated by peak-picking on a pseudo-spectral function of the form:

$$PD(\exp(j\Omega)) = \frac{1}{\sum_{i=p+1}^{M} \alpha_i |\mathbf{b}^H \mathbf{v}_i|^2} \tag{5.18}$$

where

$$\mathbf{b} = [1 \ \exp(j\Omega) \ \ldots \ \exp(j(M-1)\Omega)]^T. \tag{5.19}$$

or by finding the roots of a filter of the form:

$$C(q^{-1}) = \sum_{i=p+1}^{M} \alpha_i V_i(q^{-1}) \tag{5.20}$$

where

$$V_i(q^{-1}) = \sum_{k=0}^{M-1} v_i(k) q^{-k} \tag{5.21}$$

is the *eigenfilter* associated with the $i-th$ eigenvector.

Several frequency estimation techniques encompassed under this approach are detailed below:

- **Pisarenko Harmonic decomposition** with frequency estimation function given by [55]:

$$PD(\exp(j\Omega) = \frac{1}{|\mathbf{b}^H \mathbf{v}_{min}|^2} \tag{5.22}$$

and filter

$$C(q^{-1}) = V_{min}(q^{-1}) = \sum_{k=0}^{M-1} v_{min}(k) q^{-k} \tag{5.23}$$

where v_{min} represents eigenvector associated with minimum eigenvalue.

- **MUltiple SIgnal Classification** (MUSIC) with frequency estimation function given by [55]:

$$PD(\exp(j\Omega)) = \frac{1}{\sum_{i=p+1}^{M} |\mathbf{b}^H \mathbf{v}_i|^2}, \tag{5.24}$$

and filter

$$C(q^{-1}) = \sum_{i=p+1}^{M} V_i(q^{-1}). \tag{5.25}$$

- **Minimum norm algorithm** with frequency estimation function given by [55]:

$$PD_{MN}(\exp(j\Omega)) = \frac{1}{|\mathbf{b}^H \mathbf{c}_{MN}|^2}, \tag{5.26}$$

and filter

$$C(q^{-1}) = \sum_{k=0}^{M-1} c_{MN}(k) q^{-k} \tag{5.27}$$

where $\mathbf{c}_{MN}$ is a vector lying on the noise subspace with minimum norm and first element equal to one. In terms of noise eigenvectors of the autocorrelation matrix, this vector can be found as [55] :

$$\mathbf{v}_{MN} = \frac{(\mathbf{V}_\eta \mathbf{V}_\eta^H)\mathbf{u}_1}{\mathbf{u}_1^H (\mathbf{V}_\eta \mathbf{V}_\eta^H)\mathbf{u}_1}, \tag{5.28}$$

where

$$\mathbf{u}_1 = [1\ 0\ \ldots\ 0]^T. \tag{5.29}$$

These techniques have been extensively used in the past providing an indirect way to estimate angle of arrival of multiple plane waves.

5.3 Direction of arrival estimation for multiple non-stationary plane waves

Measuring time-varying spatial frequencies is not a trivial task as the characteristics of the analysed signals are non-stationary making inappropriate the stationary approaches described in the previous section. Despite the difficulty of this problem, the necessity of solving it has motivated the search for appropriate signal processing techniques and several solution have been proposed recently.

Among the techniques studied are:

- Adaptive eigenvalue methods.
- Direct recursive update of the angles of arrival.
- Adaptive null-steering.

These techniques will briefly introduced in the following lines to set the context background for the approach proposed in this thesis.

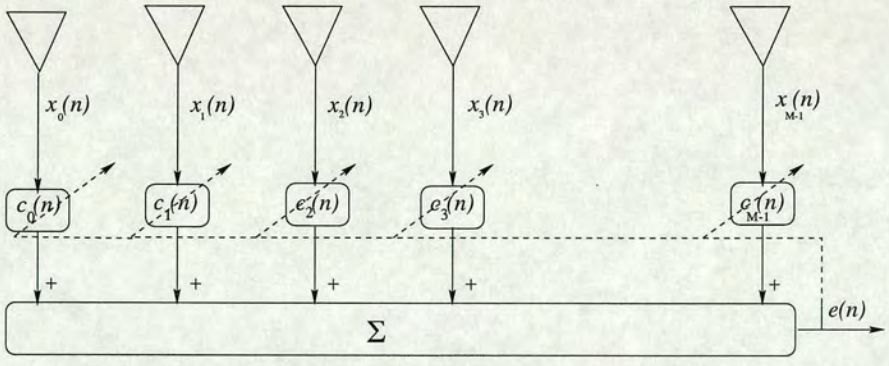

Figure 5.5: *Adaptive array*

5.3.1 Adaptive subspace techniques

The idea behind this approach is to adaptively estimate the eigenvalues belonging to the noise subspace. Algorithms exploiting this approach are characterised by two stages: A first stage used to update the noise eigenvectors and a second stage to estimate the roots of the resulting filter polynomial. As both stages aim at the appropriate utilisation of previously estimated parameters, efficient eigenvector and root updating algorithms have been proposed.

In the following lines, this idea is illustrated with the description of one algorithm for the adaptive estimation of the least eigenvector.

Adaptive estimation of the least eigenvector (adaptive Pisarenko)
The Pisarenko eigenvalue problem is equivalent to the minimisation of [79]:

$$\mathbf{c}^T\mathbf{R}_\mathbf{x}\mathbf{c} = min \tag{5.30}$$

subject to the constraint

$$\mathbf{c}^T\mathbf{c} = 1. \tag{5.31}$$

The solution to this minimisation problem is the *least eigenvector*:

$$\mathbf{c} = \mathbf{v}_{min}. \tag{5.32}$$

This minimisation problem can be solved iteratively by using a constrained Lest Mean Squares algorithm [80][57]:

$$\mathbf{c}(n+1) = \bar{\mathbf{c}}(n) + \Delta\mathbf{c}(n) \tag{5.33}$$

$$\Delta\mathbf{c}(n) = 2\mu\bar{\mathbf{c}}^H(n)\mathbf{x}(n)\mathbf{x}(n) \tag{5.34}$$

$$\bar{\mathbf{c}}(n+1) = \frac{\mathbf{c}(n+1)}{||\mathbf{c}(n+1)||} \tag{5.35}$$

This adaptive approach can be used in conjunction with a root extraction step to adaptively estimate the angles of arrival of multiple plane wave. However, as the parameters of interest are

5.3.1 Adaptive subspace techniques

The idea behind this approach is to adaptively estimate the eigenvalues belonging to the noise subspace. Algorithms exploiting this approach are characterised by two stages: A first stage used to update the noise eigenvectors and a second stage to estimate the roots of the resulting filter polynomial. As both stages aim at the appropriate utilisation of previously estimated parameters, efficient eigenvector and root updating algorithms have been proposed.

In the following lines, this idea is illustrated with the description of one algorithm for the adaptive estimation of the least eigenvector.

Adaptive estimation of the least eigenvector (adaptive Pisarenko)
The Pisarenko eigenvalue problem is equivalent to the minimisation of [79]:

$$\mathbf{c}^T \mathbf{R}_\mathbf{x} \mathbf{c} = min \tag{5.30}$$

subject to the constraint

$$\mathbf{c}^T \mathbf{c} = 1. \tag{5.31}$$

The solution to this minimisation problem is the *least eigenvector*:

$$\mathbf{c} = \mathbf{v}_{min}. \tag{5.32}$$

This minimisation problem can be solved iteratively by using a constrained Lest Mean Squares algorithm [80][57]:

$$\mathbf{c}(n+1) = \bar{\mathbf{c}}(n) + \Delta\mathbf{c}(n) \tag{5.33}$$

$$\Delta\mathbf{c}(n) = 2\mu\bar{\mathbf{c}}^H(n)\mathbf{x}(n)\mathbf{x}(n) \tag{5.34}$$

$$\bar{\mathbf{c}}(n+1) = \frac{\mathbf{c}(n+1)}{||\mathbf{c}(n+1)||} \tag{5.35}$$

This adaptive approach can be used in conjunction with a root extraction step to adaptively estimate the angles of arrival of multiple plane wave. However, as the parameters of interest are

the roots and not the coefficients of the filters, some researchers have explored the possibility of directly adapting these roots .

Adaptive root tracking algorithms

In [79] a technique to directly adapt the roots (zeros) of the filter instead of its coefficients was proposed. The update of the zeros is performed to make the algorithm equivalent to the LMS algorithm. This ideas will be briefly explained in the following lines.

A filter of the form:

$$\mathbf{C}(q^{-1}, n) = c_0(n) + c_1(n)q^{-1} + c_2(n)q^{-2} + ... + c_{M-1}(n)q^{-(M-1)} \tag{5.36}$$

can be factored as:

$$= c_0(1 - z_1(n)q^{-1})(1 - z_2(n)q^{-1})...(1 - z_{M-1}(n)q^{-1}) \tag{5.37}$$

where $z_l(n)$ represents the $l - th$ complex root of the polynomial $\mathbf{C}_i(q^{-1}, n)$.

Using a the gradient based algorithm, the $l - th$ root update formula is given by:

$$z_l(n+1) = z_l(n) + \Delta z_l(n) \tag{5.38}$$

where the increment $\Delta z_l(n)$ can be determined in a way that is equivalent to the LMS algorithm to ensure the asymptotic convergence of $z_l(n)$ to its optimal value.

From (5.37) an increment in a root value can be expressed as a function of the coefficients of the filter through:

$$\Delta z_l(n) = \sum_{m=0}^{M-1} \frac{\partial z_l(n)}{\partial c_m(n)} \Delta c_m(n) \tag{5.39}$$

where the partial derivatives are given by:

$$\frac{\partial z_l(n)}{\partial c_m(n)} = -\frac{1}{c_0(n)} \frac{z_l(n)^{(M-1-m)}}{\prod_{k \neq j}(z_j(n) - z_k(n))} \tag{5.40}$$

the roots and not the coefficients of the filters, some researchers have explored the possibility of directly adapting these roots .

Adaptive root tracking algorithms

In [79] a technique to directly adapt the roots (zeros) of the filter instead of its coefficients was proposed. The update of the zeros is performed to make the algorithm equivalent to the LMS algorithm. This ideas will be briefly explained in the following lines.

A filter of the form:

$$\mathbf{C}(q^{-1}, n) = c_0(n) + c_1(n)q^{-1} + c_2(n)q^{-2} + ... + c_{M-1}(n)q^{-(M-1)} \tag{5.36}$$

can be factored as:

$$= c_0(1 - z_1(n)q^{-1})(1 - z_2(n)q^{-1})...(1 - z_{M-1}(n)q^{-1}) \tag{5.37}$$

where $z_l(n)$ represents the $l - th$ complex root of the polynomial $\mathbf{C}_i(q^{-1}, n)$.

Using a the gradient based algorithm, the $l - th$ root update formula is given by:

$$z_l(n+1) = z_l(n) + \Delta z_l(n) \tag{5.38}$$

where the increment $\Delta z_l(n)$ can be determined in a way that is equivalent to the LMS algorithm to ensure the asymptotic convergence of $z_l(n)$ to its optimal value.

From (5.37) an increment in a root value can be expressed as a function of the coefficients of the filter through:

$$\Delta z_l(n) = \sum_{m=0}^{M-1} \frac{\partial z_l(n)}{\partial c_m(n)} \Delta c_m(n) \tag{5.39}$$

where the partial derivatives are given by:

$$\frac{\partial z_l(n)}{\partial c_m(n)} = -\frac{1}{c_0(n)} \frac{z_l(n)^{(M-1-m)}}{\prod_{k \neq j}(z_j(n) - z_k(n))} \tag{5.40}$$

Using the LMS algorithm, the increment in the filter coefficients $\Delta c_m(n)$ can be expressed as:

$$\Delta c_m(n) = 2\mu e(n) x_m(n) \tag{5.41}$$

where $e(n)$ represents the output of the array. A detailed derivation of the above algorithm can be found in [79] in conjunction with a convergence and stability analysis. This approach was used in [80] in conjunction with the adaptive Pisarenko technique, to separate directional signals using a master-slave structure.

Other algorithms have been proposed in [81] [82] and [83] to adaptively estimate a filter associated with the eigenvector lying on the noise subspace combined with efficient root updating schemes to adapt the roots of the filter. However, these approaches constitute however indirect ways to compute the angles of arrival which has motivated the research work presented in the next chapter to directly update the electrical angles (*spatial frequencies*) estimates.

5.3.2 Direct recursive update of the angles estimates

This approach first proposed in [84] and later refined in [85], consists of the direct recursive updating of the angles estimates by relating the changes in the autocorrelation matrix to those in the values of the angles.

$$\mathbf{R} = \sigma^2 \mathbf{I} + \mathbf{B}\mathbf{P}\mathbf{B}^H \tag{5.42}$$

The unrefined algorithm proposed in [84] can be briefly described in the following steps:

1. Compute a first estimate of the array output autocorrelation matrix $\mathbf{R_x}(0)$. Apply the MUSIC algorithm to obtain initial estimates of the angles of arrival $\bar{\theta} = [\theta_1\ \theta_2\ ..\ \theta_L]$, the noise power σ^2, the direction matrix $\mathbf{B}(0)$ and the signal autocorrelation matrix $\mathbf{R_x}(0)$ by solving Eq. (5.42)

2. Recursively estimate the angles by solving the equation:

$$\mathbf{G}\Delta\theta = \mathbf{y} \tag{5.43}$$

where

$$\mathbf{G} = j\frac{2\pi}{\lambda}d \begin{bmatrix} \cos(\theta_1)\gamma_1\psi_1 & \dots & \cos(\theta_L)\gamma_L\psi_L \\ 2\cos(\theta_1)\gamma_1^2\psi_1 & \dots & 2\cos(\theta_L)\gamma_L^2\psi_L \\ . & \dots & . \\ . & \dots & . \\ (M-1)\cos(\theta_1)\gamma_1^{(M-1)}\psi_1 & \dots & (M-1)\cos(\theta_L)\gamma^(M-1)_L\psi_L \end{bmatrix} \tag{5.44}$$

where

$$\gamma_i = \exp(j2\pi d\sin(\theta_i)/\lambda)$$

$$\Delta\bar{\theta}(k) = \bar{\theta}(k) - \bar{\theta}(k)$$

$[\psi_1, \psi_2, ..., \psi_M]^T$ =first row of $\mathbf{A}_{k-1}\mathbf{R}_\mathbf{x}$

$\mathbf{y}$= first column of $\Delta\mathbf{R}$ with first element deleted

3. Update the angle estimates and go to step 1.

5.3.3 Adaptive null steering

A final approach reviewed here is the design of spatial filters to direct nulls at directional signal researched in [89] and [90]. The idea in this approach consists on directing nulls at directional signals by using a gradient-based techniques to minimise the array's output power.

For a spatial filter of the form:

$$C(q^{-1}) = 1 + \sum_{k=1}^{M-1} c_k q^{-k} \tag{5.45}$$

which can be expressed in factored form as:

$$C(q^{-1}) = \prod_{k=1}^{M-1} (1 + z_k q^{-1}) \tag{5.46}$$

where z_k is the $k - th$ complex response zero.

If the filter coefficients are chosen in such a way that z_k corresponds to a phase shift ω_k, the filter will have nulls at $M - 1$ directions defined as:

$$\omega_k = \frac{2\pi d \sin(\theta)}{\lambda}, \quad k = 1, ..., M - 1. \tag{5.47}$$

A way to estimate each complex zero in a cyclical manner is by using the LMS algorithm in conjunction with a filter decomposing scheme. For example, if we want to compute the zero z_l, the filter $C(q^{-1})$ can be decomposed in the form :

$$C(q^{-1}) = (q - z_l) C_l(q^{-1}), \tag{5.48}$$

where

$$D_l(q^{-1}) = \prod_{\substack{k=1 \\ \neq l}} (q - z_k). \tag{5.49}$$

This structure is depicted in figure (5.6) where the zero z_l is the complex weight in the last stage of the structure.

Finally, the LMS algorithm [57]can be used to update the complex zero z_l on a sample-by-sample basis according to :

$$z_l(n + 1) = z_l(n) + \mu e^* v_l \tag{5.50}$$

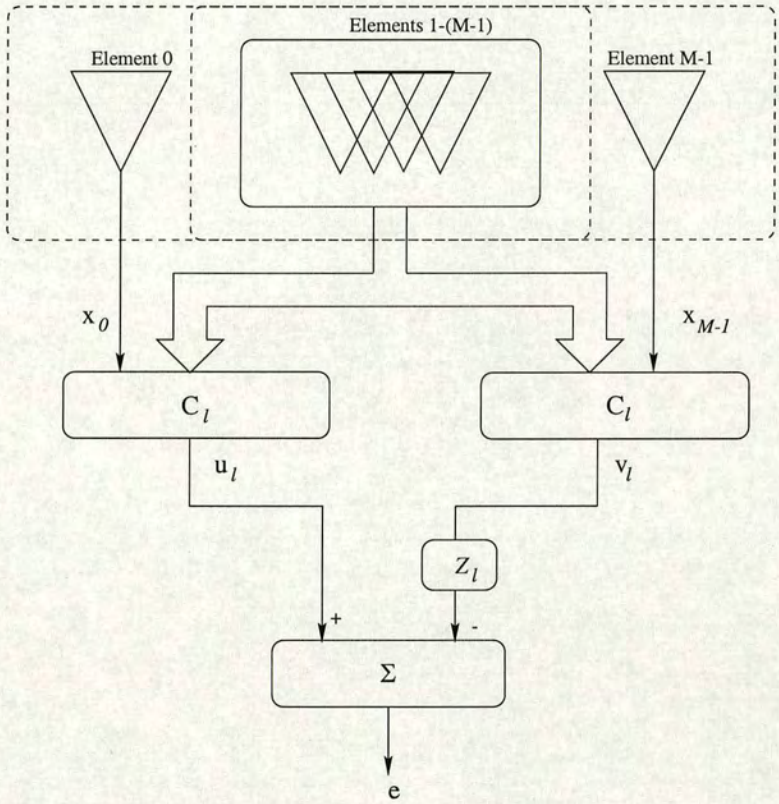

Figure 5.6: *Processing structure for adjusting the filter zeros with two spatially shifted M-element subarrays.*

5.4 Adaptive zeros for direct multi-frequency tracking. Spatial domain case

The approach proposed in this chapter is based on the concepts of adaptive nulling introduced in the previous section which have been used in the past to reduce the effect of narrow-band interference and to estimate the directions of arrival of multiple plane waves. In this approach, each directional signal is first isolated by using an spatial filter whose zeros are found to cancel all other directional signals. Once the directional signal is isolated, a second stage is used to estimate the angle of arrival using a gradient descent technique that, due to the decomposition procedure, is proven to lead to one only optimal solution. Although the algorithm proposed has the theoretical pre-requisite of the initial zeros being chosen to cancel (to a sufficient level) directional signals, this has proven empirically to be a non-restrictive requisite.

Despite its close relation to previously proposed techniques, the algorithm proposed here makes use of a gradient descent technique to ***directly estimate*** the electrical angles. This emphasis although subtle allows the on-line angle tracking procedure presented here.

5.4.1 Direct estimation of electrical angle based on a gradient-descent technique: single component case

The algorithm proposed here can be decomposed into two sections: the first allows the spatial decomposition of the array output while the second is used to estimate the angle of the isolated component. The analysis will be started by studying the case of a single wave impinging on the array. For this case, the output of an spatial error predictor filter (first-order) applied to the array output can be defined as:

$$e(m,n) = x(m,n) - z\, x(m-1,n) \tag{5.51}$$

where $z = \hat{\rho}\exp(j\hat{\omega})$ represents the filter's zero and $x(m,n)$ the output of the m-th sensor at discrete-time instant n. The mean square error (MSE) of the filter output, assuming spatio-temporal stationarity and zero constrained to be on the unit circle ($\hat{\rho} = 1$), can be defined as:

$$\xi = E[e(m,n)e^*(m,n)],$$

$$= 2(r(0) - |(r(1))| \cos(\arg\{r(1)\} - \hat{\omega})), \tag{5.52}$$

where the spatial correlations $r(0)$ and $r(1)$ are given by:

$$r(0) = E[x(m,n)x^*(m,n)], \tag{5.53}$$

and

$$r(1) = E[x(m,n)x^*(m-1,n)]. \tag{5.54}$$

Modelling the array output as :

$$x(m,n) = s(n) \exp(j\omega(n)(m-1)) + \eta(m,n) \tag{5.55}$$

where $\eta(m,n)$ represents spatio-temporally white Gaussian noise with variance σ^2, it can be shown that:

$$r(1) = E[x(m,n)x^*(m-1,n)] = P \exp j\omega(n) \tag{5.56}$$

and

$$r(0) = E[x(m,n)x^*(m,n)] = P + \sigma^2 \tag{5.57}$$

where

$$P = E[|s(n)|^2].$$

An optimal phase for the spatial predictor predictor (with zero constrained to be on the unit circle) can be computed using a gradient descent technique to minimise the MSE (5.52):

$$\hat{\omega}^o = argmin[\xi]. \tag{5.58}$$

In this case the update equation is given by:

$$\hat{\omega}(k+1) = \hat{\omega}(k) + \Delta\hat{\omega}(k) \tag{5.59}$$

where:

$$\Delta\hat{\omega}(k) = -\mu\frac{\partial\xi}{\partial\hat{\omega}} \tag{5.60}$$

and where:

$$\frac{\partial\xi}{\partial\hat{\omega}} = j(r(1)^* \exp(j\hat{\omega}) - r(1)\exp(-j\hat{\omega})), \tag{5.61}$$

$$= |(r(1))| \sin(\arg\{r(1)\} - \hat{\omega}).$$

5.4.2 Isolating and tracking multiple spatially distributed sources

In this section it will be shown how a decomposed spatial predictor can be used to isolate the components of the array output to permit the subsequent use of the gradient-based estimation procedure proposed in the previous section to estimate the instantaneous angle of the residual signal.

Suppose that in the course of tracking the directions-of-arrival of several plane waves an initial estimate of the desired angles is available. The array output can then be suppressed with a spatial predictor whose zeros are located at these angles:

$$e_{tot}(m) = \mathrm{x}^T(m)\mathbf{wtot} \tag{5.62}$$

where:

$$\mathrm{x}^T(m,n) = [x(m,n), x(m-1,n), ..., x(m-p,n)]$$

and

$$\mathbf{wtot} = \prod_{i=1}^{p}(*)[1, -z_i]$$

where $\prod(*)$ represents the multiple convolution operation, and $z_i = \exp(j\hat{\omega}_i)$ the $i-th$ cancelling zero. A spatial component can be isolated in similar way by implementing a partial

predictor imposing zeros in all angles except at the one of interest.

$$e_l(m) = \mathrm{x}^T(m)\mathrm{w}_l \tag{5.63}$$

where

$$\mathrm{w}_l = \prod_{\substack{i=1 \\ i \neq l}}^{p} (*)[1, -z_i]$$

The lag-one spatial correlation (5.54) of the partial residual (5.63) is given by:

$$\hat{r}_l(1) = E[e_l(m)e_l^*(m-1)] = \mathrm{w}_l^H \mathrm{Q}^T \mathrm{w}_l \tag{5.64}$$

where Q is a p by p matrix :

$$\mathrm{Q} = E[\mathrm{x}(m)\mathrm{x}^H(m-1)] \tag{5.65}$$

and where:

$$\mathrm{x}^T(m,n) = [x(m,n), x(m-1,n), ..., x(m-(p-1),n)]$$

for $m \geq M - p + 1$. The elements of this matrix are then given by:

$$q_{i,j} = r(\alpha_{i,j}) = E[x(m,n)x^*(m-\alpha_{i,j},n)] \tag{5.66}$$

where $\alpha_{i,j} = i - j + 1$ for $i, j = 1, 2, ..., p$. An estimate of these elements from the available data can be computed as:

$$\hat{q}_{i,j} = \frac{1}{(M-\alpha_{i,j})N} \sum_{n=1}^{N} \sum_{m=1+\alpha_{i,j}}^{M} x(m,n)x^*(m-\alpha_{i,j},n) \tag{5.67}$$

where $\alpha_{i,j} = i - j + 1$ for $i, j = 1, 2, ..., p$.

Finally equations (5.59)-(5.61) and (5.64) can be combined to estimate the angle of the isolated component with the following algorithm:

Initialise $\{\hat{\omega}_l(0),\ for\ l = 1, 2..p\}$ by distributing their values in the interval $[0, \pi]$.

For $k = 1, .., K$ Do

For $l = 1, ...p$ Do

$$\hat{r}_l(1,k) = \mathrm{w}_l(k)^H \mathrm{Q}^T \mathrm{w}_l(k) \tag{5.68}$$

$$\frac{\partial \xi}{\partial \hat{\omega}_l} = \|(\hat{r}(1,k))\| \sin(\arg\{\hat{r}_l(1,k)\} - \hat{\omega}_l(k)) \tag{5.69}$$

$$\Delta\hat{\omega}_l(k) = -\mu \frac{\partial \xi}{\partial \hat{\omega}_l} \tag{5.70}$$

$$\hat{\omega}_l(k+1) = \hat{\omega}_l(k) + \Delta\hat{\omega}_l(k) \tag{5.71}$$

End

For $l = 1, ...p$ Do

$$\mathrm{w}_l(k+1) = \prod_{i=1, i\neq l}^{p} (*)[1, -exp(\hat{\omega}_l(k+1))] \tag{5.72}$$

End

End

where K represents the number of iterations.

The structure of the resulting spatial filtering and estimation process is illustrated in figure 5.7 which had been previously proposed in [90] [89] [91] [92]. It is therefore worth emphasising that the main contribution of the algorithm proposed here, which is considered to be subtle but

significant; is that, a gradient-descent technique is used to ***directly estimate*** the electrical angles ω_l enabling the angle tracking task.

As a consequence of using the smoothing structure shown in figure 5.7, the conclusions reached in [92] stating that using an spatial a smoothing structure requires more than $\frac{2}{3}(L+1)$ elements to resolve L coherent signals, are applicable here.

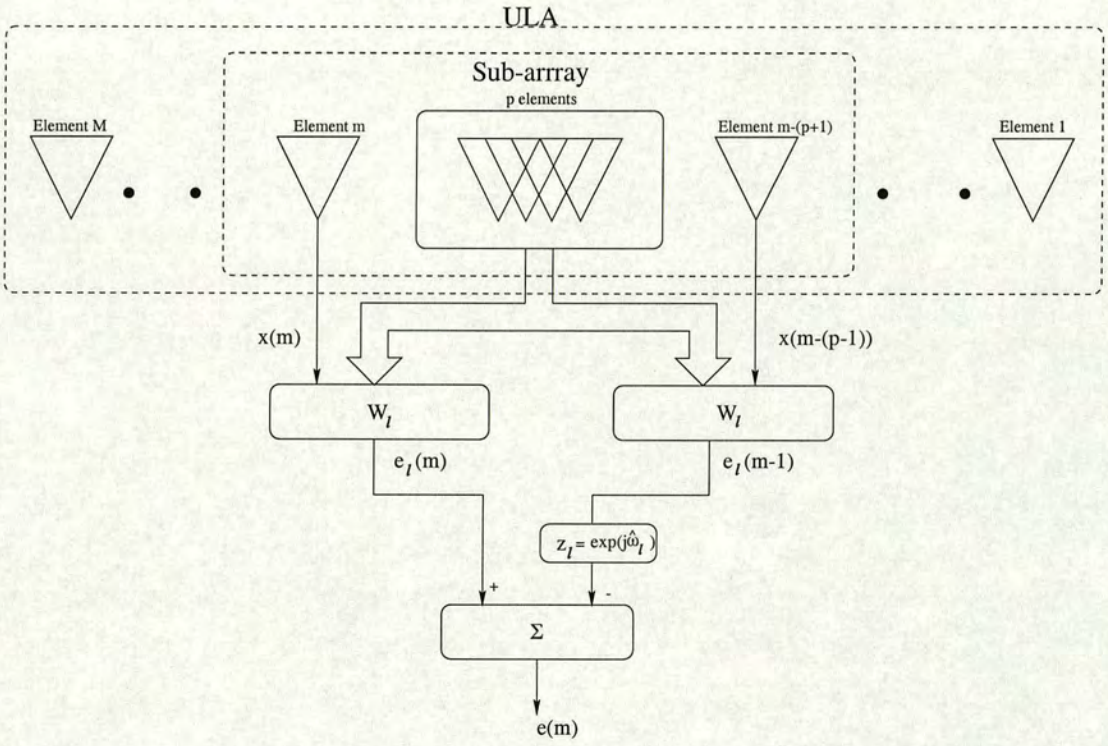

Figure 5.7: *Spatial smoothing for resolving coherent sources with adaptive null steering.*

5.4.3 Convergence analysis

In this section, the convergence characteristics of the algorithm will be explained.
In equation (5.52), it can be seen how the MSE for a predictor of first order is a function with a unique minimum at:

$$\hat{\omega}^o = \arg\{r(1)\}. \tag{5.73}$$

In the case of one spatial sinusoid (resulting from spatially-sampling one plane wave) in additive spatially-decorrelated noise, the phase of the lag-one spatial correlation ($\arg\{r(1)\}$) will equal the frequency of the sinusoid (electrical angle of the impinging plane wave):

$$\hat{\omega}^o = \arg\{r(1)\} = \omega. \tag{5.74}$$

This means that a gradient-descent algorithm to estimate the electrical angle ω, based on the minimisation of the MSE, should converge to its optimal unique solution.

In the case of several spatial sinusoids (corresponding to several plane waves), the output of the array can be modelled as:

$$x(m,n) = \sum_{l=1}^{L} s_l(n) \exp(j(m-1)\omega_l(k)) + \eta(m,n) \tag{5.75}$$

this can be expressed as :

$$x(m,n) = \sum_{l=1}^{L} s_l(n) \exp(j(m-1))\omega_l(k) + int(m,n) + \eta(m,n) \tag{5.76}$$

where

$$int_l(m,n) = \sum_{\substack{k=1 \\ k \neq l}}^{L} s_k(n) \exp(j(m-1)) \tag{5.77}$$

represents the $l-th$ "interference".

The lag-one spatial correlation of the output of the $l-th$ filtering section ($\mathbf{w}_l$) will be given by:

$$\hat{r}_l(1) = E[e_l(m)e_l^*(m-1)] \tag{5.78}$$

$$= E[\mathbf{w}_l^H((\mathbf{a}_l(m)s_l(n) + \mathbf{int}(m,n) + \vec{\eta}(m,n))$$

$$(\mathbf{a}_l(m)\exp(-j\omega_l)s_l(n) + \mathbf{int}(m-1,n) + \vec{\eta}(m-1,n))^H)^T\mathbf{w}_l]$$

where

$$\mathbf{int}_l(m,n) = \sum_{\substack{k=1 \\ k\neq l}}^{L} \mathbf{a}_k s_k(n), \tag{5.79}$$

$$\mathbf{int}_l(m-1,n) = \sum_{\substack{k=1 \\ k\neq l}}^{L} \mathbf{a}_k s_k(n)\exp(-j\omega_k), \tag{5.80}$$

$$\mathbf{a}_l(m) = [\exp(jm\omega_l)\ \exp(j(m-1)\omega_l)\ \ldots\ \exp(j(m-p)\omega_l)]^T, \tag{5.81}$$

and

$$\vec{\eta}(m,n) = [\eta(m,n)\ \eta(m-1,n)\ \ldots\ \eta(m-p,n)]^T. \tag{5.82}$$

The lag-one correlation at the output of the $l-th$ filter can be rewritten as:

$$\hat{r}_l(1) = P_l|\mathrm{a}_l^T\mathrm{w}_l|^2\exp(j\omega_l) + \hat{r}_l(1)_{bias} \tag{5.83}$$

where $\hat{r}_l(1)_{bias}$ will be in part dependent on the autocorrelations of the $l-th$ interference $\mathbf{int}_l(m-1,n)$ an its cross-correlations with $\mathbf{a}_l(m)s_l(n)$ and $\vec{\eta}(m,n)$. However, if the $l-th$ interference is "sufficiently" cancelled by the respective $l-th$ filter w_l (as would naturally result in the case of tracking) , the bias will be reduced to:

$$\hat{r}_l(1)_{bias} \approx \frac{C_l}{|\mathrm{a}_l^T\mathrm{w}_l|^2 SNR} \tag{5.84}$$

where

$$C_l = \mathrm{w}_l^H \begin{bmatrix} 0 & 0 & \dots & 0 & 0 \\ 1 & 0 & \dots & 0 & 0 \\ 0 & 1 & \dots & 0 & 0 \\ 0 & 0 & \dots & 0 & 0 \\ 0 & 0 & \dots & 1 & 0 \end{bmatrix}^T \mathrm{w}_l, \tag{5.85}$$

and $SNR = \frac{P_l}{\sigma^2}$.

Finally, the optimal phase (in the MSE sense) of the $l-th$ zero ($\hat{\omega}_l^o$) will be given by:

$$\hat{\omega}_l^o = \arg\{\hat{r}_l(1)\} = \arg\{P_l|\mathrm{a}_l^T\mathrm{w}_l|^2\exp(j\omega_l) + \hat{r}_l(1)_{bias}\} \tag{5.86}$$

$$= \arg\{\exp(j\omega_l) + \frac{\hat{r}_l(1)_{bias}}{P_l|\mathrm{a}_l^T\mathrm{w}_l|^2}\}$$

which in the case of "locked tracking" (when the spatial filters place nulls near the electrical angles of the waves) reduces to:

$$\hat{\omega}_l^o \approx \arg\{\exp(j\omega_l) + \frac{C_l}{|\mathrm{a}_l^T\mathrm{w}_l|^2 SNR}\} \tag{5.87}$$

This proves that a gradient-descent algorithm to estimate the electrical angle ω_l, based on the minimisation of the MSE, should converge to the biased solution given in equation (5.86) which in the case of "locked tracking" reduces to equation (5.87).

5.4.4 Computer simulations

In order to show the applicability of the proposed approach in the task of tracking the direction of arrival of non-stationary plane waves, several simulations are performed. In all the simulations the case of an uniform linear array of isotropic sensors with elements spaced a distance of half the wavelength is considered.

In all examples the output of the array was modelled as:

$$x(n,m) = s_1(n)\exp(j(m-1)\omega_1(n)) + s_2(n)\exp(j(m-1)\omega_2(n)) + \eta(n), \tag{5.88}$$

where

$$\omega_i(n) = \pi sin(\theta_i(n)) \quad for \quad i = 1, 2. \tag{5.89}$$

and

$$s_i(n) = A_i \exp(\phi_i(n)) \quad for \quad i = 1, 2. \tag{5.90}$$

being $\phi_1(n)$ and $\phi_2(n)$ two independent random variables uniformly distributed in the interval $[0, \pi]$.

Case A.

The first simulation consists of two coherent non-stationary sources with equal power ($A_1 = A_2$) impinging on an array of 30 elements with angles of arrival $\theta_1(t) = 20 - 5t$ and $\theta_2(t) = -20 + 5t$ contaminated by spatially decorrelated noise at a signal to noise ratio (defined as A_i^2/σ^2) of 10 dB.

A predictor of order four was used in this case with two of its zeros (intended to track the desired angles) being constrained to be on a circumference with unitary radius while the other two were constrained to be on a circumference of radius 0.7. The number of samples per time index is 5 ($n = 5t$) and the algorithm is iterated 10 times with $\mu = 0.4$.
The results of this simulation are shown in Fig. 5.8. There, it can be observed how the proposed algorithms produces good angle estimates before and after the crossing point. It must be remarked that, although the tracking zeros "exchange sources" after the crossing point, the "real trajectory" of each source can be recovered by comparing consecutive angle estimates to detect sudden changes in direction.

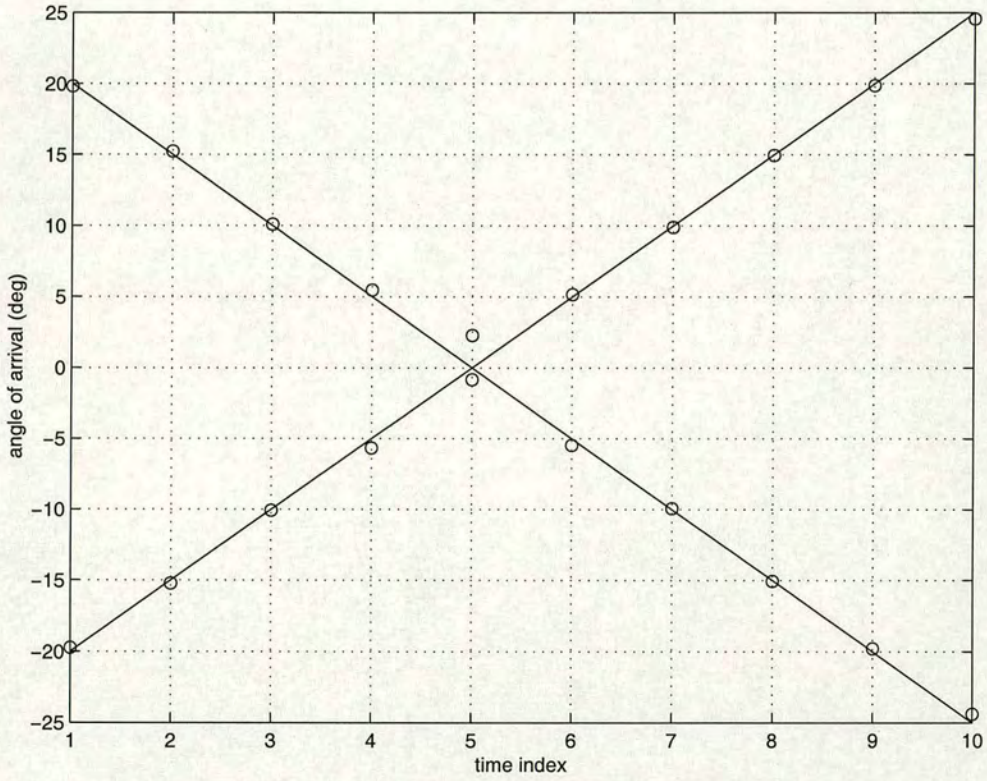

Figure 5.8: *Angle tracks for two coherent source: proposed approach, M=30, SNR=10dB ('o' estimated angles, '- 'real track).*

Case B.

A second simulation consists of two coherent non-stationary sources with equal power ($A_1 = A_2$) impinging on an array of 20 elements with angles of arrival $\theta_1(t) = 20 - 5t$ and $\theta_2(t) = -20 - 5t$ contaminated by spatially decorrelated noise at a signal to noise ratio of 3 dB.

The number of samples per time index in this case is 50 and the algorithm is iterated 10 times per time index with $\mu = 0.4$. The results of this simulation are shown in Fig. 5.9. The mean square error in the angle estimates obtained in this simulation was $0.3\ deg^2$.

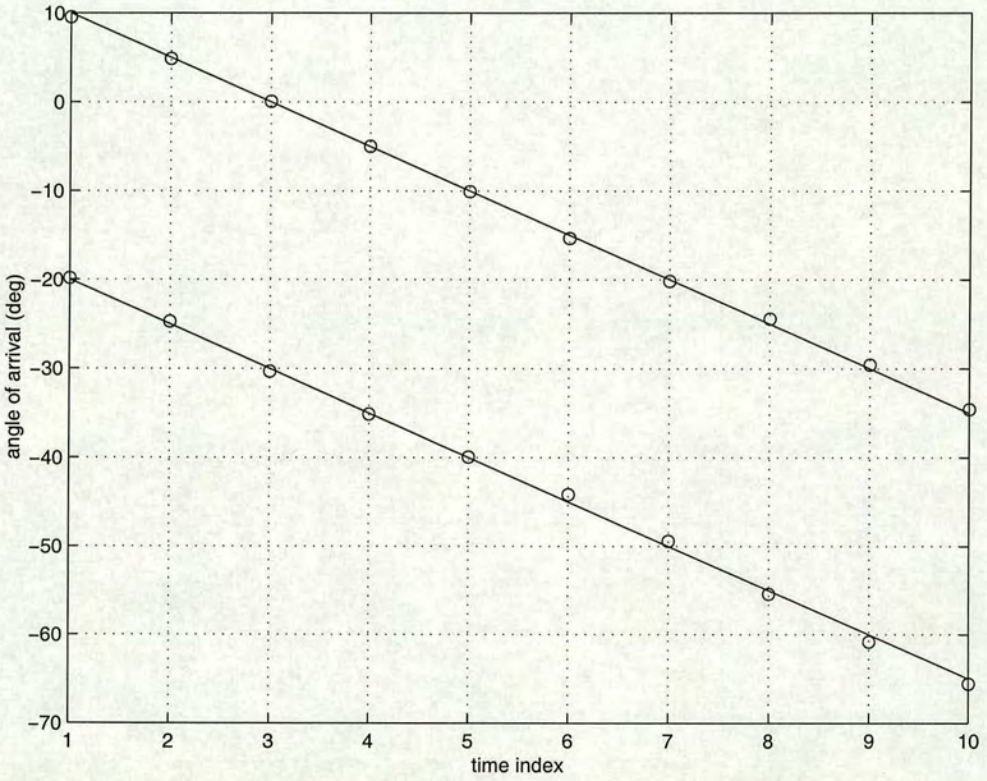

Figure 5.9: *Angle tracks for two coherent sources, proposed approach, M=20, SNR=3dB ('o' estimated angles, '-' real track).*

Case C.

In order to prove the effect of model order selection in the performance of the algorithm, the previous simulation is repeated (SNR=10 dB) for:

a) a filter consisting of two zeros (Fig.5.10), one on the unit circle (red circle in the figure) and another with radius of 0.7 (blue circle in the figure),
b)a filter consisting of one zero (Fig.5.11) on the unit circle(red circle in the figure),
c) a filter consisting of four zeros (Fig.5.12) ,three on a circumference with unitary radius (black, blue and green circles in the figure) and one with radius of 0.7 (red circle in the figure).

In the first case, it can be observed how the trajectories are still tracked by the zeros despite one of them being well inside a circumference with unitary radius.

In the second case, the zero tracks the median angle trajectory reflecting the optimum output-power-cancelling "fuction" of the proposed adaptive algorithm.

Finally, in the third case, it can be observed how the trajectories are tracked by two of the zeros on a circumference with unitary radius, the third zero on a circumference with unitary radius and the zero inside the circumference cover the rest of the angle space. In order to prove the "validity" of a given source trajectory estimate, it is necessary to include additional information such as the power of the signal at a given direction which can be obtained by using beamforming techniques[93].

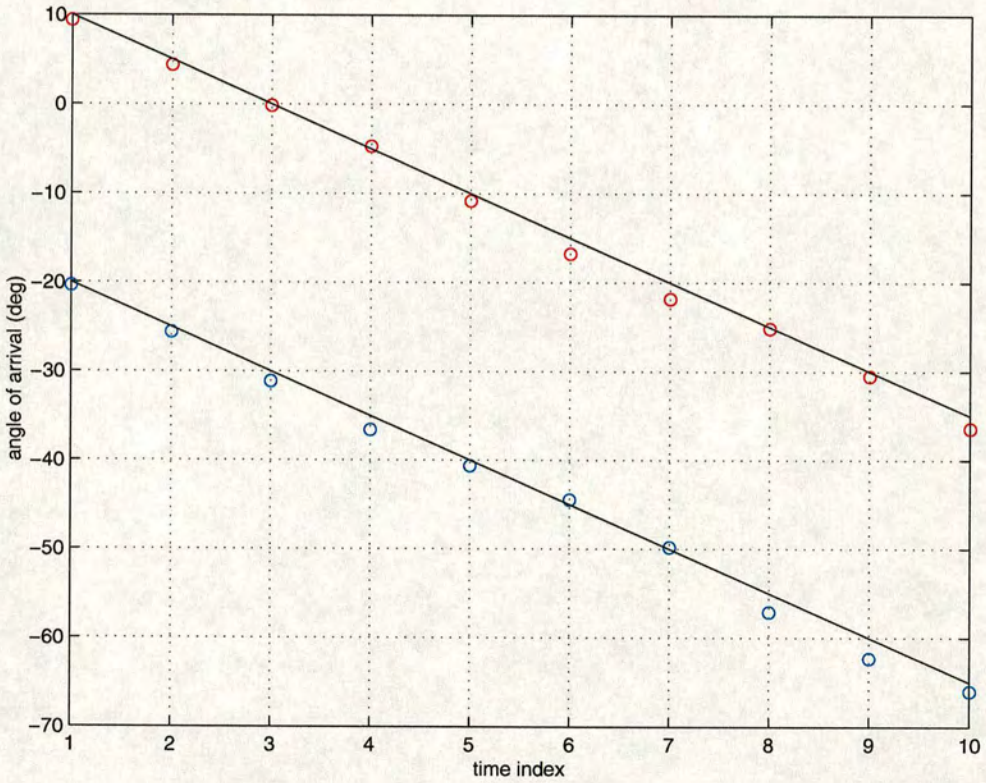

Figure 5.10: *Angle tracks for two correlated sources obtained with two adaptive zeros , M=20, SNR=10dB('o' angles estimated with proposed approach,'-' real track).*

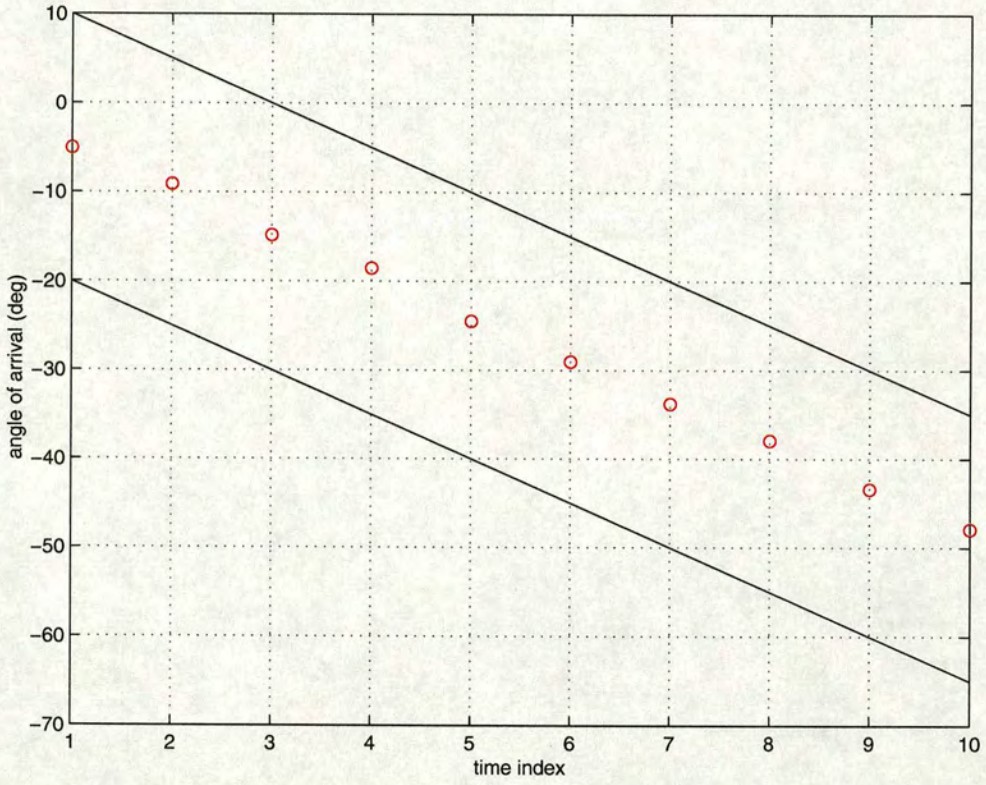

Figure 5.11: *Angle trajectory obtained with one adaptive zero for the case of two correlated sources, M=20, SNR=10dB('o' angle estimated with proposed approach,'-' real track).*

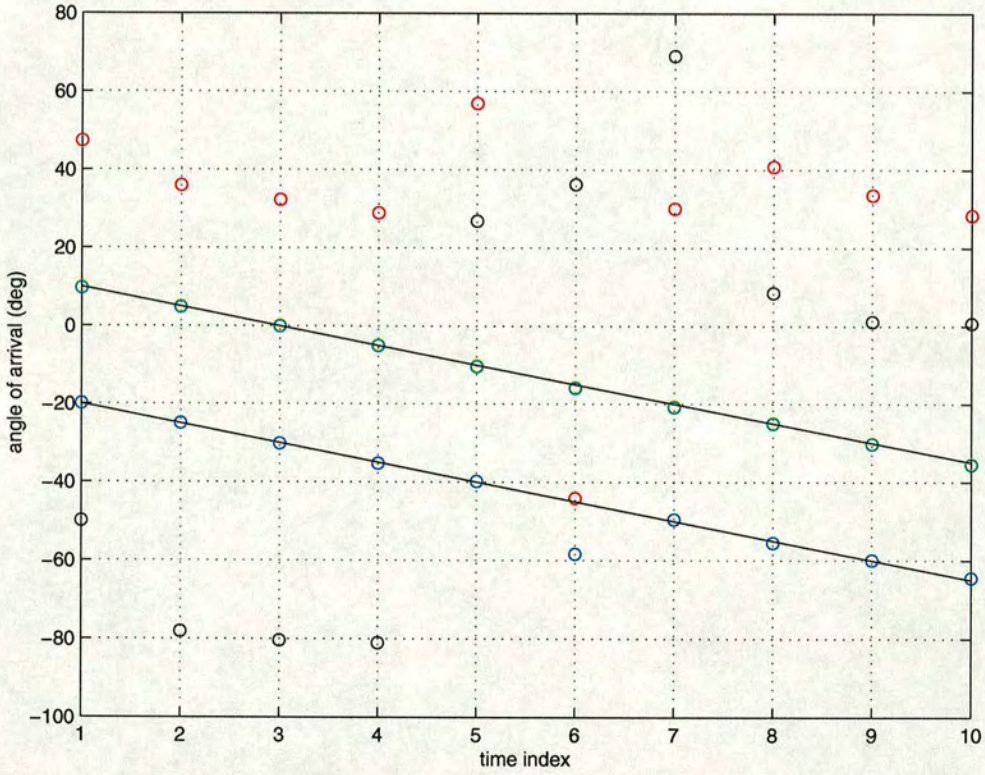

Figure 5.12: *Angle tracks for two correlated sources obtained with four adaptive zeros M=20, SNR=10dB ('o' angle estimated with proposed approach,'-' real track).*

SNR (dB)	$MSE(dB)$	
	Proposed	root-MUSIC
15	- 21.2	- 41
10	-15.43	-36
5	-7.33	-29.2

Table 5.1: *MSE of the angle estimate for the proposed an root-MUSIC approaches*

Case D.

In order to compare the performance of the algorithm proposed, a simulation consisting of two uncorrelated sources with equal power and angles of arrival $\theta_1(t) = 43 - 52t$ and $\theta_2(t) = -43 + 52t$ (M=30, N=10) is implemented.

For the proposed algorithm, a filter containing four zeros was implemented with two zeros constrained to be on a circumference with unitary radius while the other two were constrained to have a radius of 0.4. Only the zeros on a circumference with unitary radius are shown in the figure.

The MSE of the angle measurement for several values of SNR are shown in Tab. 1, and the angle tracks obtained using both techniques are plotted in Fig 5.13. The results show that the proposed algorithm successfully tracks the angle trajectories with less accuracy that the root-MUSIC [95] [94]algorithm. However, one must take into account that the root-MUSIC algorithm required the ED of a $M \times M$ correlation matrix plus polynomial root estimation at each time-index, which represents high-accuracy at the expense of high computational load.

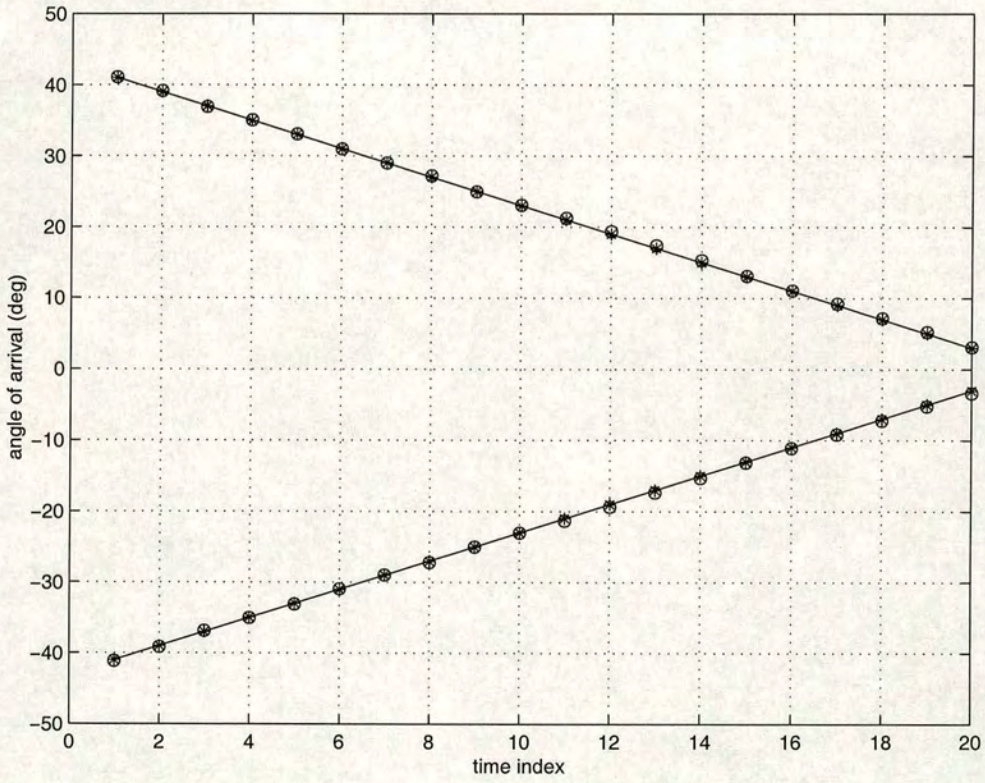

Figure 5.13: *Angle tracks for two uncorrelated sources, proposed approach in comparison to root-MUSIC, M=30, SNR=15dB ('o' angles estimated with proposed approach,'*' estimated angles (root-MUSIC),'-' real track).*

Case E.

Finally, the case of two closely spaced uncorrelated sources is considered.In this case a ULA of 50 sensors is simulated with 10 snaposhots per time index and signal-to-noise ratio of 20 dB. The performance of the algorithm is this case is displayed in Fig. 5.14. In this figure, it can be observed how the proposed algorithm successfully tracks the linear angle trajectories as they approach up to a separation of 2 degrees.

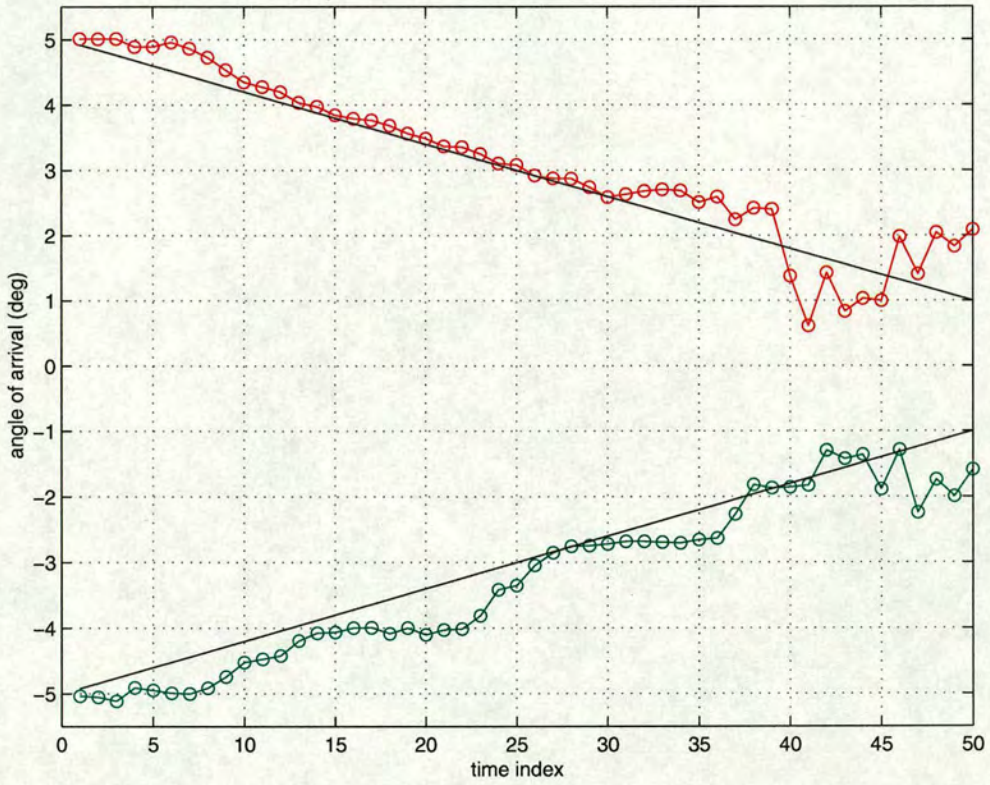

Figure 5.14: *Angle tracks for two closely spaced uncorrelated sources, M=50, N=10, SNR=20dB ('o'angles estimated with proposed approach,'-' real track).*

5.5 Conclusions

In this chapter, the concepts of multiple nonstationary spatial frequencies have been defined in conjunction with a brief description of some of the signal processing technqiues that have been used in the past to estimate and track these frequencies. It was explained in the chapter, how the output measurements of a linear array with uniformly spaced sensors (antennas) upon which impinge several nonstationary planar electromagnetic waves, can be modelled as time-varying exponential signals. It was also explained how these frequencies provide information about the angle of incidence of the planar waves on the linear array.

Eigenvalue-decomposition-based techniques where presented as the most commonly used techniques (due to their associated high resolution) to obtain estimates of the frequencies of stationary spatial exponentials.

For the problem of nonstationary waves, three approaches for tracking the nonstationary angles of arrival were subsequently reviewed. These approaches have been grouped under the three general classes:

- Adaptive subspace techniques,
- Direct recursive update of the angles estimates, and
- Adaptive null-steering,

which illustrate the common goal of providing a recursive way to adapt the parameters of spatial filters to "track" information in non-stationary scenarios.

After the presentation of the general background review, a technique was proposed to directly estimate and track the direction of arrival of multiple nonstationary plane waves impinging on a linear array of sensors. The proposed approach, which is based on spatial signal separation and direct angle estimation, has been successfully tested for the case of simulated nonstationary coherent sources.

Computer simulations show that the accuracy of the proposed algorithm in the estimation of multiple angle tracks is lower than that obtained with the root-MUSIC algorithm. However the proposed technique represents an advantage due to its direct estimation approach which translates as an efficient reutilisation of previously estimated parameters. Additionally the proposed approach is suitable for use in the case of correlated signals and in large array applications .

Chapter 6
Conclusions and suggestions for future work

6.1 Conclusions

In this thesis, the development of an adaptive technique to measure the instantaneous frequency of multiple non-stationary sinusoids was presented.

The second chapter of the thesis provided a review of some of the many approaches that have been used in the past to estimate the instantaneous parameters of multiple non-stationary sinusoids, as well as as brief explanation of some potential applications of the estimation of these parameters in the design of communication systems and in the area of speech analysis where resonances of the vocal tract have been modelled in the past as non-stationary sinusoidal signals.

A detailed review of the adaptive FIR filters approach to analyse non-stationary multicomponent signals, which is the centre of study in this research work, was provided in chapter three to describe the general background of the technique that has been explored in the thesis.

The main ideas explored in the research described here, which focused on the direct estimation and tracking of the frequency trajectory of several superimposed sinusoids using a cascade of second-order filters, were then presented in chapter four. There, a gradient-based re-estimation technique was used to adapt the parameters of each zero associated to each section of the cascade.

It was explained in the thesis that if the parameters of the zeros are adjusted to minimise the total output error for multiple superimposed non-stationary sinusoids, the angle of the zeros are actually estimates of the frequencies of the sinusoids.

These ideas were tested in computer simulations where the performance of the proposed approach was illustrated by tracking single and multiple instantaneous frequencies of synthetic and real signals. The most remarkable of these simulations consisted of the analysis of a

segment of voiced speech where the novel algorithm was used to successfully track formant frequency trajectories of the sonorous segment.

In addition to the frequency estimation algorithm proposed in chapter four, another technique was presented there to estimate the amplitude envelope of a mono-component sinusoidal signal. This technique was extended to the case of multiple sinusoids by first using a separation stage to isolate the components of the signal. This separation was performed relying on a cascade of adaptive notch filters tuned to previously estimated frequency trajectories.

By directly adjusting the angle of the zeros, it is possible to provide a direct estimate of the frequencies of the sinusoids which is particularly beneficial in the case of multi-frequency tracking.

The idea of adaptive zeros for multi-frequency estimation was also extended to the spatial domain case by designing an adaptive spatial filter to track the electrical angles and therefore the angles of arrival of multiple plane waves impinging on a linear array of uniformly spaced sensors.

An introduction to the problem of tracking the direction of arrival of multiple plane waves was given in chapter 5 followed by a detailed description of the proposed spatial approach. The resulting adaptive zero tracking algorithm belongs to a class of adaptive nulling structures that had been proposed in the past for the task of interference suppression in linear arrays and source tracking.

Adapting the zeros of an spatial filter proved to be a successful approach in computer simulations with straightforward applications in the case of large arrays and coherent scenarios.

The main emphasis of the proposed estimation technique was explained to be the direct estimation of the electrical angle of each tracked spatial signal using a gradient-based technique offering significant computational saving over eigen-decomposition based techniques. This task had not been explored in the past and constitutes the basis of the tracking technique proposed in chapter 6.

6.2 Suggestion for future Work

Tracking the instantaneous frequency of multiple non-stationary sinusoids has many potential applications especially in the area of speech processing where the task of formant tracking has captivated the attention of many researchers for many years. This special interest in tracking the frequencies of speech resonances is due to the fact that these frequencies are recognised as important features in the process of speech perception and understanding.

New research work could be oriented towards the incorporation of formant frequency estimates in the development of systems for speech synthesis, coding and recognition. This task is not new as it has been explored in the past in numerous research works [96] [97] [98] [100] [101] but as no satisfactory proposition has yet been made, the proposed technique could offer a new window of research in this subject.

In the case of tracking spatial frequencies, the proposed approach has proved successful in computer simulations of the problem, leaving open the question of the applicability of this technique in real-world scenarios. Additionally it would be interesting researching possible improvements to the proposed algorithms to increase its robustness to noise and estimation accuracy.

Appendix A
Boundaries for the adaptation constants

Boundary for μ_ω

For a complex mono-component signal:

$$s_c(n) = a(n)\exp[j\phi(n)], \tag{A.1}$$

the instantaneous error obtained after passing it through a filter composed of one zero $z(n) = \hat{\rho}\exp[j\hat{\omega}(n)]$ will be:

$$e_c(n) = s_c(n) - s_c(n-1)z(n) \tag{A.2}$$

$$= a(n)\exp[j\phi(n)] - \frac{a(n)}{\rho(n)}\exp[j\phi(n) - j\omega(n)]\hat{\rho}(n)\exp[j\hat{\omega}(n)]. \tag{A.3}$$

This implies that the absolute instantaneous error for a real valued signal:

$$s(n) = s_c(n) + s_c^*(n) \tag{A.4}$$

will have the following upper bound:

$$|e(n)| < 2a|1 - \frac{\hat{\rho}(n)}{\rho(n)}\exp[j\hat{\omega}(n) - j\omega](n)| \tag{A.5}$$

which can be simplified assuming $\hat{\rho}(n) = \rho(n)$ as:

$$|e(n)| < 2a(n)|1 - \exp[j\hat{\omega}(n) - j\omega(n)]| \tag{A.6}$$

or

$$\frac{|e(n)|}{2a(n)} < |(\exp(j\hat{\omega}(n) - j\omega(n)) - 1)|. \tag{A.7}$$

As

$$|(\exp(j\hat{\omega}(n) - j\omega(n)) - 1)| < |\hat{\omega}(n) - \omega(n)| = |\omega v(n)| \ . \tag{A.8}$$

which leads to

$$\frac{|e(n)|}{2a(n)} < |\omega v(n)|, \tag{A.9}$$

if we want

$$\mu_\omega |e(n)| < |\omega v(n)|, \tag{A.10}$$

we must choose

$$\mu_\omega < \frac{1}{2a(n)}. \tag{A.11}$$

Finally, for $a(n) = 1$, we obtain

$$\mu_\omega < \frac{1}{2}. \tag{A.12}$$

Boundary for μ_ρ

As stated before, we have for a real-valued monocomponet signal:

$$\frac{|e(n)|}{2a(n)} < |1 - \frac{\hat{\rho}(n)}{\rho(n)} \exp[j\hat{\omega}(n) - j\omega(n)]| \tag{A.13}$$

or

$$\frac{|e(n)|}{2a(n)} < \frac{1}{\rho(n)}|\rho(n) - \hat{\rho}(n)| = \frac{1}{\rho(n)}|\rho v|. \tag{A.14}$$

In order to obtain

$$\mu_\rho |e(n)| < |\rho v(n)|, \tag{A.15}$$

we should choose

$$\mu_\rho < \frac{\rho(n)}{2a(n)}. \tag{A.16}$$

Finally, for $a(n) = 1$, we obtain

$$\mu_\rho < \frac{\rho(n)}{2}. \tag{A.17}$$

Appendix B
Associated Publications

J. Vargas and M. Jack, "Cascade adaptive predictors with improved sensitivity for speech decorrelation through decomposition into exponential signals," *Electronics Letters*, vol. 34, p.1809, September 1998.

J. Vargas and S. Mc. Laughlin, "Adaptive predictors in cascade form to analyse superimposed exponential signals with time-varying parameters." Accepted for publication in *Signal Processing* (Elsevier Press) on May 2001.

J. Vargas and S. Mc. Laughlin, 'Tracking direction of arrival with adaptive decomposed filters" Submitted to *Signal Processing* (Elsevier Press) on January 2001 , and re-submitted after review on May 2001.

References

[1] J. Proakis J. Deller and J. Hansen, *Discrete-time processing of speech signals*. Macmillan, 1993.

[2] B. S. Atal and S. L. Hanauer, "Speech analysis and synthesis by linear prediction of the speech wave," *Journal of the Acoustic Society of America*, vol. 50, pp. 637-655, 1971.

[3] J. I. Makhoul, "Linear prediction: A tutorial review," *Proc. IEEE*, vol. 63 (III), pp. 561-580, April 1975.

[4] D. Gabor, "Theory of communication," *Proc. IEE*, vol. 93 (III), pp. 429–457, 1946.

[5] R. W. Schafer and L. R. Rabiner, "System for automatic formant analysis of voiced speech," *Journal of the Acoustic Society of America*, vol. 47, pp. 634–648, Feb. 1970.

[6] R. J. McAulay and T. F. Quatieri , "Speech analysis/synthesis based on a sinusoidal representation," *IEEE Trans. Acoust. Speech Signal Processing*, vol. 34, no. 4, pp. 744–754, 1986.

[7] L. S. Marques and L. B. Almeida. "Frequency-varying sinusoidal modeling of speech," *IEEE Trans. Acoust. Speech Signal Processing*, vol. 37, no. 5, pp. 763–765, May 1989.

[8] J. F. Kaiser, "On Teager's energy algorithm and its generalization to continuous signal," in *Proc. 4th IEEE Digital Signal Processing Workshop*, vol. 1, (New Paltz, NY), Sept. 1990.

[9] J. F. Kaiser, "On a simple algorithm to calculate the 'energy' of a signal," in *Proc. IEEE Int. Conf. Acoustics, Speech, and Signal Processing*, vol. 1, (Albuquerque), pp. 381–384, Apr. 1990.

[10] P. Maragos, J. F. Kaiser and T. F. Quatieri, "On amplitude and frequency demodulation using energy operators," *IEEE Transactions on Signal Processing*, vol. 41, pp. 1532–1550, April 1993.

[11] P. Maragos, J. F. Kaiser and T. F. Quatieri, " Energy separation in signal modulations with application to speech analysis," *IEEE Transactions on Signal Processing*, vol. 41, no. 10, pp. 3024–3051, October 1993.

[12] R. A. Baxter and T. F. Quatieri, "Shunting networks for multiband AM-FM decomposition," in *Proc. IEEE Workshop on applications of signal processing to audio and acoustics*, New Platz, New York, pp. 227-230, 1999.

[13] B. Santhanam and P. Maragos, "Demodulation of discrete multicomponent AM-FM signals using periodic algebraic separation and energy demodulation," in *Proc. IEEE Int. Conf. Acoust., Speech, Signal Process.*, pp. 2409-2412, 1987.

[14] K. T. Assaleh and R. J. Mammone, "Spectral temporal decomposition of multicomponent signals," in *Proc. IEEE Sixth Workshop on Statistical and Array Processing*, pp. 206-209, 1992.

[15] L. B. Fertig and J. H. McClellan, "Instantaneous frequency estimation using linear prediction with comparisons to the DESA's," *IEEE Signal Processing Letters*, vol. 3, pp. 54–6, 1996.

[16] T. S. Rao, "The fitting of non-stationary time series models with time-dependent parameters," *J. Royal Statist. Soc. series B*, vol. 32, no. 2, pp. 312–322, 1970.

[17] L. A. Liporace "Linear estimation of non-stationary signals"*Journal of the Acoustic Society of America*, vol. 58, no. 6, pp. 1288–1295, 1975.

[18] Y. Grenier, "Time-dependent ARMA modeling of non-stationary signals," *IEEE Trans. Acoust. Speech Signal Processing*, vol. ASSP-31, pp. 899–991, August 1983.

[19] S. Conforto and T. D'Allesio, "Optimal estimation of power spectral density by means of a time-varying autoregressive approach," *Signal Processing*, vol. 72, pp. 1–14, Jan 1999.

[20] A. Akan and L. F. Chaparro, "Adaptive time-varying parametric modeling," in *1994 IEEE International Conference on Acoustics, Speech and Signal Processing*, vol. 4, pp. 13–16, 1994.

[21] S. Mukhopadhyay and P. Sircar, "Parametric modeling of non-stationary signals: A unified approach," *Signal Processing*, Elsevier, pp.135-152, July 1997.

[22] A. S. Kayan, "Difference equation representation of chirp signals and instantaneous frequency/amplitude estimation," *IEEE Trans. Acoust. Speech Signal Processing*, vol. 44, pp. 2948–2958, December 1996.

[23] K. C. Sharman, "Time varying autoregressive modelling of a class of nonstationary signals," in *Proc. IEEE Int. Conf. Acoust., Speech, Signal Process.*, pp. 22.2.1–22.2.4, 1984.

[24] E. W. Kamen and Hafez, "Algebraic theory of linear time-varying systems," *SIAM J. Contr. Optimiz.*, vol. 17, no. 4, pp. 500–510, 1980.

[25] E. W. Kamen, "The poles of a linear time-varying system," *Linear Algebra Appl.*, vol. 98, pp. 263–289, 1988.

[26] B. Boashash, "Estimating and interpreting the instantaneous frequency of a signal. II. Algorithms and applications.," *Proceedings of the IEEE*, vol. 80, pp. 540–568, April 1992.

[27] B. Boashash, "Estimating and interpreting the instantaneous frequency of a signal. I. Fundamentals," *Proceedings of the IEEE*, vol. 80, pp. 520–538, April 1992.

[28] S. Mallat, *A wavelet tour of signal processing*. Academic Press, 1998.

[29] L. Cohen, *Time Frequency Analysis*. Englewood Cliffs, NJ:Prentice-Hall, 1995.

[30] L. Cohen, "Time-frequency distributions-a review," *Proceedings of the IEEE*, vol. 77, pp. 942–81, July 1989.

[31] E. P. Wigner, "On the quantum correction for thermodynamic equilibrium," *Phys. Rev.*, vol. 40, pp. 749–759, 1932.

[32] H. I. Choi and W. J. Williams, "Improved time-frequency representations of multi-component signals using exponential kernels," *IEEE Trans. Acoust., Speech, Sig. Proc.*, vol. 37, no. 6, pp. 862–871, 1989.

[33] J. Ville, "Theory et applications de la notion de signal analytique," *Cables et Transm.*, vol. 2, pp. 61–74, 1948.

[34] C. Wang and M. Amin, "Time-frequency distribution spectral polynomials for instantaneous frequency estimation," *Signal Processing*, vol.768, pp. 211-217, 1999.

[35] Z. Hussain and B. Boashash, 'Adaptive instantaneous frequency estimation of multi-component FM signals," in *2000 IEEE International Conference on Acoustics, Speech and Signal Processing*, vol. 2, pp. 675–660, 2000.

[36] J. P. Costas, "Residual signal analysis," *Proceedings of the IEEE*, vol. 68, no. 10, pp. 1352–1352, 1980.

[37] A. B. Fineberg and R. J. Mammone, "A method for instantaneous frequency tracking of multiple narrow-band signals," *Signal Processing*, vol. 29, no. 1, pp. 29-44, 1992.

[38] C. S. Ramalingam and R. Kumaresan, "Voiced-speech analysis based on the residual interfering signal canceler (RISC) algorithm," in *1994 IEEE International Conference on Acoustics, Speech and Signal Processing*, vol. 1, pp. 473–6, 1994.

[39] C. S. Ramalingam, A. Rao, R. Kumaresan, "Time-frequency analysis using the residual interference signal canceller filter bank," in *Proceedings of the IEEE-SP International Symposium on Time-Frequency and Time-Scale Analysis*, pp. 500–503, 1994.

[40] T.F. Quatieri T. E Hanna G. C. O'Leary, "AM-FM separation using auditory-motivated filters," *IEEE Trans. Acoust., Speech, Sig. Proc.*, vol. 5, pp. 465–480, Sept. 1997.

[41] K. Saberi and E. K. Hafter, 'A common neural code for frequency-modulated and amplitude-modulated sounds," *Nature*, vol. 374, no. 3, pp. 537-539, 1995.

[42] W. Torres and T. F. Quatieri, "Estimation of modulation based on FM-to-AM transduction: two-sinusoid case," *IEEE Transactions on Signal Processing*, vol. 47, pp. 3084–97, 1999.

[43] P. Guillemain and R. Kronland-Martinet, "Characterisation of acoustic signals through continuous linear time-frequency representations," *Proc. IEEE*, vol. 84, no. 2, pp. 561–585, 1996.

[44] A. Rao Ramalingam and R. Kumaresan, "Dynamic tracking filters for decomposing non-stationary sinusoids," in *1995 IEEE International Conference on Acoustics, Speech and Signal Processing*, vol. 3, pp. 917-920, 1995.

[45] A. Rao and R. Kumaresan , "Model-based approach to envelope and positive instantaneous frequency estimation of signals with speech applications," *Journal of the Acoustic Society of America*, vol. 105, no. 3, pp. 1912-1924, 1999.

[46] A. Rao and R. Kumaresan , "On decomposing speech into modulated components," *IEEE Transactions on Speech Audio Processing*, vol. 8, no. 3, pp. 240-254, 2000.

[47] S. Haykin, *Communication Systems*. New York, USA: Wiley, 1987.

[48] G. M. Miller, *Modern Electronic Communication*. Englewood Cliff, USA, Prentice Hall, fith ed., 1996.

[49] J. R. Carson, "Notes on the theory of modulation," *Proc. IRE*, vol. 10, pp. 57–64, 1922.

[50] B. van der Pol, "Frequency modulation," *Proc. IRE*, vol. 18, pp. 1194–1205, July 1930 1930.

[51] E. H. Armstrong, "A method of reducing disturbances in radio signaling by a system of frequency modulation," *Proc. IRE*, vol. 24, pp. 689–740, May 1936.

[52] H. M. Teager, "Some observations of oral airflow during phonation," *IEEE Trans. Acoust., Speech, Sig. Proc.*, vol. 28, pp. 599–661, October 1980.

[53] H. M. Teager, "Evidence for noonlinear sound production mechanisms in the vocal tract," in *Speech Production and Speech Modelling*,William J. Hardcatle and Alain Marchal, Eds. (NATO adavaced Study institute Series D, vol 55, Bonas, France, July 17-29, 1998). Boston, MA: Kluwer, pp. 241-261, 1990.

[54] N. Wiener, *Extrapolation, interpolation, and Smoothing of Stationary Time Series with Engineering applications*. Press, Cambridge, MA, 1949.

[55] M. Hayes, *Statistical Digital Signal Processing and Modeling*. John Wiley Sons, 1996.

[56] S. Haykin, *Adaptive Filter Theory*. Englewood Cliff, USA, Prentice Hall, 1996.

[57] B. Widrow and S. D. Stearns, *Adaptive Signal Processing*. Englewood Cliffs, NJ:Prentice-Hal, 1985.

[58] L. J. Griffiths, "Rapid measurement of digital instantaneous frequency," *IEEE Transactions on Acoustics, Speech, Signal Processing*, vol. ASSP-23, no. 2, pp. 207–222, 1975.

[59] D. H. Youn, V. J. Mathews, S. H. Cho , "An efficient lattice predictor algorithm for instantaneous frequency estimation," *Signal Processing*, vol. 10, no. 1, pp. 75–81, 1986.

[60] P. R. Chitrapu and Z. Pan, 'Constrained least squares estimation of sinusoidal frequencies and application to time frequency analysis of chirp signals," in *Proceedings of IEEE Workshop on VLSI Signal Processing*, pp. 20-22, 1993.

[61] D. Hush, N. Ahned and R. David, "Instantaneous frequency estimation using adaptive linear prediction weights," *IEEE Transactions on Aerospace and Electronic Systems*, vol. 22, no. 44, pp. 422–431, 1986.

[62] S. Ghaemmaghami, M. Deriche and B. Boashash, "Hierarchical approach to formant detection and tracking through instantaneous frequency estimation," *Electronics Letters*, vol. 33, pp. 17–18, Jan. 1997.

[63] M. L. Honig and D. G. Messerschmitt, "Convergence properties of an adaptive digital lattice filter," *IEEE Trans. Acoust., Speech, Sig. Proc.*, vol. ASSP-29, pp. 642–653, 1981.

[64] E. H. Satourius and S. Alexander, "Channel equalization using adaptive lattice algorithms," *IEEE Trans. Comm.*, vol. COM-27, pp. 899–905, 1979.

[65] W. Hodgkiss and J. Presley, "Adaptive tracking of multiple sinusoids whose power levels are widely separated.," *IEEE Transactions on Circuits Systems*, vol. CAS-28, pp. 550–561, June 1981.

[66] P. J. Davies and M. G. Amin, "Frequency tracking-adaptive filtering vs. time-frequency distributions.," in *Proc. IEEE Int. Conf. Acoust., Speech, Signal Process.*, vol. 5, , pp. 3225–3228, IEEE, 1991.

[67] L. B. Jackson and S. L. Wood, "Linear prediction in cascade form," *IEEE Transactions on Acoustics, Speech ,Signal Processing*, vol. ASSP-26, pp. 518–528, December 1978.

[68] P. C. Ching and C. Goodyear, "LMS algorithm for sequentially adapting all-zero digital filters in modified cascade form," *Electronics Letters*, vol. 16, no. 7, pp. 270–1271, March 1980.

[69] P. C. Ching and C. Goodyear, "Adaptive cascade filter for speech anlaysis," *IEE Proceedings-E: Computers and Digital Techniques*, vol. 130, no. 1, pp. 11–18, January 1983.

[70] Y. H. Tam, P. C. Ching and Y. T. Chan , "Adaptive recursive filters in cascade form," *IEE Proceedings, Part F: Communications, Radar signal Processing*, vol. 134, no. 3, pp. 245-252, June 1987.

[71] U. Forssen, "Analysis of adaptive FIR filters in cascade form," *IEEE Transactions on Circuits ,Systems II-Analog , Digital Signal Processing*, vol. 41, pp. 392–401, June 1994. USA.

[72] L. C. Coradine, J. M. T. Romano and M. G. Bellanger, "Adaptive filtering in cascade form using a fast multichannel RLS algorithm," *IEEE Transactions on Circuits and Systems II-Analog and Digital Signal Processing*, vol. 44, pp. 757–762, Sept. 1997.

[73] P. Prandoni and M. Vetterli, "An FIR cascade structure for adaptive linear prediction," *IEEE Transactions on Signal Processing*, vol. 46, pp. 2566–2571, September 1998.

[74] G. Zakaria and A. Beex, "Cascade recursive least squares with subsection adaptation for AR parameter estimation.," in *Proc. IEEE Int. Conf. Acoust., Speech, Signal Process.*, vol. 2, (New York, NY, USA), pp. 953–956, IEEE, 1998.

[75] J. Vargas and M. Jack, "Cascade adaptive predictors with improved sensitivity for speech decorrelation through decomposition into exponential signals," *Electronics Letters*, vol. 34, p. 1809, September 1998.

[76] A. Nehorai, "A minimal parameter adaptive notch filter with constrained poles and zeros," *IEEE Trans. Acoust., Speech, Signal Processing*, vol. 33, pp. 983–996, Aug. 1985.

[77] S. S. Haykin, *Array Signal Processing*. Englewood Cliffs: Prentice-Hall, 1985.

[78] S. J. Orfanidis, *Optimum Signal Processing*. New:York:McGraw-Hill, 1988.

[79] S. J. Orfanidis and L. M. Vail, "Adaptive pole estimation," *IEEE Transactions on Acoustics, Speech, Signal Processing*, vol. ASSP-34, pp. 1566–1572, December 1986.

[80] T. J. Shan and T. Kailath, "Directional signal separation by adaptive arrays with a root tracking algorithm," in *Proc. IEEE Int. Conf. Acoust., Speech, Signal Process.*, vol. 4, pp. 2288–91, 1987.

[81] B. Yang, "Projection approximation suspace tracking," *IEEE Trans. Signal Processing*, pp. 95–107, January 1995.

[82] K.-B. Yu, "High-resolution multiple target angle tracking," *IEEE Aerospace and Electronic Systems Magazine*, vol. 6, no. 5, pp. 8–12, 1991.

[83] K. V. S. Babu,Y. Yoganandam , V.U. Reddy, "Adaptive estimation of eigensubspace and tracking the directions of arrival.," *Signal Processing*, vol. 68, no. 3, pp. 317–339, 1998.

[84] C. K. Sword, M Simaan and E. W. Kamen, "Multiple angle tracking using sensor array outputs," *IEEE Trans. Aerospace and Elec. Systems*, vol. 26, pp. 367–373, Mach. 1990.

[85] K. W. Lo and C. K. Li, "An improved multiple target angle tracking algorithm," *IEEE Transactions on Aerospace and Electronic Systems*, vol. 28, no. 3, pp. 797–805, 1992.

[86] D. E. N. Davies, "Independent angular steering of each zero of the directional pattern for a linear array," *IEEE Trans.* , vol. 15, pp. 296-298, 1967.

[87] M. K. Leavitt, "A phase adaptation algorithm," *IEEE Transactions on antennas and Propagation* , vol. 24, pp. 754-756, 1976.

[88] J. E. Hudson, *Adaptive array principles*. Peregrinus on behalf of the Institute of Electrical Engineers, 1981.

[89] C.C. Ko , K.L. Thum, W. Ser, T.S. Quek , "A simple fast adaptive zero tracking algorithm," *Signal Processing*, vol. 20, pp. 315–23, Aug. 1990.

[90] C. Ko, "A fast adaptive null-steering algorithm based on output power meaurements," *IEEE Transactions on Aerospace and Electronic Systems*, vol. 29, no. 3, 1993.

[91] C. C. Ko, "Resolution of coherent sources by using a fast phase shifting based null steering algorithm.," *Signal Processing*, vol. 25, pp. 11–22, Oct. 1991.

[92] C. C. Ko, "Resolution of coherent sources in power inversion arrays with a fast zero tracking algorithm.," *IEE Proceedings-I Communications Speech Vision*, vol. 139, pp. 45–52, Feb. 1992.

[93] B. D. Van Veen and K. m. Buckley, "Beamforming a versatile approach to Spatial filtering,"*IEEE ASSP Magazine*, pp. 4-24, April 1998.

[94] A. J. Barabell, "Improving the resolution performance of eigenstructure-based direction-finding algorithms," in *Proc. ICASSP-83*, vol. 1, pp. 336-339, 1983.

[95] B. D. Rao and K.V.S. Hari, "Performance analysis of root-MUSIC,"*IEEE Trans. Acoust. Speech and Signal Proc.*, vol. 37, pp. 1939-1949 , 1989.

[96] J. L. Flanagan, "Automatic extraction of formant frequencies from continuous speech," *Journal of the Acoustic Society of America*, vol. 28, pp. 110-118, 1956.

[97] R. W. Schafer, L. R. Rabiner, " System for automatic formant analysis of voiced speech," *Journal of the Acoustic Society of America*, vol. 47, no. 2.2 , pp. 634-648, 1970.

[98] S. S. McCandless, "An algorithm for automatic formant extraction using linear prediction spectra," *IEEE Trans. Acoust. Speech and Signal Proc.*, vol. 22, no. 2 pp. 1350-1341, 1974.

[99] B. Yegnanarayana, "Formant extraction from Linear-prediction Phase Spectra," *Journal of the Acoustic Society of America*, vol. 63, pp. 1638-1640, 1978.

[100] J. Holmes et al., "Using formant frequencies in speech recognition," in *Proc. 5th European Conf. Speech Communication Technology*, vol. 34,, pp. 2083-2086, 1997.

[101] L. Welling and H. Hey, "Formant estimation for speech recognition," *IEEE Trans. Acoust. Speech and Signal Proc., vol. 6, no. 1, pp. 36-48, 1998.*